ANALYTICAL REPRESENTATION OF FLAT PLATE STRUCTURES UNDER VERTICAL AND LATERAL LOADS

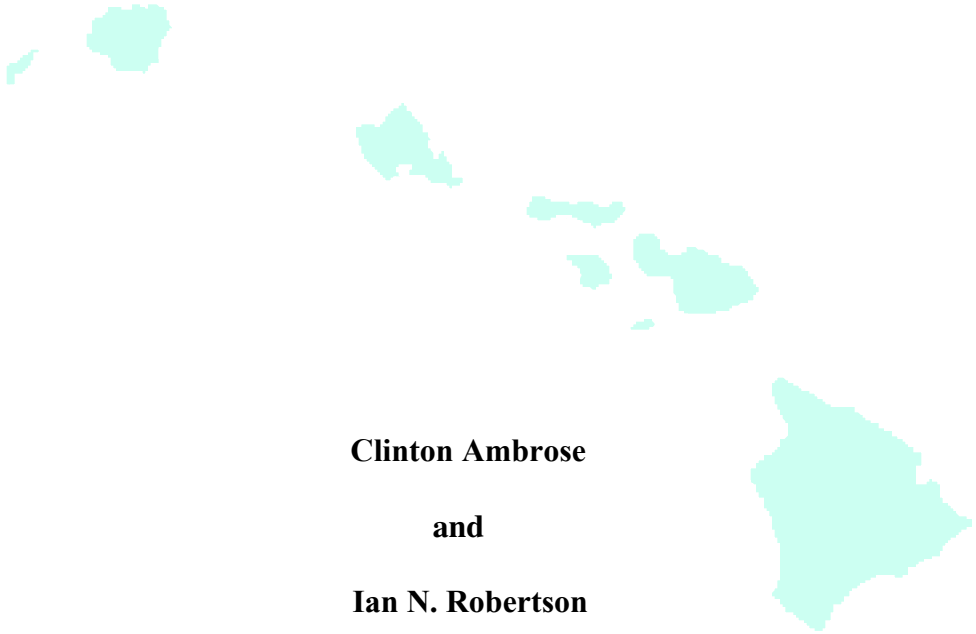

Clinton Ambrose

and

Ian N. Robertson

UNIVERSITY OF HAWAII
COLLEGE OF ENGINEERING

DEPARTMENT OF CIVIL AND ENVIRONMENTAL ENGINEERING

Research Report UHM/CE/96-01

April 1996

ANALYTICAL REPRESENTATION OF FLAT PLATE STRUCTURES UNDER VERTICAL AND LATERAL LOADS

by

Clinton Ambrose, and

Ian N. Robertson

University of Hawaii at Manoa

April 1996

Abstract

The effective beam width method is used extensively for two- and three-dimensional analysis of flat plate structures subjected to combined gravity and lateral loading. Typically, the member stiffnesses are assumed constant throughout each span. This approach is shown to produce unreliable estimates of lateral drift and slab bending moments when compared with the results of previously reported experimental programs performed by other researchers.

This paper presents a two-beam effective width model in which different section properties are used in negative and positive bending regions of the slab. Proposed slab stiffnesses for use in this model are based on a correlation between the experimental data and analytical analysis results. The application of the two-beam model using the proposed slab stiffness factors to a typical flat-plate structure is demonstrated in a worked example.

ACKNOWLEDGEMENTS

This report is based on a Masters Thesis prepared by Clinton Ambrose, performed under the direct supervision of Prof. I. N. Robertson, submitted in partial fulfillment of the requirements for the degree of Master of Science in Civil Engineering.

The authors wish to thank SSFM Engineers, Inc. for their support and the use of their computer facilities. Special thanks are extended to Chad Cadiente for his assistance with CAD drafting of many of the figures in this report.

TABLE OF CONTENTS

LIST OF TABLES

LIST OF FIGURES

CHAPTER 1

INTRODUCTION

INTRODUCTION

1.1 GENERAL

For several decades, the reinforced concrete flat-plate structure has been one of the most economical structural systems. It utilizes simple formwork for construction and requires the least story height for a specified headroom. Because of its simplicity, it remains one of the most widely used slab systems for multistory construction of apartments and hotels [8, 16].

The behavior of flat-plate structures under gravity loads has been studied extensively. Empirical design methods such as the ACI Direct Design method and Equivalent Frame method have been developed to facilitate member design [25].

Under combined gravity and lateral loading, the behavior of flat-plate structures becomes more complex. Two common analytical models used to represent flat-plate structures under combined gravity and lateral loads are the effective beam width model and the equivalent frame model recommended by the ACI code [4].

The ability of these models to produce reasonable estimates of member actions and lateral drift when subjected to combined gravity and lateral loading depends on the assumed member stiffnesses. Due to a lack of comparisons between experimental data and analytical results on member actions and drift, current assumptions regarding member stiffnesses are only rough estimates. The engineer is in need of a rational approach to determine each member's stiffness. The purpose of this study will be to address the issue of estimating each member's stiffness under gravity and lateral loads based on a correlation between experimental data and analytical analysis methods.

1.2 STATEMENT OF PROBLEM

Previous research has shown that the effective beam width and equivalent frame models tend to underestimate values of lateral drift under combined gravity and lateral loading [3, 15, 18, 26]. In both methods, a single value for the effective beam width factor, alpha (α), and the stiffness reduction factor to account for cracking, beta (β), are applied throughout the entire length of the slab-beam element. However, a constant α may not adequately represent the differences between interior and exterior connection behavior. In addition, applying a constant β value does not account for the fact that portions of the slab-beam may be more severely cracked than others. This may result in unreliable estimates of drift, and incorrect moment distribution along the span. Adjustment of the α and β values along the design span may result in a better estimate of actual member stiffness under combined gravity and lateral loading.

1.3 RESEARCH OBJECTIVES

Alpha (α) and β values suggested by past researchers [3, 7, 10, 18, 23, 28] are rough estimates based on analytical studies and limited experimental observations [9, 12, 13, 19, 21]. In this study, the effective beam width and equivalent frame methods are applied to two identical experimental concrete flat-plate specimens previously tested by Kirk and Scavuzzo [27]. The effective beam width method is also applied to an experimental concrete flat-plate specimen previously tested by Hwang and Moehle [14]. Analysis of the three-dimensional Moehle specimen is performed using the effective beam width method only, since the equivalent frame method is limited to two-dimensional frame analysis. The

models are analyzed using the ETABS [11] analysis program. The analytical and experimental results are then compared.

A two-beam model is introduced and applied to the Kirk specimens using both the effective beam width and equivalent frame methods. The two-beam model is applied to the Moehle specimen using only the effective beam width method. The analytical and experimental results are then compared. Recommended α and β values for effective beam width two-beam model analysis are developed. Due to the fact that the three-dimensional Moehle specimen is a more realistic approximation of an actual flat-plate structure, the recommended α and β values are based on the results of the two-beam model analysis of the Moehle specimen only. The results of the two-beam model analysis of the Kirk specimens are used to verify the recommended α and β values.

CHAPTER 2

ANALYTICAL METHODS

ANALYTICAL METHODS

2.1 EFFECTIVE BEAM WIDTH METHOD

The effective beam width method may be applied to two- and three-dimensional flat-plate frames (Figure 1). The columns are represented directly using actual dimensions. The slab is modeled as individual beams spanning between the columns. Each beam has an effective width equal to the centerline-to-centerline slab width, l_2, multiplied by an effective width factor, α. The beam depth is equal to the actual slab depth.

According to Vanderbilt and Corley [28], "the effective width factor α is obtained from the requirement that the stiffness of a prismatic beam of width αl_2 must equal the stiffness of the plate of width l_2." Several analytical procedures for evaluating effective beam width coefficients have been developed and are summarized in their paper [28].

The effective beam width method does have a drawback. Cano and Kingner [5] report that the effective beam width method does not incorporate the effects of moment leakage. The assumption of the effective beam width method is that all moments pass through the slab column connection. However, loaded spans may transfer moment to adjacent spans through the torsional flexibility of the slab on either side of the column.

Much research has focused on the evaluation of the effective beam width factor, α. Unfortunately, the approach taken by researchers has been based on elastic theory, neglecting the effects of cracking. A summary of past research on effective width follows.

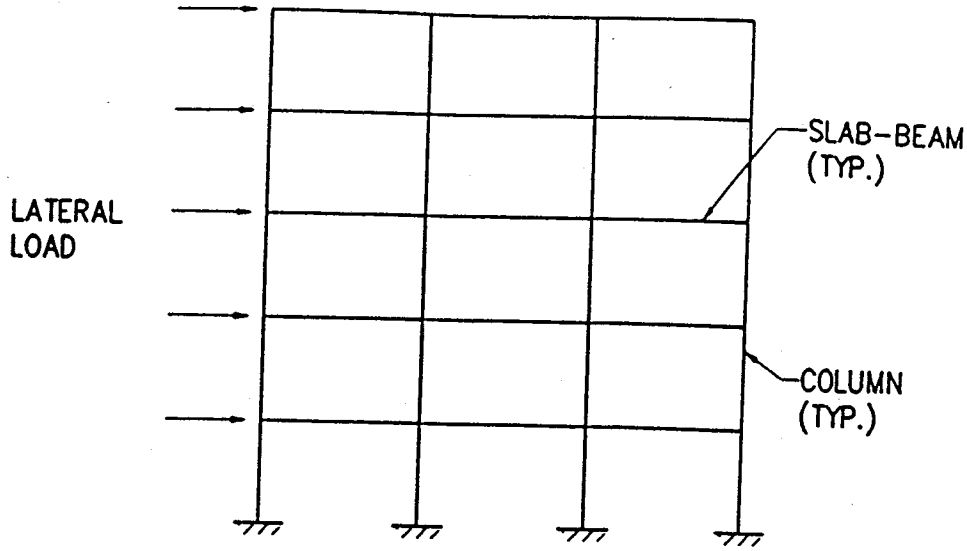

2 - DIMENSIONAL FRAME

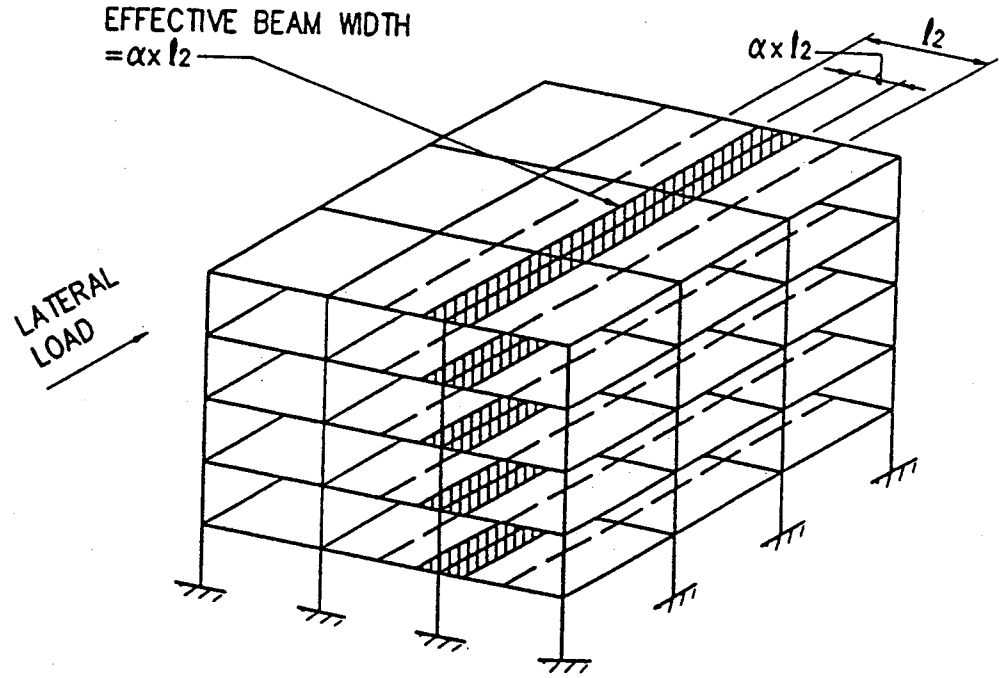

3 - DIMENSIONAL FRAME

Figure 1 Effective Beam Width Model

2.1.1 AALAMI

In 1972, Aalami [1] attempted to represent slab stiffness through the use of a moment-rotation coefficient. To further understand the column-slab stiffness relation, Aalami attempted to evaluate upper and lower limits to the rotational stiffness of a floor plate at the column-slab junction. The rotational stiffness coefficient is used to determine the portion of unbalanced moment transferred to the slab at the column-slab junction. For his study, Aalami assumed elastic behavior of concrete.

In the lower limit, the floor plate is assumed to be uniform and continuous at the column-slab interface; the column adding no additional bending stiffness in this region. The applied bending moment which is used for analysis at the center of the column-slab interface is represented by a linearly varying triangular distribution.

The upper limit is obtained by assuming that the column makes the floor plate infinitely stiff in bending within the column-slab interface, while the region of plate outside this interface is subjected to elastic deformation. Aalami stated that the rotational stiffness of the floor plate at the column-slab interface lies between the upper and lower limits. Aalami [17] then evaluated moment-rotation coefficients for a square plate on a centralized square column using a finite difference method for various relative column sizes, c_1/l_1.

In his study, Aalami does not obtain effective width coefficients essential for flat-plate frame analysis. However, his attempt to evaluate slab moments by the use of moment-rotation coefficients provided useful insight for further effective width research.

2.1.2 PECKNOLD

In 1975, Pecknold [23] attempted to derive a simple expression for the effective width of a typical interior panel of a flat plate structure. Pecknold used elastic plate theory and a standard Levy type solution. Using a rigid column approximation, and equating the slab rotation at the center of the column-slab interface to the rotation of a beam subjected to a concentrated moment, Pecknold was able to obtain effective widths as a function of column size for different slab aspect ratios. A finite element analysis was then used to check the accuracy of the rigid column approximation, resulting in good agreement.

2.1.3 ALLEN AND DARVALL

In 1977, Allen and Darvall [3] derived upper bound effective width coefficients using a rigid column approximation and an analysis similar to that of Pecknold. The effective width coefficients were derived for plates of different aspect ratios, l_1/l_2, column cross section aspect ratios, c_1/c_2, and relative column sizes, c_1/l_1. Experimental values of effective width coefficients were obtained from work carried out on steel and microconcrete plates. Allen and Darvall found the experimental and theoretical values to correlate well. Despite their efforts to determine effective width coefficients for effective beam width analysis, Allen and Darvall failed to account for the effects of cracking on slab stiffness.

2.1.4 MULCAHY AND ROTTER

In 1983, Mulcahy and Rotter [20] discussed the results from their experimental study of slab-column joints in a flat plate structure subjected to lateral loads. Mulcahy and Rotter concluded that the behavior of these joints is complex and nonlinear. Mulcahy and Rotter suggest that the flexible column theory gives a better representation of the slab stiffness

when elastic slab theory is used without regard for cracking. The authors also concluded that the application of elastic isotropic theoretical models to the slab-column joints leads to underestimation of drift in design calculations.

To account for a reduction in lateral load stiffness due to cracking, a stiffness reduction factor, β, is applied to the slab-beam. Beta (β) is defined as the effective moment of inertia of the cracked slab-beam divided by the gross moment of inertia of the slab-beam. Vanderbilt and Corley [28] recommend a β value of 1/3 for the slab-beam, while Moehle and Diebold [18] suggest a value between 1/3 and 1/2.

2.2 EQUIVALENT FRAME METHOD

Developed by Corley and Jirsa [6] for gravity loads, the equivalent frame method adopted by the ACI Code [4] analyzes a three dimensional flat-plate structure as a series of equivalent planar frames (Figure 2). The equivalent planar frames are composed of columns, slab-beams, and transverse torsional members. The transverse torsional members transfer moments from slab-beams to columns.

To further simplify analysis, the transverse torsional members are combined with the columns to create an equivalent column. The three dimensional frame is thus reduced to a series of two dimensional planar frames. The resulting planar frame is composed of slab-beam elements supported by equivalent columns. The stiffness of each equivalent column is a function of both the flexural stiffness of the column, and the torsional stiffness of the slab framing into the column transverse to the direction being analyzed. The torsional stiffness of the transverse slab elements is obtained empirically, while slab-beam and column stiffnesses are calculated using gross section properties.

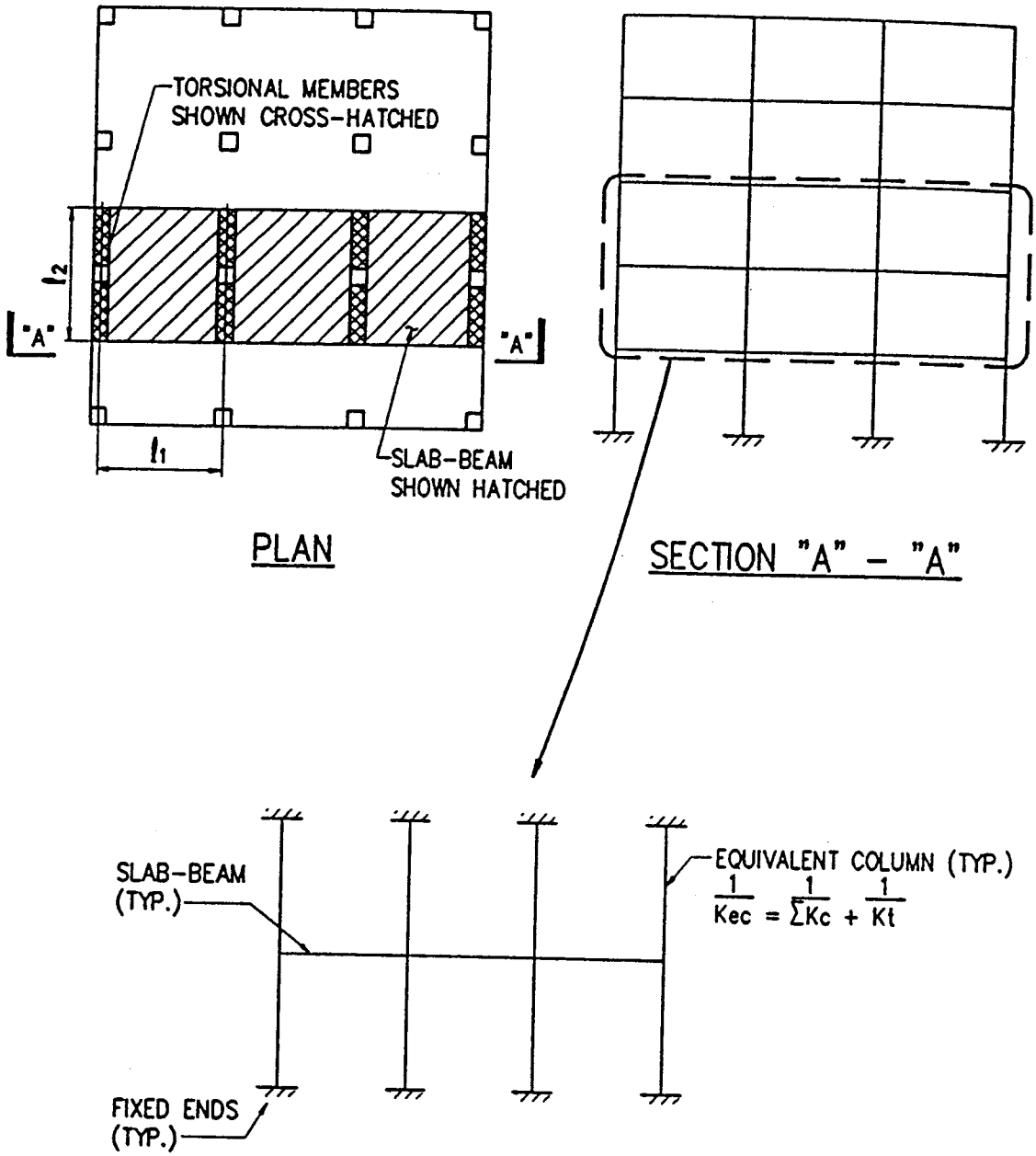

Figure 2 Equivalent Frame Model

The advantage of the equivalent frame method is that it accounts for moment leakage. However, time consuming calculations are required for the computation of the equivalent column stiffness. Problems with the application of the method may occur when analyzing multistory frames. Each column can have only one equivalent stiffness. However, torsional member properties at joints above and below a particular column may differ, resulting in two equivalent column stiffness values for the same column.

For lateral load analysis, the ACI 318-89 Code recommends that to assure lateral drift is not underestimated, cracking of slabs must be considered in stiffness assumptions [4]. To account for cracking, Vanderbilt and Corley [28] recommend a stiffness reduction factor, β, of 1/3 unless a more detailed analysis of cracking is made.

CHAPTER 3

DESCRIPTION OF TEST SPECIMENS

DESCRIPTION OF TEST SPECIMENS

3.1 KIRK SPECIMEN

3.1.1 GENERAL

The Kirk specimen is taken from research performed by Kirk and Scavuzzo [27]. The 1/3 scale specimen models a single floor of a multi-story flat-plate concrete structure. The specimen has one and a half bays in the principal direction of loading, and one bay transverse to the direction of loading. In total, four specimens were tested, each having identical dimensions but differing slab shear reinforcement.

The specimens were used to investigate the effect of shear reinforcement on the strength and ductility of exterior and interior slab-column connections in a flat-plate structure subjected to gravity and lateral loads. Of the four specimens tested, only specimens S-2 and S-4 are used in this study because they produced more complete experimental results.

3.1.2 MODEL DIMENSIONS

Development of the Kirk specimen is shown in Figure 3. The complete model is shown in Figure 4. The slab has a thickness of 2.5 in. (63.5 mm), and is 79 in. (2007 mm) wide by 118.5 in. (3010 mm) long. The length of the exterior bay, spanning from the centerline of the exterior column to the centerline of the interior column, is 76 in. (1930 mm). The length of the interior half bay measures 39.5 in. (1003 mm) from the centerline of the interior column to the edge of slab. The exterior column is 4x6 in. (102x152 mm) with the 6 in. (152 mm) dimension parallel to the direction of loading. The interior column

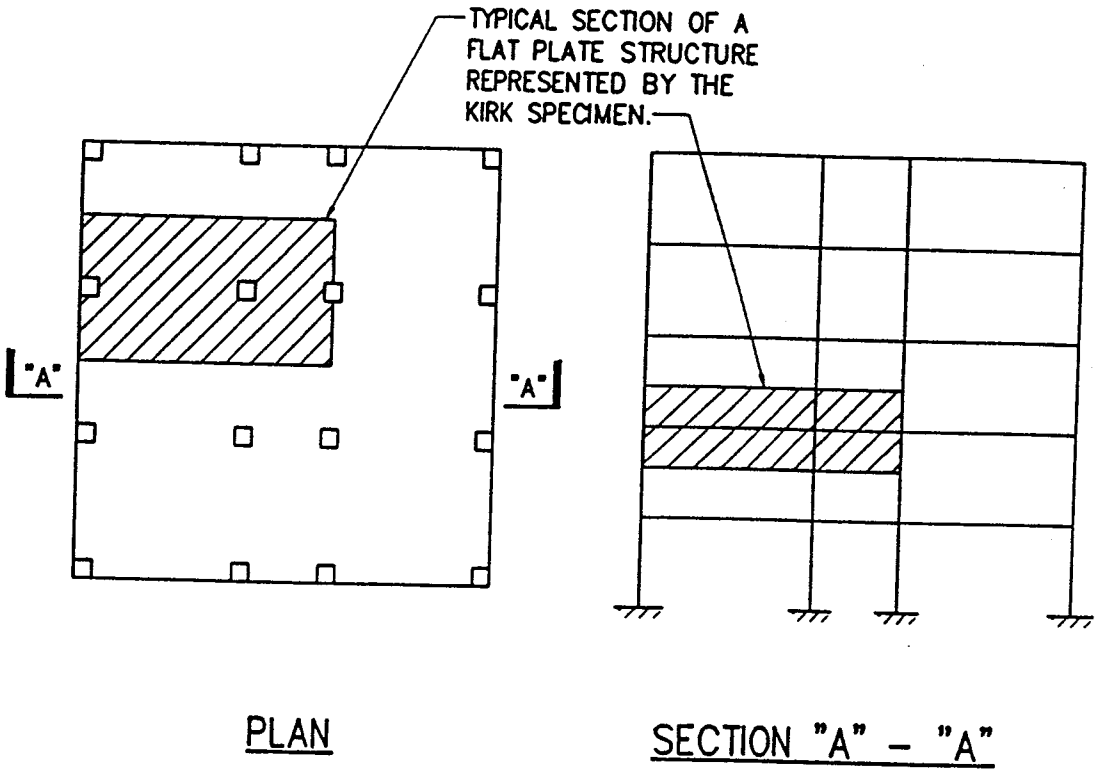

Figure 3 Development Of Kirk Specimen

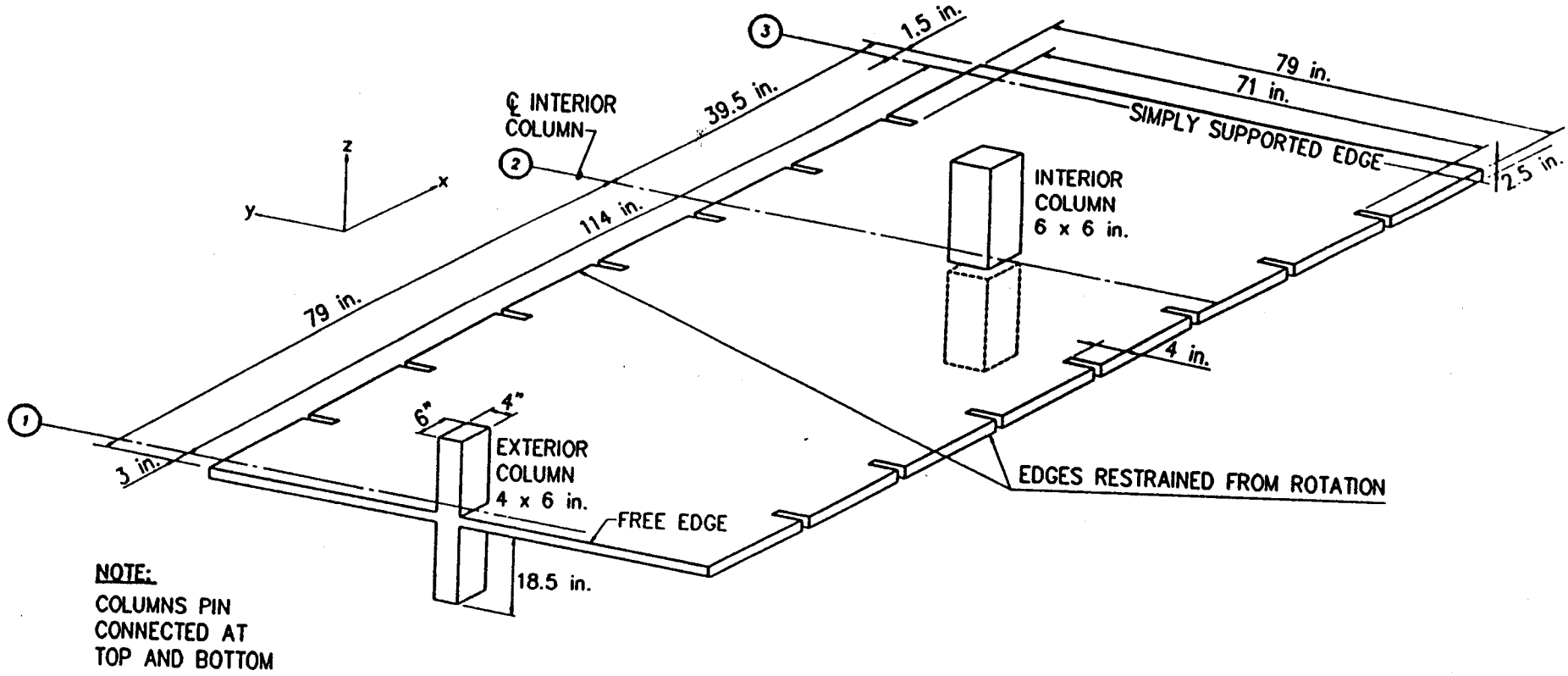

Figure 4 Kirk Specimen

2. A service gravity load of 47 psf (2.25 kPa) was applied to the interior span, while the exterior span was subjected to a service gravity load of 140 psf (6.70 kPa).

3. A service gravity load of 140 psf (6.70 kPa) was again applied on both spans. The specimens were then subjected to four cycles of increasing lateral loading reaching a maximum of 2600 pounds (11.6 kN).

Further gravity load tests were carried out to observe ultimate strength capacity, but did not include any application of lateral loading.

In their paper summarizing the test program, Pillai, Kirk, and Scavuzzo [24] report that the actual slab load measured by the reactions on the load cells was less than the applied 140 psf (6.72 kPa). The discrepancy was believed to be caused by the coarse graduation of the load cells and friction in the system.

In order to obtain the "actual" slab load applied, the summation of vertical reactions was divided by an effective slab area of 114 in. x 71 in (2896x1803 mm). These "actual" slab loads are used in this study.

3.2 MOEHLE SPECIMEN

3.2.1 GENERAL

The Moehle specimen is taken from research performed by Hwang and Moehle [14]. The four tenths scale specimen models a portion of a typical flat-plate floor of an intermediate story of a multi-story office building.

The specimen was used to investigate the lateral load stiffness of reinforced concrete slab-column framing, to study various analytical techniques for modeling the elastic

stiffness and strength of flat-plates, and to study the effectiveness of slab-edge reinforcing details. Other studies were carried out which are outlined in their report.

3.2.2 MODEL DIMENSIONS

The prototype of the Moehle specimen is shown in Figure 5. The complete specimen is shown in Figure 6. The specimen has three bays in each direction. Center to center spans in the North-South and East-West directions measured 72 in. (1829 mm) and 108 in. (2743 mm) respectively. The panel aspect ratio of 1.5:1 was selected based on practical dimensions for flat-plate construction. The slab thickness is 3.2 in. (81 mm). The columns extend four feet (1219 mm) below the slab soffit. The specimen has both square and rectangular columns with sizes shown in Figure 6 (1 in. = 25.4 mm). The variety of column sizes were chosen to study the effects of column rectangularity.

3.2.3 INSTRUMENTATION AND BOUNDARY CONDITIONS

Each column was pinned at its base and connected to a tripod reaction transducer which measured column shear and axial load. Lateral drift at slab mid-depth was measured using four horizontal displacement transducers in each direction. Two of the transducers were dial gages used to measure the imposed lateral drift. The remaining two transducers were used to monitor lateral load-drift behaviors. Slab vertical deflections and slab-column rotations were measured using dial gages attached to an overslab grid.

3.2.4 CONCRETE STRENGTH

The mean compressive strength of the precast columns was 4980 psi (34.3 MPa). The mean compressive strength of the slab was 3160 psi (21.8 MPa).

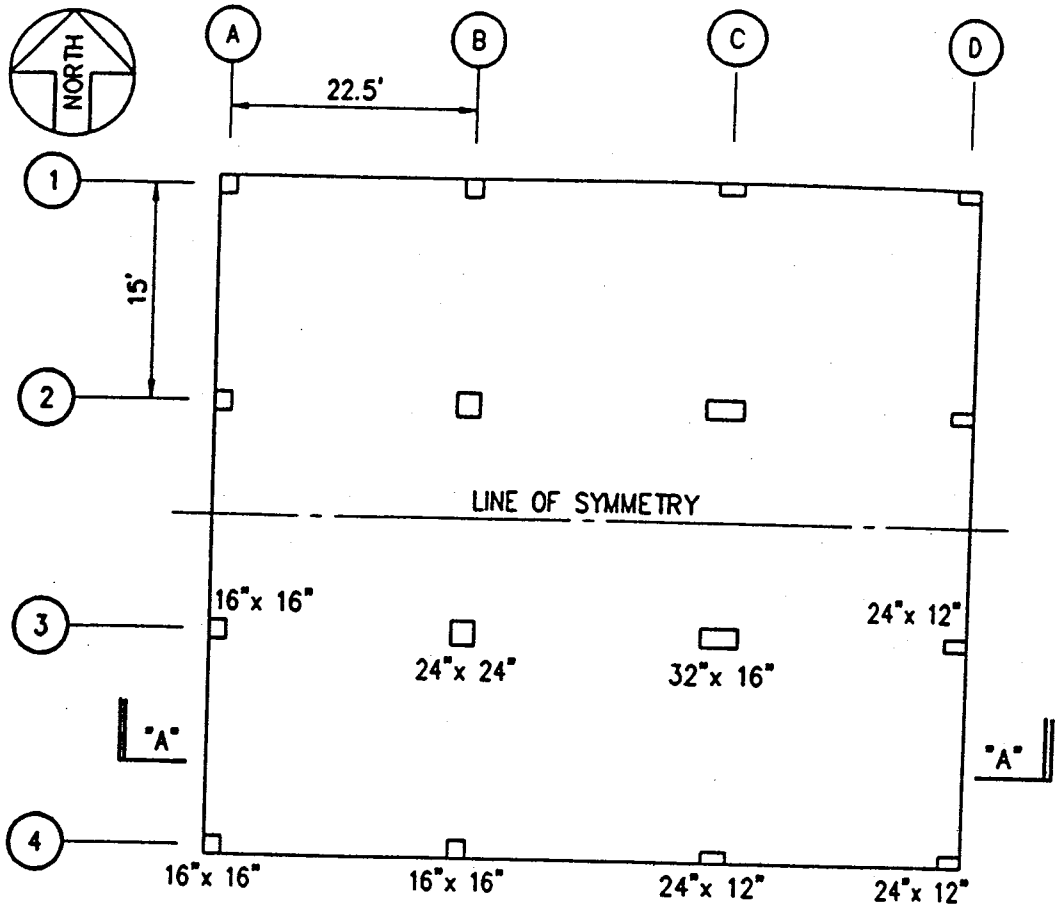

PLAN

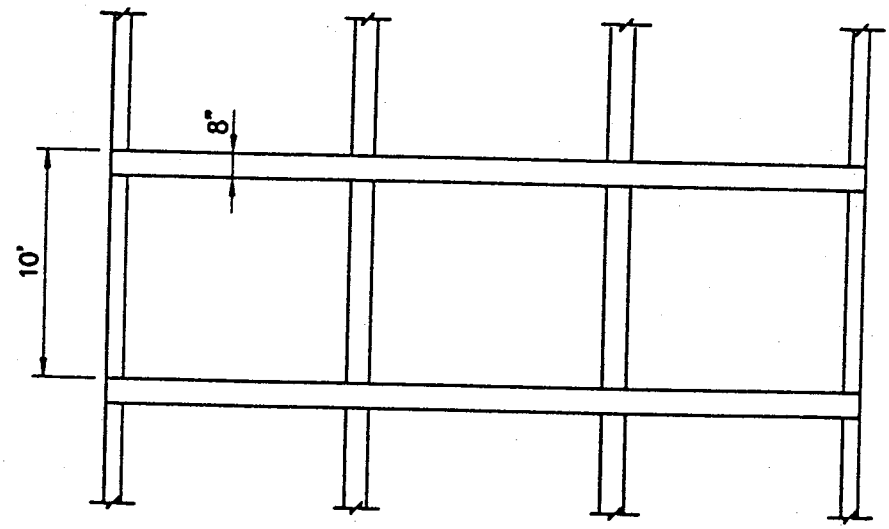

SECTION "A" – "A"

Figure 5 Prototype of Moehle Specimen

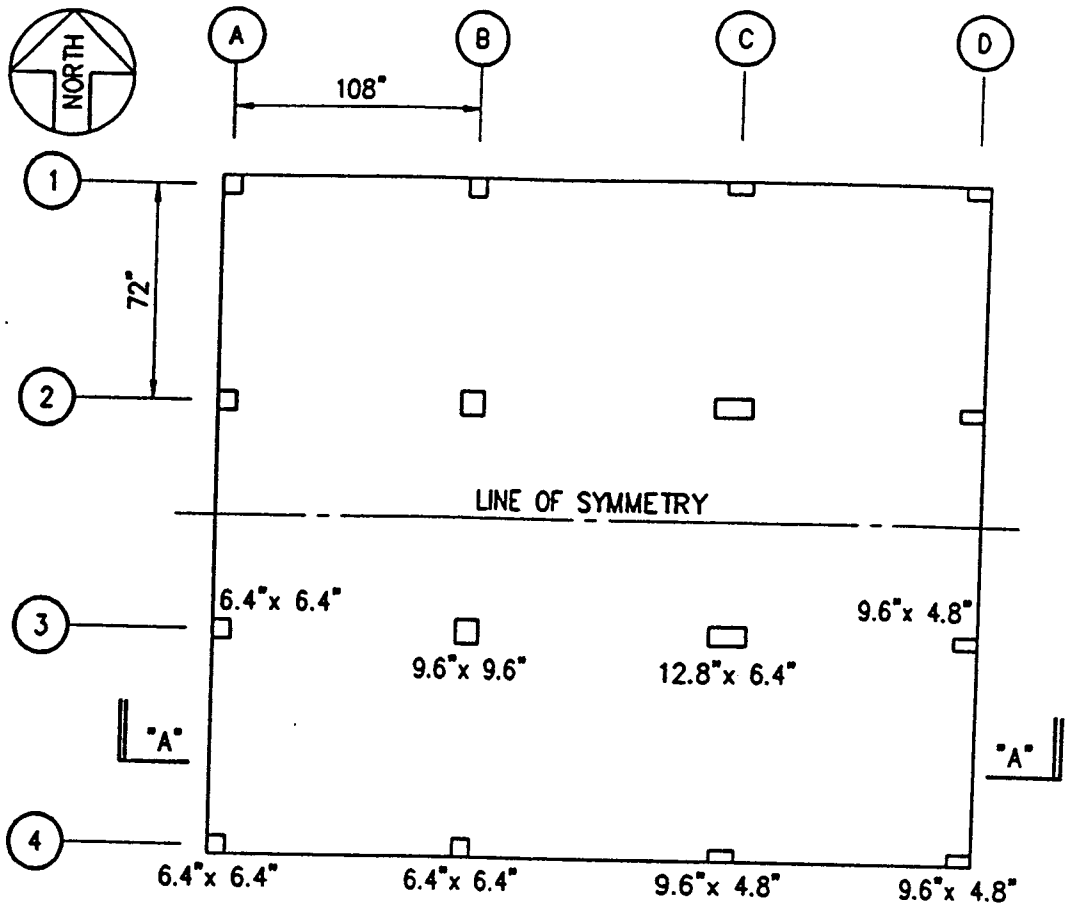

PLAN

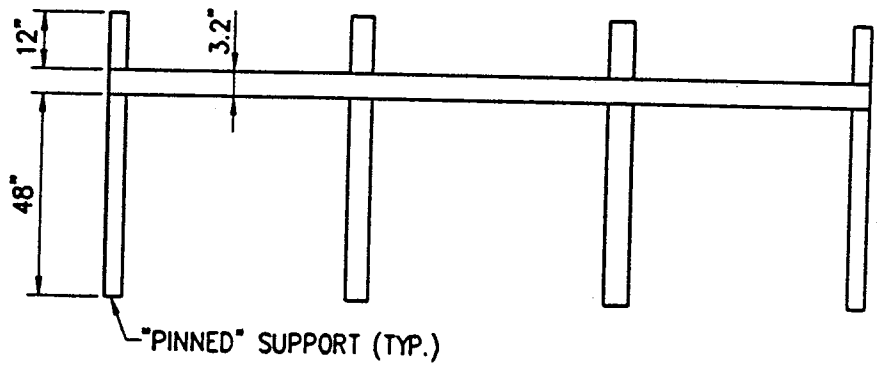

SECTION "A" – "A"

Figure 6 Moehle Specimen

3.2.5 LOADING

Gravity loading of the specimen was accomplished using lead weights placed uniformly over the slab in two layers resulting in a uniform load of 78 psf (3.73 kPa). The load of the lead weights plus the self weight of the slab totalled 118 psf (5.65 kPa).

The lateral load was applied at slab mid-depth in both directions using four reversible hydraulic actuators supported on reaction frames. The specimen was subjected to the following loading sequence:

1. Lateral loads were applied in turn in the North-South and East-West directions. The gravity load consisted of slab self-weight only (40 psf) (1.91 kPa). Maximum interstory drift was 1/800.
2. Lead weights were added to the slab producing a uniform gravity load of 78 psf (3.73 kPa). Total gravity load including slab self-weight was 118 psf (5.65 kPa). No lateral load was applied.
3. With the lead weights in place, lateral loads were again applied in each of the North-South and East-West directions with a maximum interstory drift of 1/800.
4. To approximate the effects of construction loads, an additional gravity load of 55 psf (2.63 kPa) was applied to each panel, one panel at a time.
5. After the application and removal of the construction load, lateral load tests described under (3) were repeated.

6. With the lead weights still in place, a series of lateral load tests were applied with increasing lateral drifts. At four percent drift, failure of some of the connections occurred.

CHAPTER 4

DESCRIPTION OF ANALYSIS

DESCRIPTION OF ANALYSIS

4.1 ETABS ANALYSIS PROGRAM

As part of this thesis research, analysis of the Kirk and Moehle specimens was performed using the ETABS analysis program [11]. ETABS is a three dimensional finite-element computer analysis program which simplifies three dimensional analysis of building systems by assuming that the floor slab is a rigid diaphragm. The ETABS input files were created using the graphical input file generator, ETABSIN. The specimens were modelled as closely as possible to actual test conditions.

For the Kirk model, the columns at the exterior and interior connections above and below the slab were "pinned". The support at the free edge of the interior span was modelled using a 2 inch (50 mm) square steel column "pinned" at the top and bottom, shown as the rigid link in Figure 7, which is a representation of the Kirk model.

For the Moehle model, all of the columns were "pinned" at the base. The column stubs above the slab were not included in the model. Figure 8 is a representation of the Moehle model.

4.2 BASIS FOR ANALYTICAL AND EXPERIMENTAL COMPARISON

The comparison between experimental and analytical results was made using the following two quantities:

1) Lateral drift

2) The column moment at the center of the slab-column connection

Both of these quantities were readily available from the experimental data reported for the two test programs. In addition, the centerline column moments due to lateral loads are an

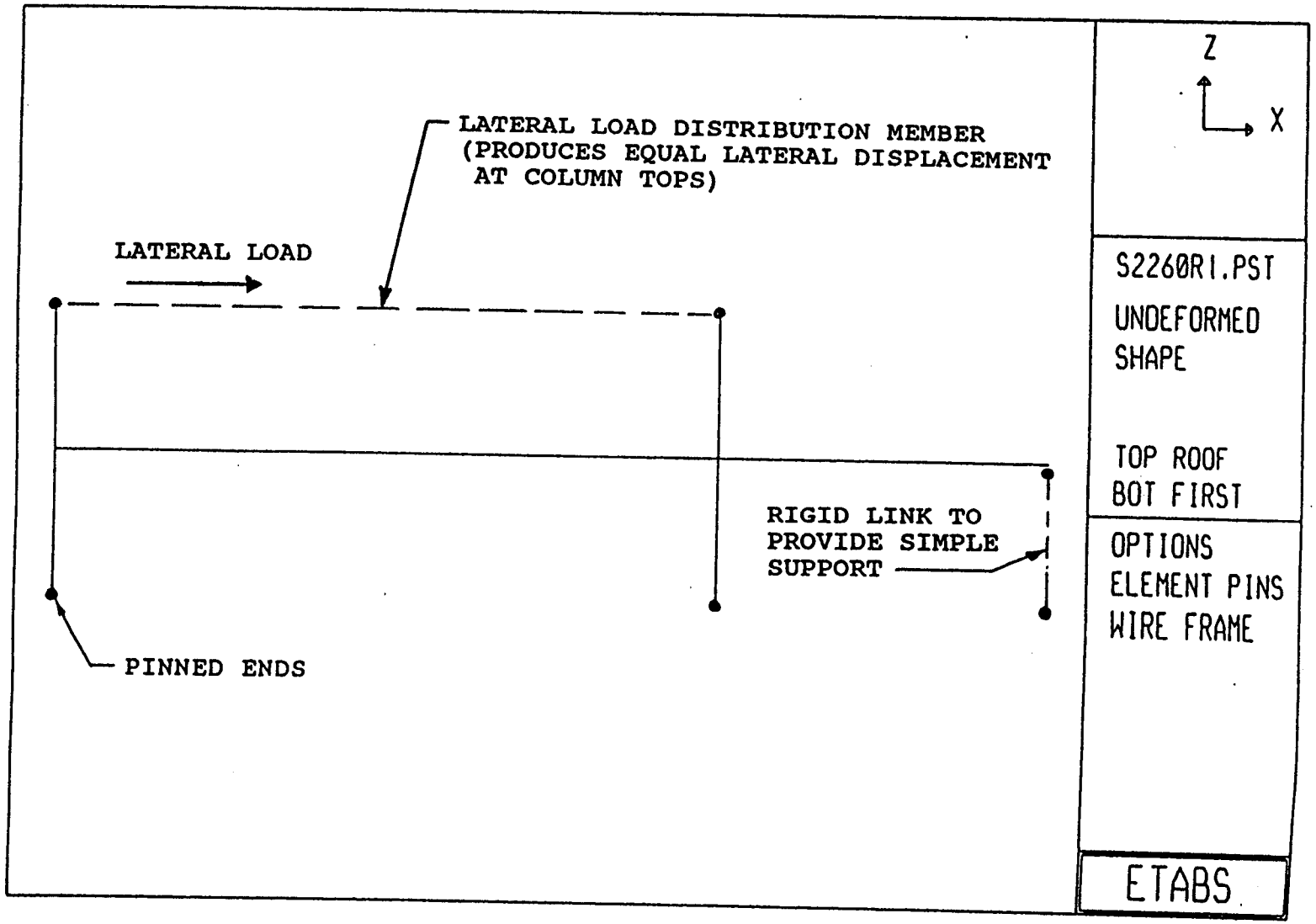

Figure 7 Kirk Model

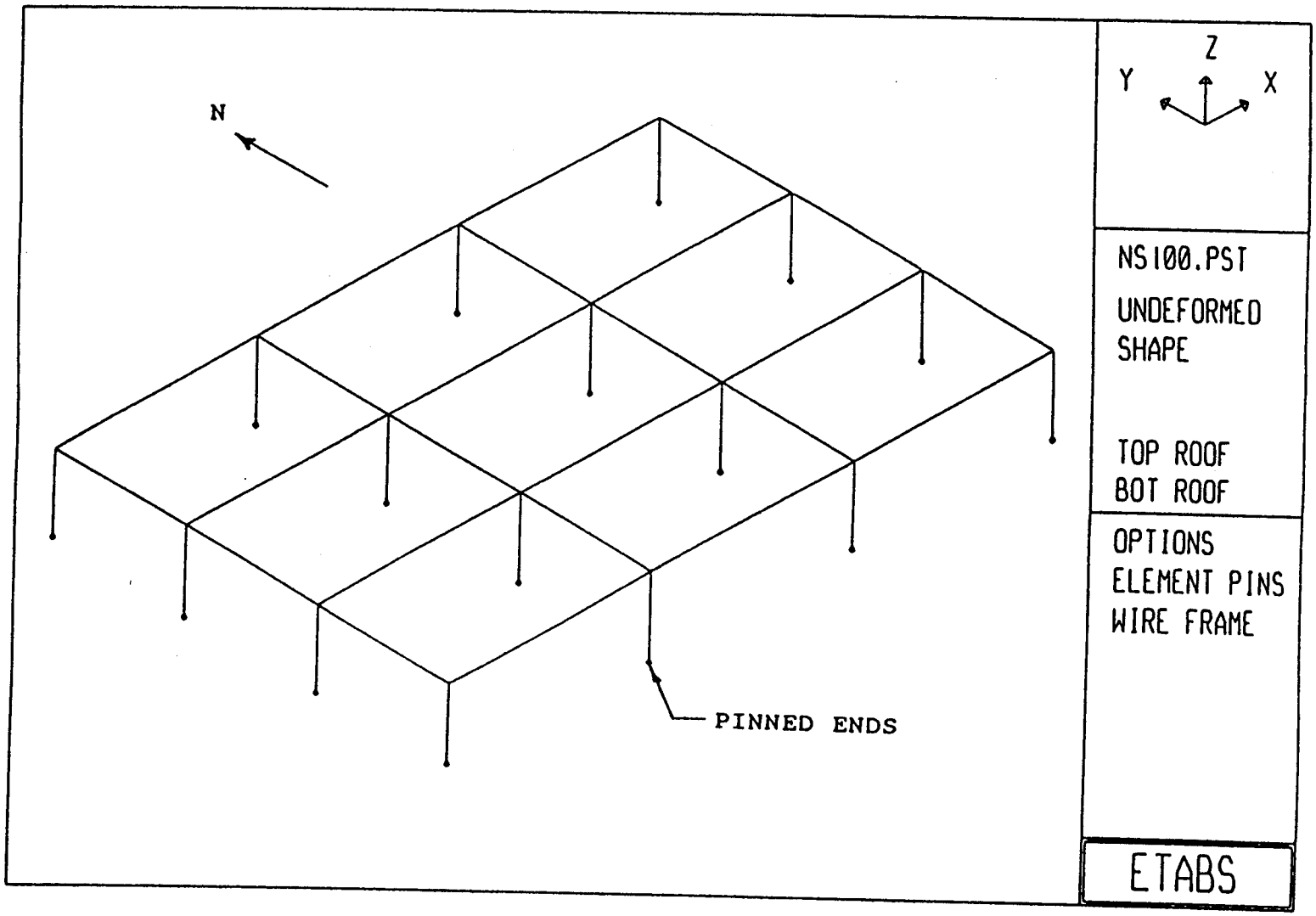

Figure 8 Moehle Model

important input requirement for computer programs such as PCACOL [22] and ADOSS [2], which design the column and slab elements of the structural frame.

4.3 APPLICATION OF ANALYTICAL METHODS TO KIRK SPECIMENS

Experimental specimen column reactions and specimen drift were readily obtained from the Masters thesis by Scavuzzo [27]. By multiplying the top and bottom column horizontal reactions by 20 inches (508 mm) (distance from center of slab to column pin) and summing the two values, the experimental moment at the centerline of the interior and exterior slab-column connections were obtained.

Due to experimental error, the summation of the experimental column reactions did not equal the applied lateral load. To obtain equilibrium, the experimental moments at the exterior and interior connections were increased by the ratio of the sum of the analytical moments over the sum of the experimental moments at the interior and exterior connections.

The lateral drift of the test specimen was based on the horizontal displacement of the exterior column. Two dial gages were located 14.5 inches (368 mm) above and below the slab on the exterior column, with a total distance of 31.5 inches (800 mm) between them. The experimental specimen drift was calculated by taking the difference of these two dial gage readings and dividing by the distance between them.

4.3.1 EFFECTIVE BEAM WIDTH METHOD APPLIED TO KIRK SPECIMENS

The effective beam width method was applied to specimens S-2 and S-4 following the procedure described in section 2.1. Each specimen was analyzed under three lateral loads, corresponding to the lateral loads applied during the experimental tests.

Specimen S-2 was analyzed under lateral loads of 1.260 kips, 2.205 kips, and 2.600 kips (5.60 kN, 9.81 kN, and 11.56 kN resp.). Specimen S-4 was analyzed under lateral loads of 1.313 kips, 1.970 kips, and 2.600 kips (5.84 kN, 8.76 kN, and 11.56 kN resp.). The gravity loads used for each analysis varied, as described in section 3.1.5.

For the initial model analysis (labeled Run 1), a lower bound effective width factor of 0.4, obtained from the report by Pecknold [23], was used. No allowance was made for cracking ($\beta = 1.0$). This resulted in a slab effective width of 28.4 inches.

A second analysis (labeled Run 2) was performed using an effective width of 0.4 and a β factor of 0.33, as suggested by Vanderbilt and Corley [28] to account for slab cracking. This β value was applied to the entire length of each span and resulted in a reduced slab effective width of 9.4 inches (239 mm). The results of these analyses are compared with the experimental results in section 4.4.2.

4.3.2 EQUIVALENT FRAME METHOD APPLIED TO KIRK SPECIMENS

The equivalent frame method was applied to specimens S-2 and S-4 following the procedures described in section 2.2. To model the equivalent columns, the actual column dimensions were used but the concrete modulus was reduced by a factor of K_{ec}/K_c to produce a resultant column stiffness equal to the required equivalent column. Kec is the stiffness of the equivalent column while K_c is the stiffness of the actual column.

Both specimens were analyzed under the gravity and lateral loading conditions described previously. The initial model analysis (labeled Run 1) was performed using

α = 1.0 and ignoring slab cracking (β = 1.0). A second analysis (labeled Run 2) was performed including cracking of the slab by using β = 0.33 throughout each beam element. The analytical results are compared with the experimental results in section 4.4.3.

4.4 ANALYTICAL VS. EXPERIMENTAL RESULTS FOR KIRK SPECIMENS

4.4.1 PRESENTATION OF RESULTS

The analytical results obtained from the analysis of the Kirk specimens are compared with the experimental results in tables 1 through 24. Each table lists the results of two analyses, labeled Run 1 and Run 2. Run 3 represents a two-beam model analysis described later in CHAPTER 5. At the top of each table is a heading describing the analysis.

When the Kirk specimens are analyzed using the effective beam width method, Run 1 is the analysis of the analytical model using α = 0.4 and β = 1.0 throughout each span. Run 2 is the analysis of the analytical model using α = 0.4 and β = 0.33 throughout each span.

When the Kirk specimens are analyzed using the equivalent frame method, Run 1 is the analysis of the model using α = 1.0 and β = 1.0. Run 2 is the analysis of the analytical model using α = 1.0 and β = 0.33.

For each "Run", the first column in the table titled CONNECTION lists the connection at which the moment is located. The location of the exterior and interior connections are shown in Figure 4. The second column titled ACTUAL MOMENT lists the experimental moment values, while the third column titled ETABS MOMENT lists the moments obtained from the analytical model.

The fourth column titled ETABS M/ACTUAL M lists the ratio of the analytical moment over the experimental moment for the exterior and interior connections. The average ratio of both connections is listed at the bottom of the column.

The fifth column titled % ERROR lists the percent error of the analytical moment as compared to the experimental moment. The percent error is defined as the absolute value of the quantity ((ETABS M/ACTUAL M - 1.0) x 100). The average percent error of moments at both connections is listed at the bottom of the column. This average error is used for comparison of the results of the various computer Runs. It should be noted that some connections may experience greater or smaller moment errors as listed in the table.

Below the results table is a listing of the alpha and beta values used in each span. See Figure 4 and Figure 7 for span locations.

At the bottom of each table is a listing of the ACTUAL DRIFT obtained from the experimental test, and the ETABS DRIFT obtained from the analytical model. Both values are listed as percent drift defined as ((lateral column displacement/column height)x100).

4.4.2 EFFECTIVE BEAM WIDTH MODEL

Tables 1, 3 and 5 list the analytical vs. experimental results for specimen S-2 for the three vertical and lateral loading conditions.

Under all three vertical and lateral loading conditions, the analytical results obtained from Run 1 showed that the effective beam width model underestimated the experimental moments at the exterior connection, and overestimated the experimental moments at the interior connection. The average error between analytical and experimental results varied

from 32% to 175%. The results also showed a significant underestimation of experimental drift.

The analytical results obtained from Run 2 showed the same trends observed in Run 1 under all three vertical and lateral loading conditions. The average error varied from 37% to over 200%. However, the results showed a slight overestimation of experimental drift.

Tables 7, 9 and 11 list the analytical vs. experimental results for specimen S-4 for the three vertical and lateral loading conditions. The same trends identified in specimen S-2 were observed for specimen S-4.

4.4.3 EQUIVALENT FRAME METHOD

Tables 13, 15 and 17 list the analytical vs. experimental results for specimen S-2 for the three vertical and lateral loading conditions.

Under all three vertical and lateral loading conditions, the analytical results obtained from Run 1 (with $\beta = 1.0$) showed an underestimation of lateral drift. However, moments at the connections compared well with the experimental results. The average error between analytical and experimental results varied from 5% to 15%.

The analytical results obtained from Run 2 (with $\beta = 0.33$ for cracking) under all three vertical and lateral loading conditions showed an improved estimation of lateral drift, with respect to Run 1. However, analytical moments at the exterior and interior connections deviated further from experimental results, with the exterior connection experiencing a smaller moment and the interior connection experiencing a larger moment than observed in the experimental specimens. The average error between analytical and experimental results varied from 16% to 108%.

Tables 19, 21 and 23 list the analytical vs. experimental results for specimen S-4 for the three vertical and lateral loading conditions. The same trends identified in specimen S-2 were observed for specimen S-4.

4.5 APPLICATION OF ANALYTICAL METHODS TO MOEHLE SPECIMEN

The Moehle specimen was analyzed using a three- dimensional analytical model. The equivalent frame method is limited to two-dimensional analysis only as described in section 2.2. For this reason, only the effective beam width method was applied to the Moehle specimen.

Experimental specimen column moments and specimen drift were readily obtained from the report by Hwang and Moehle [14]. The experimental moment at each connection was the product of the measured base shear and the distance from slab mid-depth to column pin of 49.6 inches (1260 mm).

Unfortunately, the experimental column moments excluded gravity load effects and therefore needed adjustment. Gravity loading causes a reduction in stiffness at the slab-column connections. The reduction in stiffness causes a portion of the column moment to be redistributed to the slab-beam, resulting in a reduced column base shear.

The only gravity load column base shear results available from the report by Hwang and Moehle [14] were measured after test EW400. Test EW400 was a test performed in the final loading sequence as described in section 3.2.5. In test EW400, the specimen was subjected to an average lateral load of 10.9 kips (48.5 kN) corresponding to a lateral drift of 0.25% in the East-West direction.

In order to approximate the reduction in base shear due to gravity loading, it was assumed that the gravity load column base shears from test EW400 be reduced by 15% for application to the 0.5% drift case, and by 25% for application to the 1.0% case.

To further simplify application of the gravity load effects, reduced gravity load column base shear values from column groups were averaged, and the average value applied to each column in the group. The four column groups were as follows (see Figure 6 for column locations):

1) A1, A4, D1, D4

2) B1, C1, B4, C4

3) A2, A3, D2, D3

4) B2, B3, C2, C3

The resulting gravity load column base shear at each column was then multiplied by 49.6 inches (1260 mm) and added to the lateral load moment at each column.

Adjustment was also made to the experimental column moments along gridlines 1 and 2 for analysis in the North-South direction at 0.5% and 1.0% drift.

In the design of the experimental specimen, the connections along gridlines 3 and 4 were designed for the shears and moments conforming to the ACI 318-83 Code. Along gridlines 1 and 2, a redistribution of moments between the connections was assumed. This assumption reduced the negative moments at the connections and transferred them to the positive moment regions of the slab-beams.

An estimate of the moments which might have occurred at the connections along gridlines 1 and 2 had the specimen been designed without redistribution of negative

moments was made. The experimental column moments adjusted for gravity load effects at the connections along gridlines 3 and 4 were obtained from the application of lateral load in the North direction. These moments were applied to the columns along gridlines 2 and 1 respectively. Since the lateral load applied in the South direction was larger than that applied in the North direction, the moments were factored up by the ratio of the lateral load applied in the South direction divided by the lateral load applied in the North direction. The adjustment was done for the 0.5% and 1.0% drift cases.

The experimental specimen drift was defined as the lateral deflection of the slab divided by the column clear height of 48 inches (1219 mm).

4.5.1 EFFECTIVE BEAM WIDTH METHOD APPLIED TO MOEHLE SPECIMEN

The effective beam width method was applied to the Moehle specimen in the North-South and East-West directions, following the procedures described in section 2.1. The specimen was analyzed under lateral loads corresponding to the lateral loads applied during the experimental tests.

In the North-South direction, the specimen was analyzed under lateral loads of 15.15 kips (67.39 kN) and 23.74 kips (105.6 kN) applied in a Southerly direction. These loads corresponded to 0.5% drift and 1.0% drift respectively. In the East-West direction, the specimen was analyzed under lateral loads of 17.93 kips (79.75 kN) and 24.93 kips (110.9 kN) applied in a Westerly direction. These loads corresponded to 0.5% and 1.0% drift respectively. The gravity load for each analysis was described in section 3.2.5.

For the initial model analysis (labeled Run 1) in both the North-South and East-West directions, a lower bound effective width factor α of 0.4 obtained from the report by Pecknold [23] was applied to the entire length of each span in the direction of analysis. No allowance was made for cracking ($\beta = 1.0$). An α value of 0.4 was applied to the entire length of each span transverse to the direction of analysis, with no allowance made for cracking ($\beta = 1.0$).

A second analysis (labeled Run 2) was performed in the North-South and East-West directions using $\alpha = 0.4$ and $\beta = 0.33$ as suggested by Vanderbilt and Corley [28] to account for slab cracking. This β value was applied to the entire length of each span in the direction of analysis. Again, an α value of 0.4 was applied to the entire length of each span transverse to the direction of analysis, with no allowance made for cracking.

4.6 ANALYTICAL VS. EXPERIMENTAL RESULTS FOR MOEHLE SPECIMEN

4.6.1 PRESENTATION OF RESULTS

The results obtained from the analysis of the Moehle specimen are listed along with the experimental results in tables 25 through 36. At the top of each table is a heading describing the analysis. Run 1 is the analysis of the Moehle specimen using $\alpha = 0.4$ and $\beta = 1.0$ throughout each span, in the direction of analysis. Run 2 is the analysis of the specimen using $\alpha = 0.4$ and $\beta = 0.33$ throughout each span in the direction of analysis.

For each Run, the first column in the table titled CONNECTION lists the connection at which the moment is taken. The location of each connection is referenced from the gridline layout in Figure 6.

The second column titled ACTUAL MOMENT lists the experimental moments, while the third column titled ETABS MOMENT lists the moments obtained from the analytical model.

The fourth column titled ETABS M/ACTUAL M lists the ratio of the analytical moment over the experimental moment for each connection. The average ratio of the ETABS M/ACTUAL M for the four connections along each gridline are listed at the bottom of each gridline subsection. The total average ratio of the ETABS M/ACTUAL M for all connections is listed at the bottom of the column.

The fifth column lists the percent error of the column group along each gridline. The percent error of each column is defined as ((ETABS M/ACTUAL M) - 1.0) x 100. The percent error of the column group is the sum of the percent error of each column in the group, divided by 4. The total average percent error for the four column groups is listed at the bottom of column five.

Near the bottom of each table is a listing of the alpha and beta values used for each of the three spans (Figure 6).

Finally, at the bottom of each table is a listing of the ACTUAL DRIFT obtained from the experimental test, and the ETABS DRIFT obtained form the analytical model. Both values are listed as percent drift.

4.6.2 COMPARISON OF RESULTS IN THE NORTH-SOUTH DIRECTION

Tables 25 and 26 list the results from Runs 1 and 2 respectively in the North-South direction under a lateral load of 15.15 kips (67.39 kN)(corresponding to 0.5% drift of the experimental specimen).

The results from Run 1 show that the analytical model overestimated the moments at the exterior connections along gridlines 1 and 4. The analytical moments along gridlines 2 and 3 compared well with the experimental results, but were slightly lower on average. The analytical drift of 0.24% significantly underestimated the lateral drift of 0.5%.

The results from Run 2 showed an improved correlation between analytical and experimental moments at the exterior connections along gridline 1 with respect to Run 1. However, the analytical model further overestimated the moments at the exterior connections along gridline 4. As in Run 1, the analytical moments along gridlines 2 and 3 compared well with the experimental results, but were slightly lower on average. The analytical drift improved, matching the experimental drift of 0.5%.

Tables 28 and 29 list the results from Runs 1 and 2 respectively in the North-South direction under a lateral load of 23.74 kips (105.6 kN)(corresponding to 1.0% drift of the experimental specimen).

The results from Run 1 show that the analytical model overestimated the moments at the exterior connections along gridlines 1 and 4. The analytical model slightly underestimated the moments along gridlines 2 and 3, while analytical drift of 0.37% severely underestimated the lateral drift of 1.0%.

The same trends observed in Run 1 were observed in Run 2. However, the analytical drift improved to 0.79%, but was still significantly less than the experimental drift of 1.0%.

4.6.3 COMPARISON OF RESULTS IN THE EAST-WEST DIRECTION

Tables 31 and 32 list the results from Runs 1 and 2 respectively in the East-West direction under a lateral load of 17.93 kips (79.75 kN)(corresponding to 0.5% drift of the experimental specimen).

In Run 1, analytical moments were well below the experimental moments along gridline D; the first exterior connections in the direction of analysis. Analytical moments showed an improved correlation with experimental moments along gridlines C and B, while the analytical moments were much greater than the experimental moments along gridline A. The analytical drift of 0.43% compared well with the experimental, but remained below the actual drift of 0.5%.

The same trends observed in Run 1 were observed in Run 2. However, the analytical drift of 1.14% overestimated the experimental drift by over 100%.

Tables 34 and 35 list the results from Runs 1 and 2 respectively in the East-West direction under a lateral load of 24.93 kips (110.9 kN)(corresponding to 1.0% drift of the experimental specimen).

As in the 0.5% drift case, analytical moments from Run 1 along gridline D were well below the experimental moments. Analytical moments showed good correlation with experimental moments along gridlines B and C, while the analytical moments were greater than the experimental moments along gridline A. The analytical drift of 0.70% underestimated the experimental drift by 30%.

The same trends observed in Run 1 were observed in Run 2. However, the analytical drift of 1.57% overestimated the experimental drift by over 50%.

TWO-BEAM MODEL

5.1 GENERAL

Chapter 4 summarized the results of the effective beam width and equivalent frame method applied to the Kirk specimens. It also summarized the results of the effective beam width method applied to the Moehle specimen.

In general, the effective beam width method applied without cracking effects (β = 1.0) was observed to underestimate lateral drift. It also did not accurately predict the slab-column moments at the connections. When the effective beam width method was applied with cracking effects (β = 0.33), it slightly overestimated lateral drift. The effective beam width method's prediction of slab-column moments at the connections was again inaccurate.

The equivalent frame method (applied to Kirk specimens only) gave a good prediction of slab-column moments at the connections. However, it underestimated lateral drift. When the equivalent frame method was applied with cracking effects (β = 0.33), prediction of slab-column moments at the connections worsened, while prediction of lateral drift improved.

In order to improve the accuracy of predicted slab-column moments at the connections, and lateral drift, the behavior of flat-plate specimens under vertical and lateral loads must be examined. Under vertical loads only, the moment diagram for the slab-beam elements of a typical three-bay frame is shown in Figure 9. In the same figure, the moment diagram for the slab-beam elements under lateral load only is also shown. Under actual loading conditions, the effects of vertical and lateral loading are combined resulting in the final moment diagram shown in Figure 9. The combined loading moment diagram displays

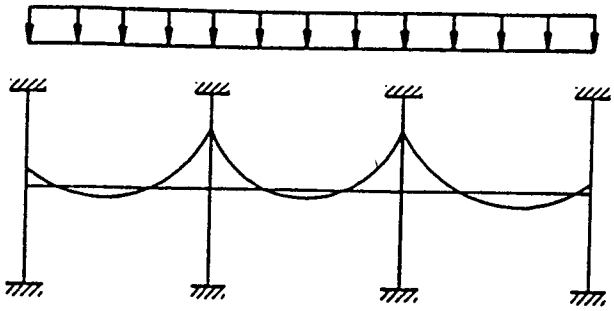

MOMENT DIAGRAM UNDER VERTICAL LOADS ONLY

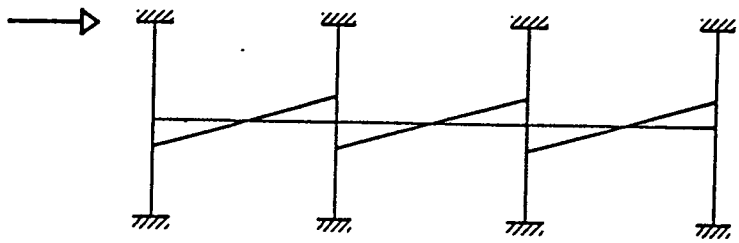

MOMENT DIAGRAM UNDER LATERAL LOADS ONLY

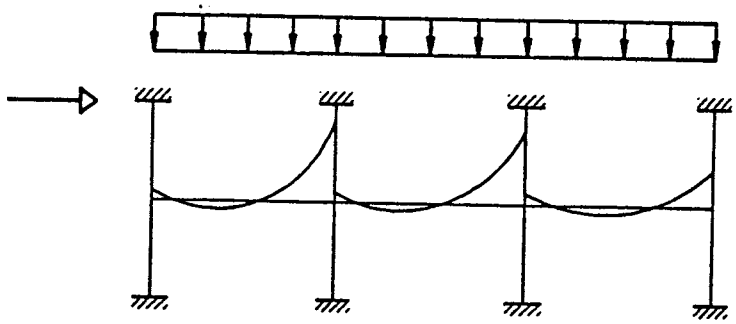

MOMENT DIAGRAM UNDER COMBINED VERTCAL AND LATERAL LOADS

NOTE:
MOMENT DIAGRAMS ARE PLOTTED IN TENSION

Figure 9 Moment Diagrams Of Typical 3-Bay Frame

increased negative moments at one end of a typical span and reduced moments at the other end. Hence, portions of the slab-beam will be more severely cracked than others. Therefore, applying a constant β value throughout the span will not accurately model the slab-beam behavior.

In order to better represent the cracking behavior under combined vertical and lateral loading, a two-beam model is proposed. The proposed two-beam model separates the slab-beam in each span into regions of positive and negative bending. The split is made at the inflection point along each span. The proposed two-beam model enables the engineer to apply reduced beta values in the regions of negative bending where more severe cracking is likely to occur.

5.2 DETERMINATION OF INFLECTION POINTS FOR TWO-BEAM MODELS

5.2.1 KIRK SPECIMEN

The inflection points obtained for Kirk specimens S-2 and S-4 were derived using the column base reactions and "actual" slab loads from Scavuzzo's thesis [27]. The "actual" slab loads were described previously in section 3.1.5. The inflection points obtained for specimens S-2 and S-4 under all experimental loading conditions were then averaged. This average value of the inflection point was utilized for both the effective beam width and equivalent frame two-beam models.

5.2.2 MOEHLE SPECIMEN

Due to the three dimensional nature of the Moehle specimen, certain assumptions were made in the calculation of the inflection points. First, the moments at the slab-column connections were calculated using the experimental column-base shears (excluding gravity

load effects). The moments at the interior connections were distributed equally to the slab-beam on each side of the connections.

Next, the vertical load moments were superimposed on the lateral load moments using a fixed-fixed beam analogy in each span. Finally, simultaneous equations were written in each span to solve for the inflection point locations. The inflection points in each span obtained for the 0.5% and 1.0% drift cases in the North-South direction were averaged together. The average value was then applied to each span in the two-beam model for both the 0.5% and 1.0% drift cases. This same procedure was then applied in the East-West direction.

The decision to use an average value of the inflection points for all models was based on the fact that engineers do not know the location of inflection points prior to their analysis. Therefore an assumption has to be made on the location of the inflection point based upon factors such as span to depth ratio, drift level, etc.

5.3 APPLICATION OF TWO-BEAM MODEL TO KIRK SPECIMENS

5.3.1 EFFECTIVE BEAM WIDTH TWO-BEAM MODEL

The application of the effective beam width two-beam model to the Kirk specimens S-2 and S-4 required a minor change to the original analytical model. Span 1-2 was separated at the inflection point located 50.7 inches (1288 mm) from gridline 1. No modification was made to span 2-3. Both specimens were analyzed under the loadings described in section 4.3.1. The effective beam width two-beam model of the Kirk specimens is shown in Figure 10.

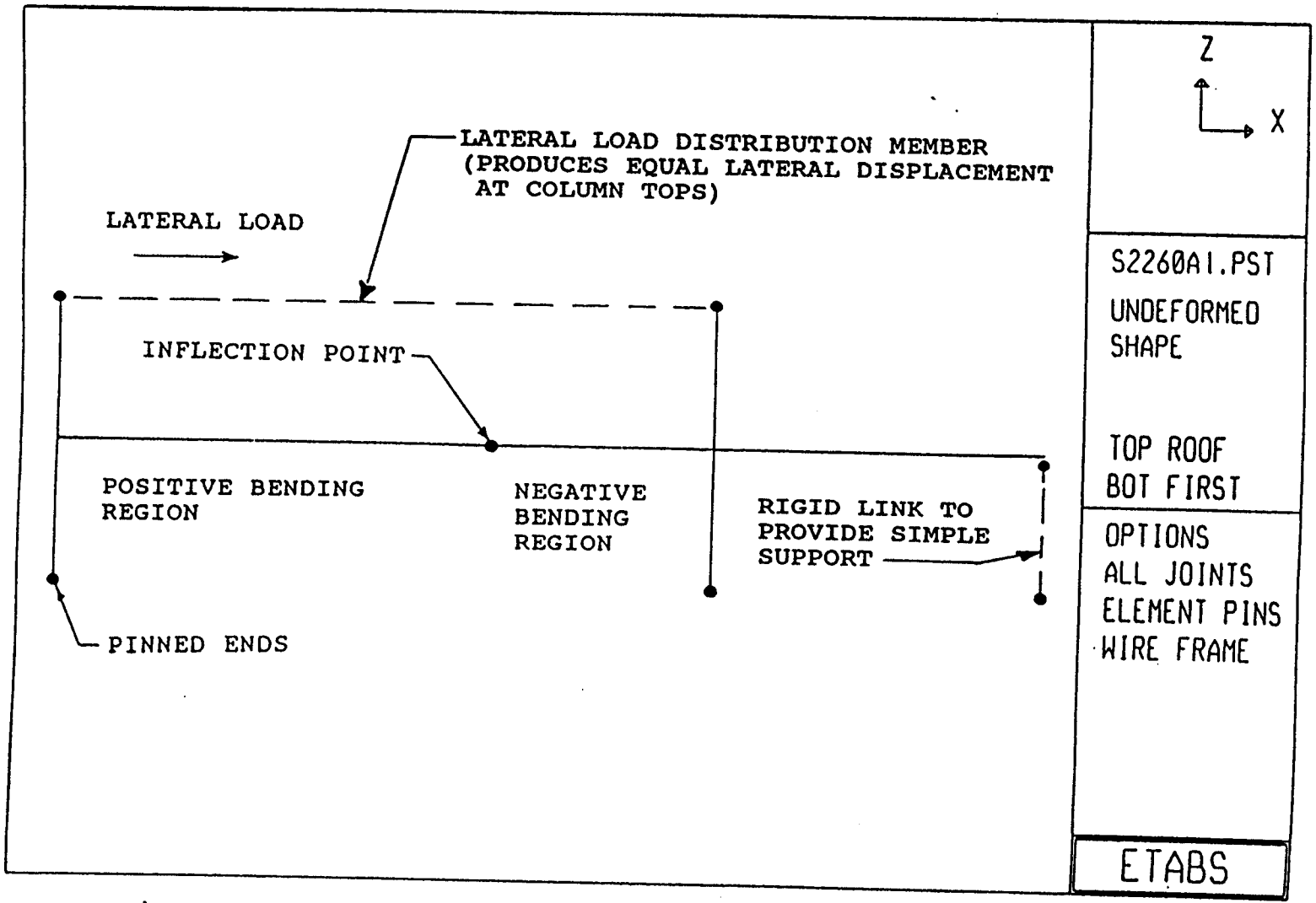

Figure 10 Kirk Effective Beam Width and Equivalent Frame Two-Beam Model

For the two-beam model analysis, an alpha value of 0.4 was used throughout. The beta values were then adjusted by trial and error until the moments at the slab-column connections and lateral drift matched the experimental values.

5.3.2 EQUIVALENT FRAME TWO-BEAM MODEL

The equivalent frame two-beam model was prepared by splitting span 1-2 of the original equivalent frame model at the inflection point located 50.7 inches (1288 mm) from gridline 1. No modification was made to span 2-3. Again, both specimens were analyzed under the loadings described in section 4.3.1. The equivalent frame two beam model of the Kirk specimens is shown in Figure 10.

In the original equivalent frame model, the full width of slab was assumed as being effective. In the equivalent frame two-beam model, the analysis was done using an alpha value of 0.4 throughout. Beta values were then adjusted by trial and error until the moments at the slab column connections and lateral drift matched experimental results.

5.4 OBSERVATIONS OF TWO-BEAM MODEL APPLIED TO KIRK SPECIMENS

5.4.1 PRESENTATION OF RESULTS

The results obtained from the analysis along with the experimental results are listed in tabular form as previously described in section 4.4.1. The heading on each table titled "Run 3" denotes the results of the two-beam model analysis.

However, the table listing the α and β values used in each span was modified. The first column lists the region of positive or negative bending in which the α and β values are

being applied along the beam span. The second and third columns list the span in which the factors are being applied (see Figure 4), along with the α and β values used.

5.4.2 EFFECTIVE BEAM WIDTH TWO-BEAM MODEL

Tables 2 and 8 list the analytical vs. experimental results at approximately 0.5% drift for specimens S-2 and S-4 respectively. At the 0.5% drift level, most cracking is expected to occur at the interior connection where negative bending is predominant, while the region of positive bending is expected to be uncracked. The adjusted β values of 1.0 in the region of positive bending and 0.3 in the region of negative bending are consistent with the expected cracking behavior.

Figures 11 and 13 show the effective beam widths of specimens S-2 and S-4 respectively at approximately 0.5% drift for Runs 1 through 3. Figures 12 and 14 show a graphical comparison of the TOTAL AVERAGE PERCENT ERROR OF MOMENTS and PERCENT ERROR OF DRIFT of specimens S-2 and S-4 respectively at approximately 0.5% drift for Runs 1 through 3. The TOTAL AVERAGE % ERROR OF MOMENTS is used for comparing the results of the various computer Runs. It should be noted that some connections may experience greater or smaller moment errors. The PERCENT ERROR OF DRIFT is defined as ((ETABS DRIFT (%) - ACTUAL DRIFT (%))/ACTUAL DRIFT) (%)) x 100. A positive (+) value of PERCENT ERROR OF DRIFT represents the ETABS DRIFT (%) greater than the ACTUAL DRIFT (%). A negative (-) value of PERCENT ERROR OF DRIFT represents the ETABS DRIFT (%) less than the ACTUAL DRIFT (%).

Tables 4 and 10 list the analytical vs. experimental results at approximately 0.75% drift for specimens S-2 and S-4 respectively. At the 0.75% drift level, increased cracking is

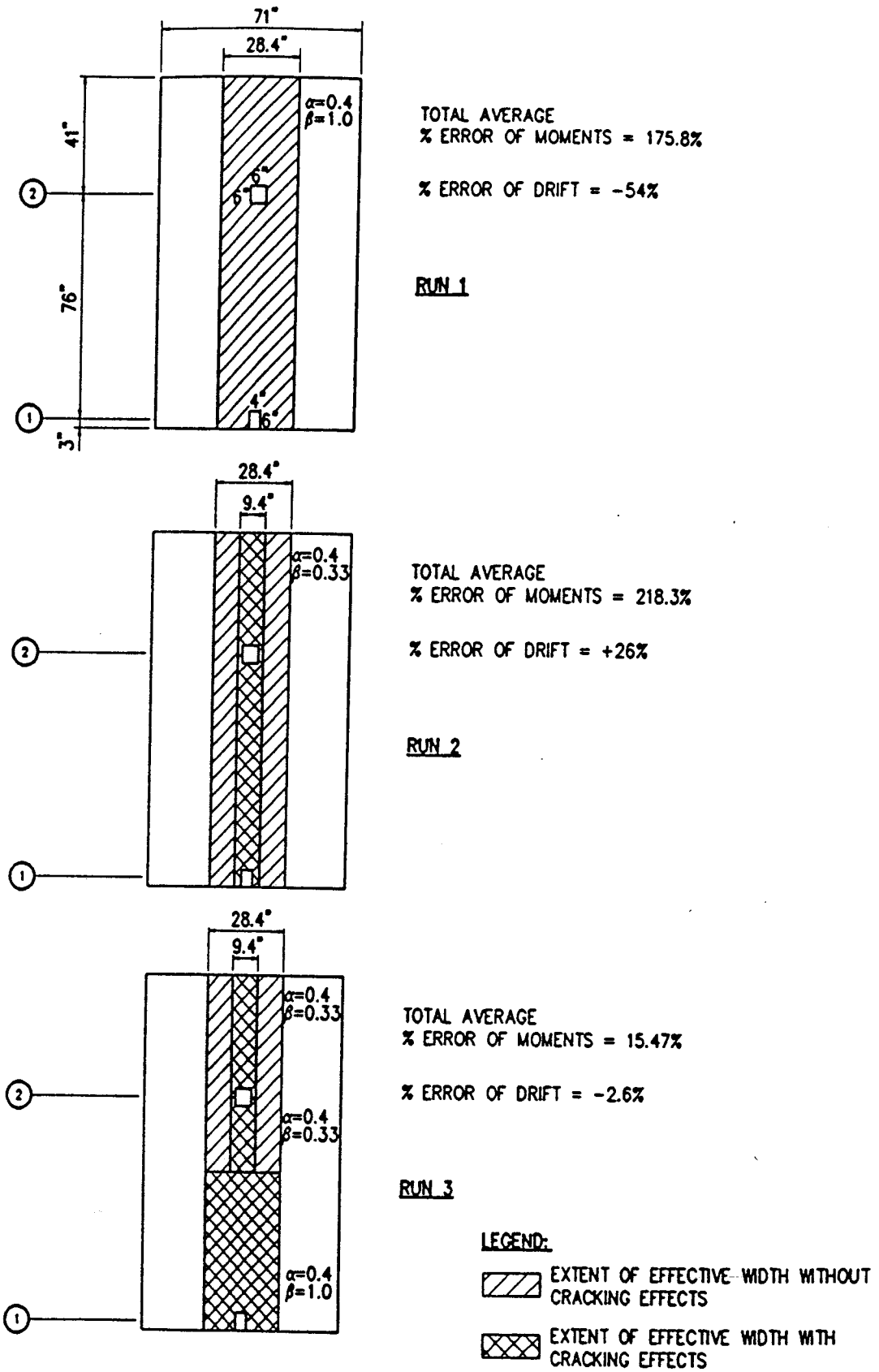

Figure 11 Effective Beam Widths Of Kirk Specimen S-2
At 0.39% Drift For Runs 1, 2 And 3

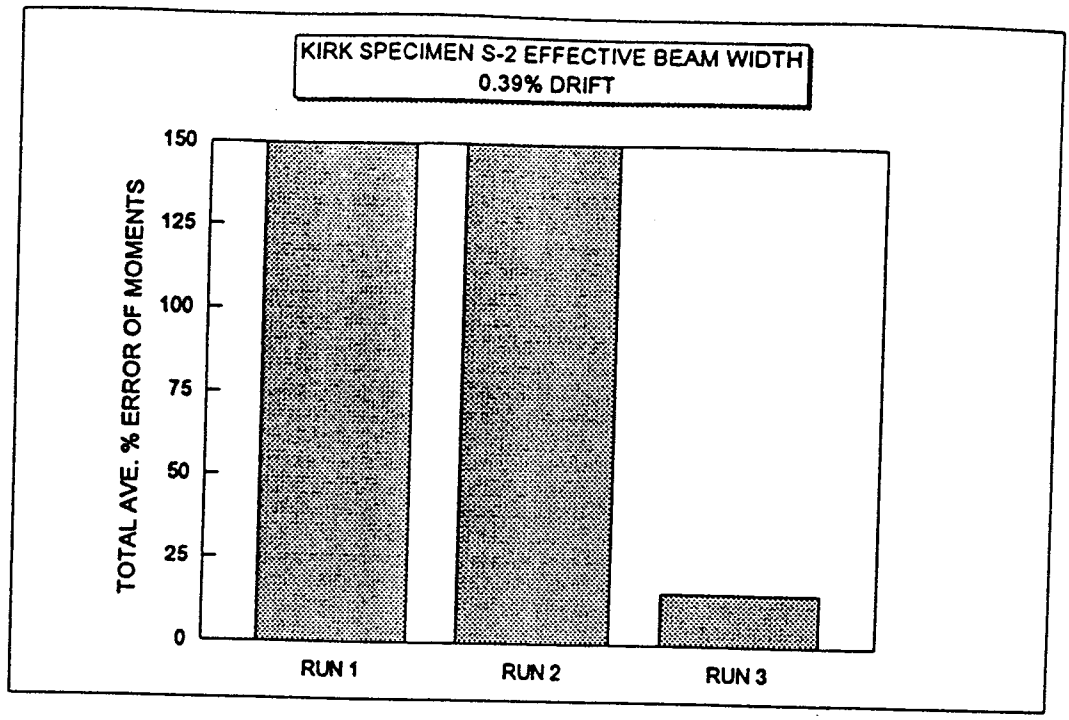

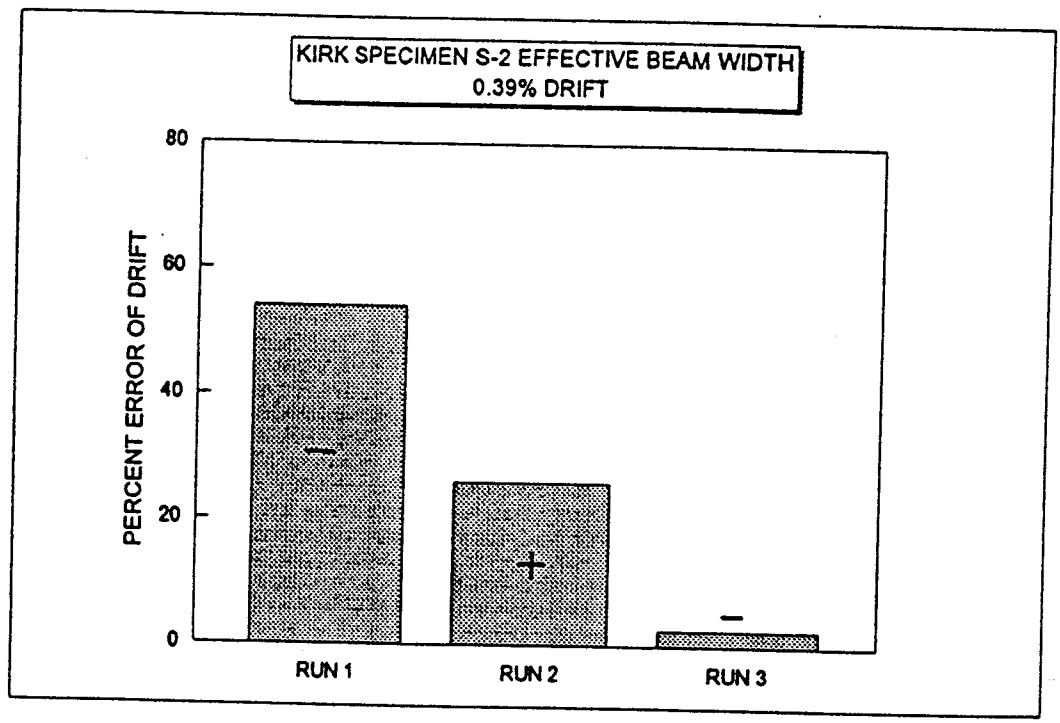

Figure 12 Total Average Percent Error Of Moments And Percent Error Of Drift Of Kirk Specimen S-2 At 0.39% Drift For Runs 1, 2 And 3

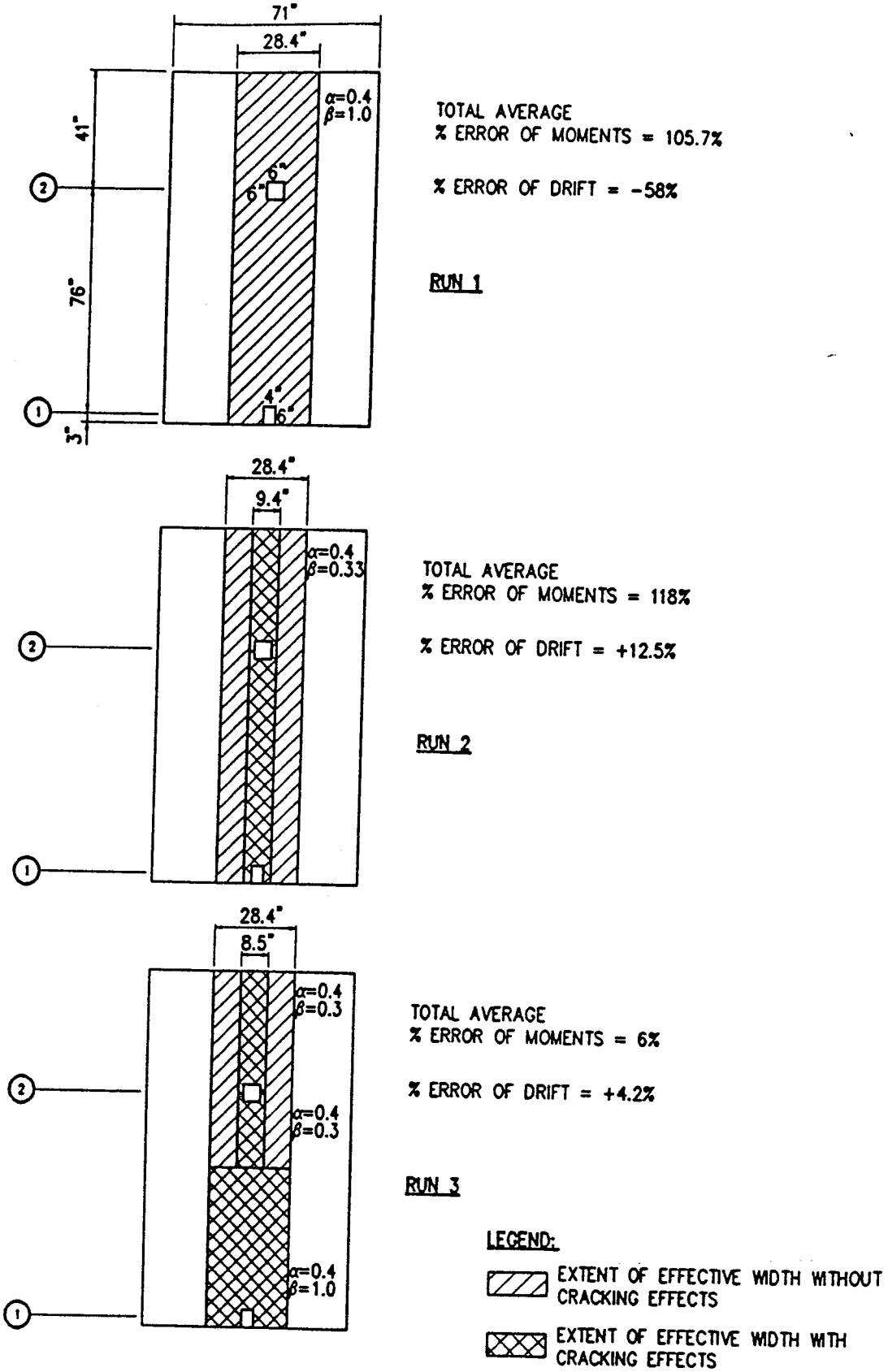

Figure 13 Effective Beam Widths Of Kirk Specimen S-4
At 0.48% Drift For Runs 1, 2 And 3

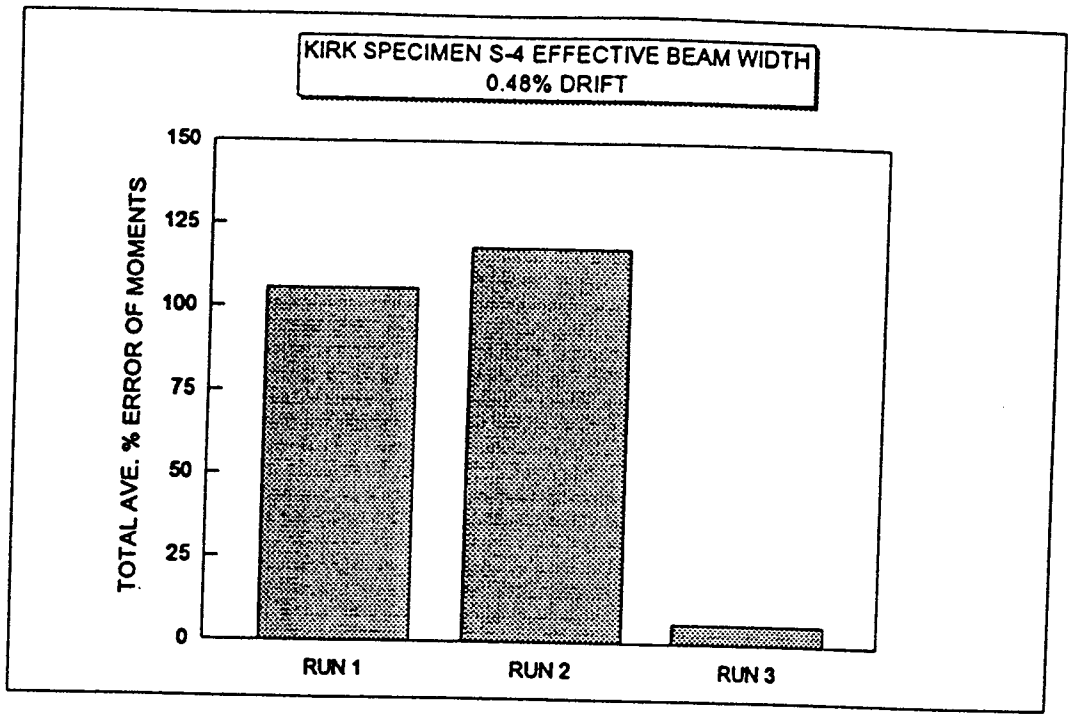

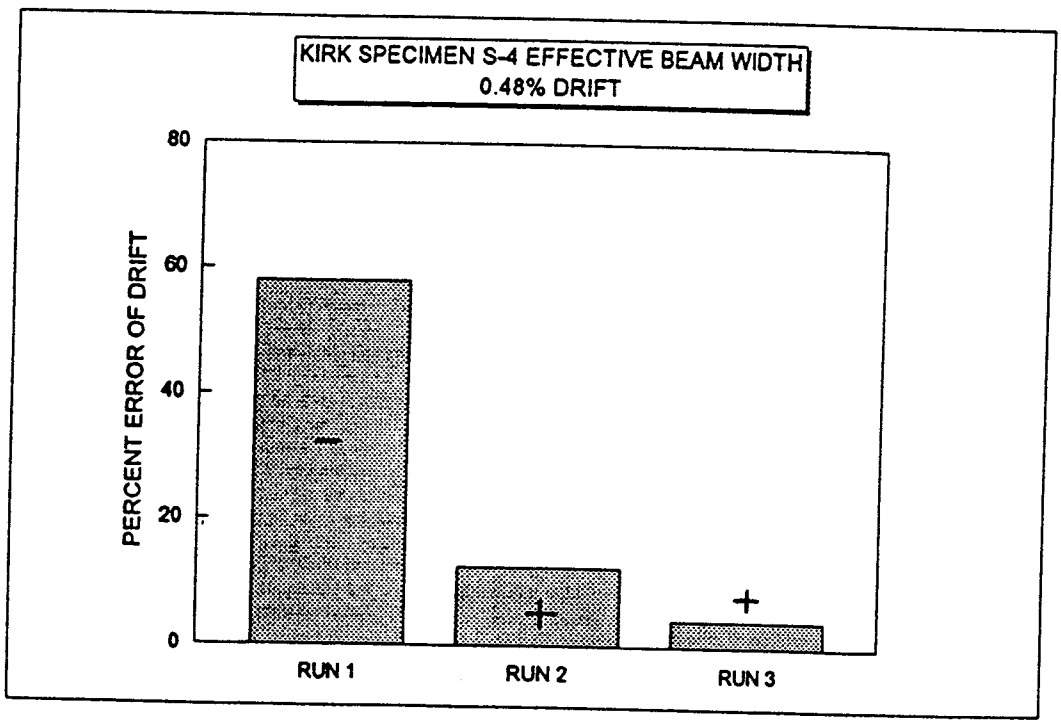

Figure 14 Total Average Percent Error Of Moments And Percent Error Of Drift Of Kirk Specimen S-4 At 0.48% Drift For Runs 1, 2 And 3

expected in the region of negative bending, while cracking in the region of positive bending should start to occur. The adjusted β values of 0.75 in the region of positive bending and 0.25 in the region of negative bending are consistent with the expected cracking behavior.

Tables 6 and 12 list the analytical vs. experimental results at approximately 1.0% drift for specimens S-2 and S-4 respectively. At the 1.0% drift level, a redistribution of negative moment is expected to occur resulting in increased cracking in the region of positive bending. The adjusted β values of 0.6 in the region of positive bending and 0.25 in the region of negative bending are consistent with the expected cracking behavior.

Figures 15 and 17 show the effective beam widths of specimens S-2 and S-4 respectively at approximately 1.0% drift for Runs 1 through 3. Figures 16 and 18 show a graphical comparison of the TOTAL AVERAGE PERCENT ERROR OF MOMENTS and PERCENT ERROR OF DRIFT of specimens S-2 and S-4 respectively at approximately 1.0% drift for Runs 1 through 3.

For specimens S-2 and S-4 analyzed under their respective loading cases, the two-beam model with adjusted β values brought the total average ratio of ETABS/ACTUAL moment closer to unity. This significantly reduced the % ERROR of ETABS to ACTUAL moment as compared to the % ERROR observed in Runs 1 and 2. Not only did the correlation between analytical and experimental moments improve, but so did the comparison between analytical and experimental drift.

5.4.3 EQUIVALENT FRAME TWO-BEAM MODEL

Tables 14 and 20 list the analytical vs. experimental results at approximately 0.5% drift for specimens S-2 and S-4 respectively. At the 0.5% drift level, the adjusted β values

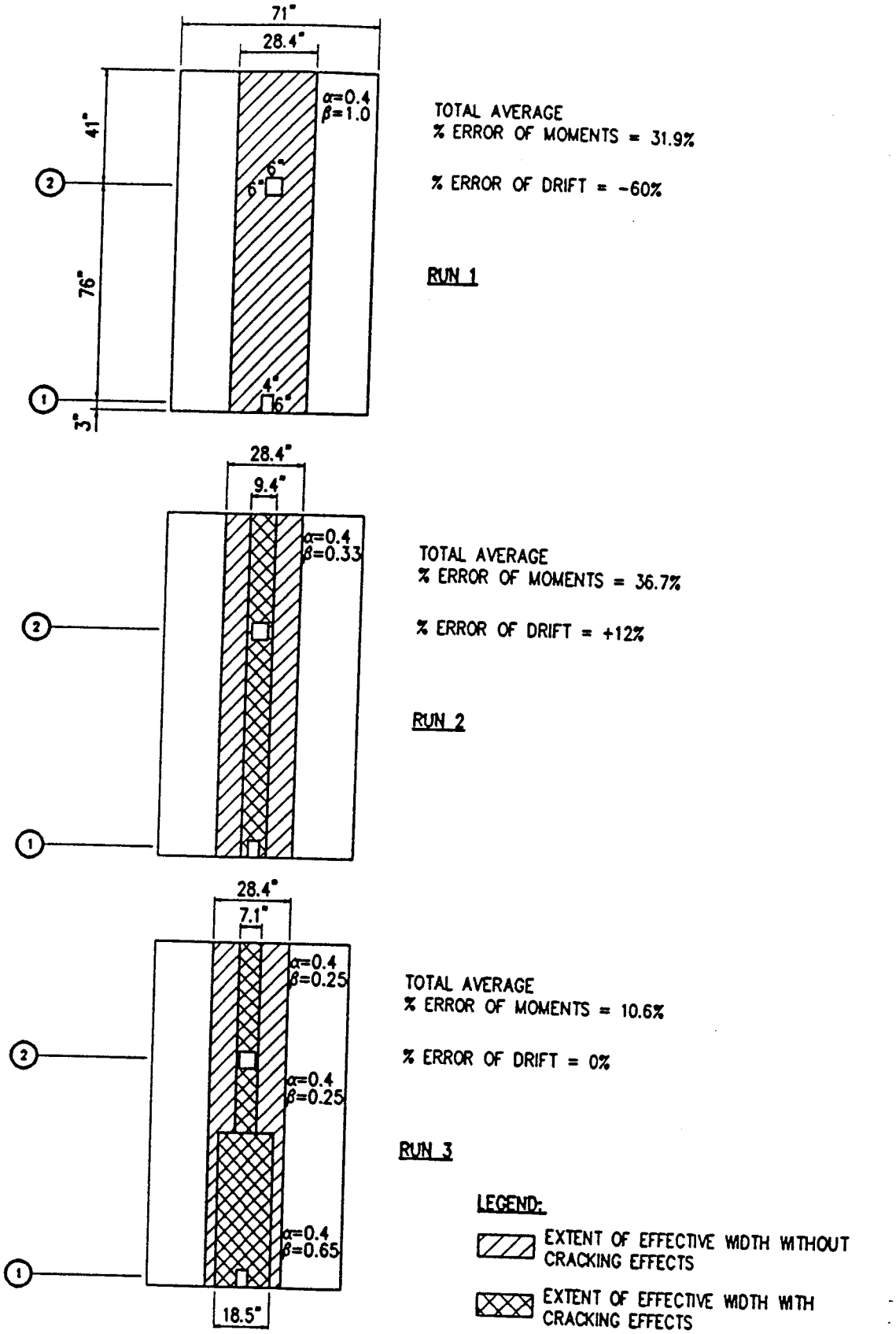

Figure 15 Effective Beam Widths Of Kirk Specimen S-2 At 0.84% Drift For Runs 1, 2 And 3

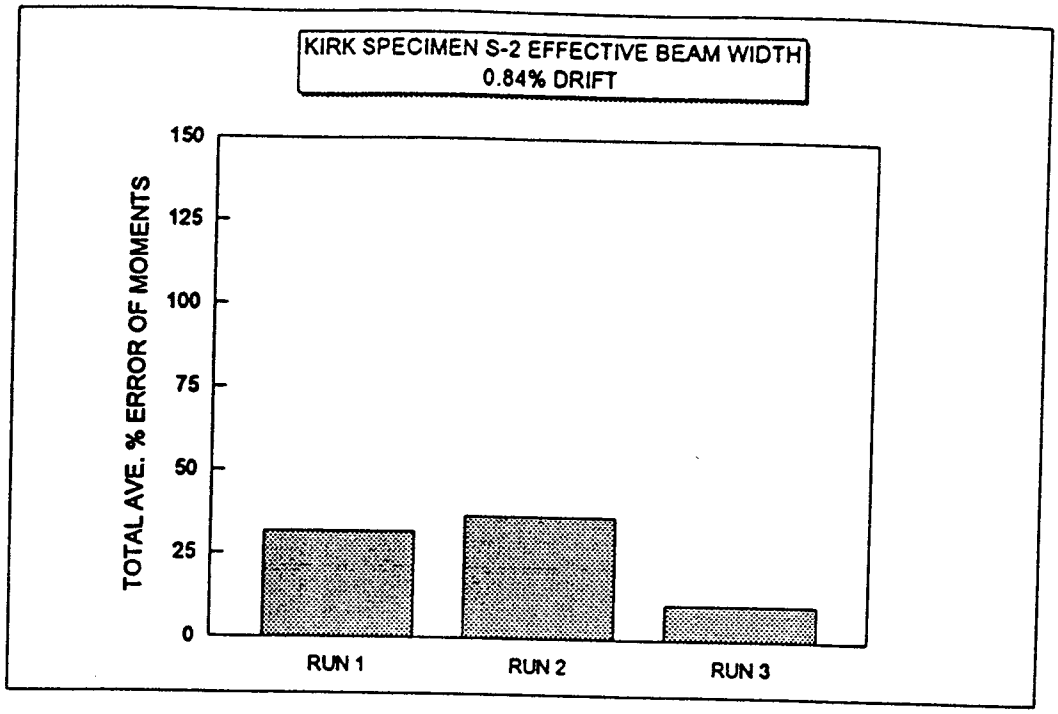

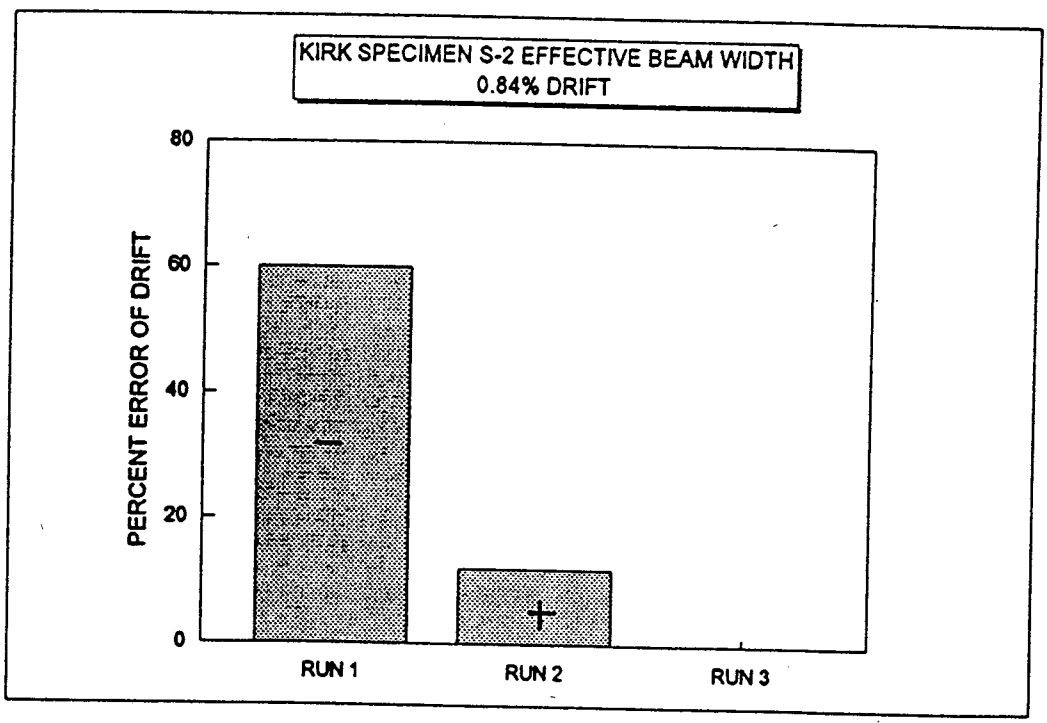

Figure 16 Total Average Percent Error of Moments And Percent Error Of Drift Of Kirk Specimen S-2 At 0.84% Drift For Runs 1, 2 And 3

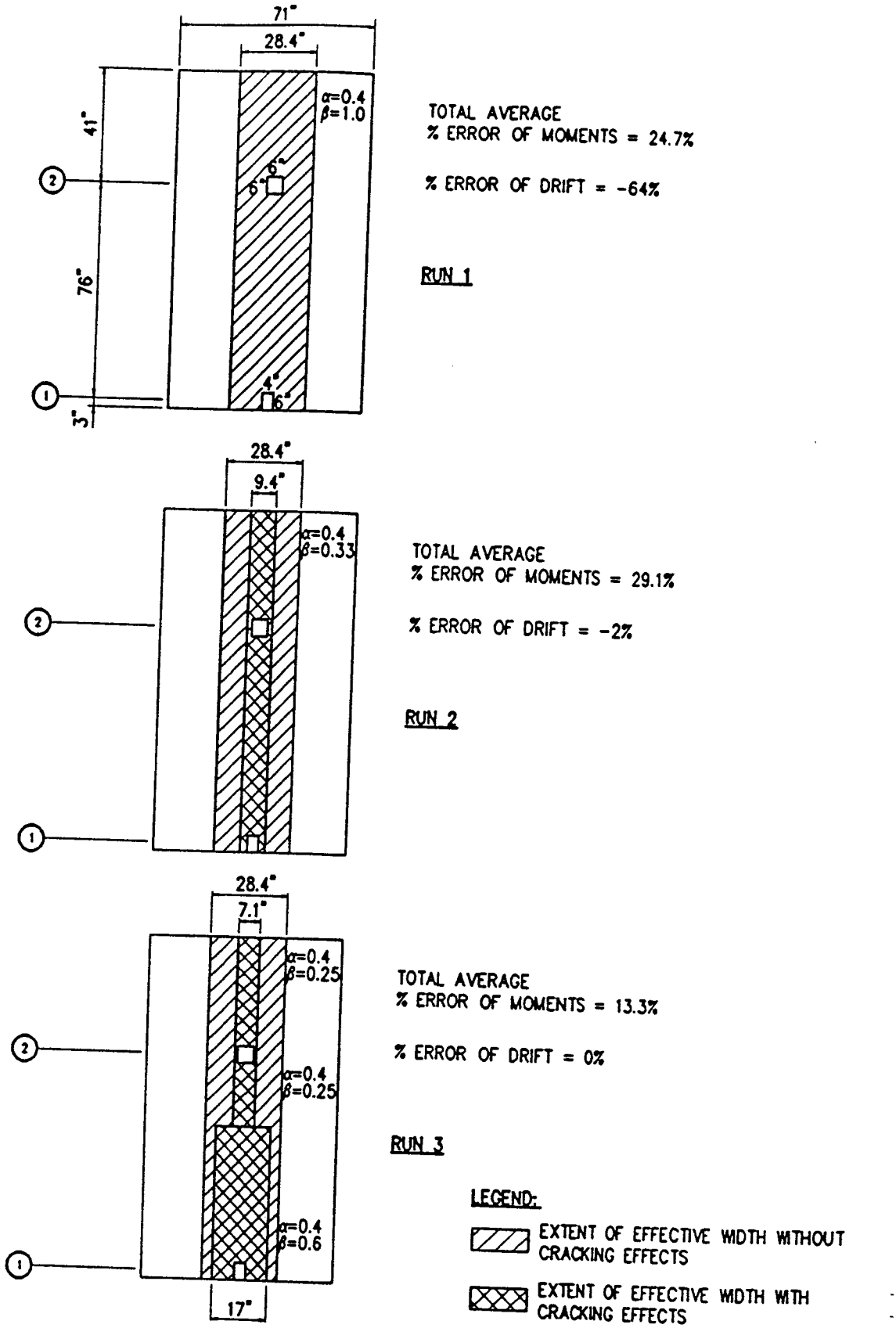

Figure 17 Effective Beam Widths Of Kirk Specimen S-4 At 0.98% Drift For Runs 1, 2 And 3

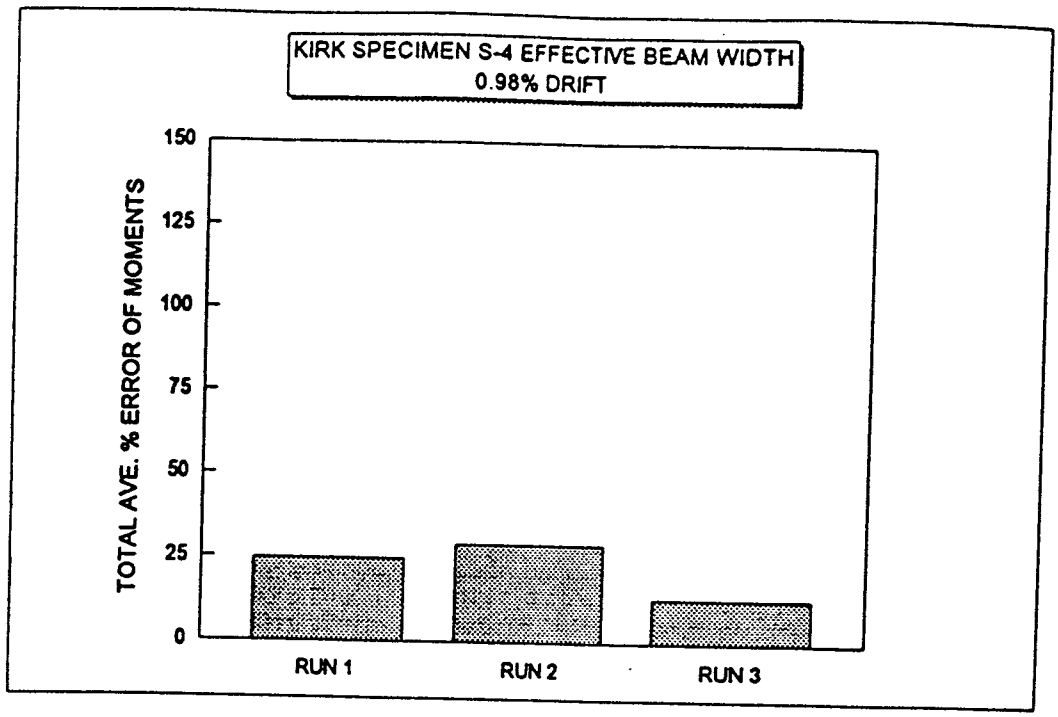

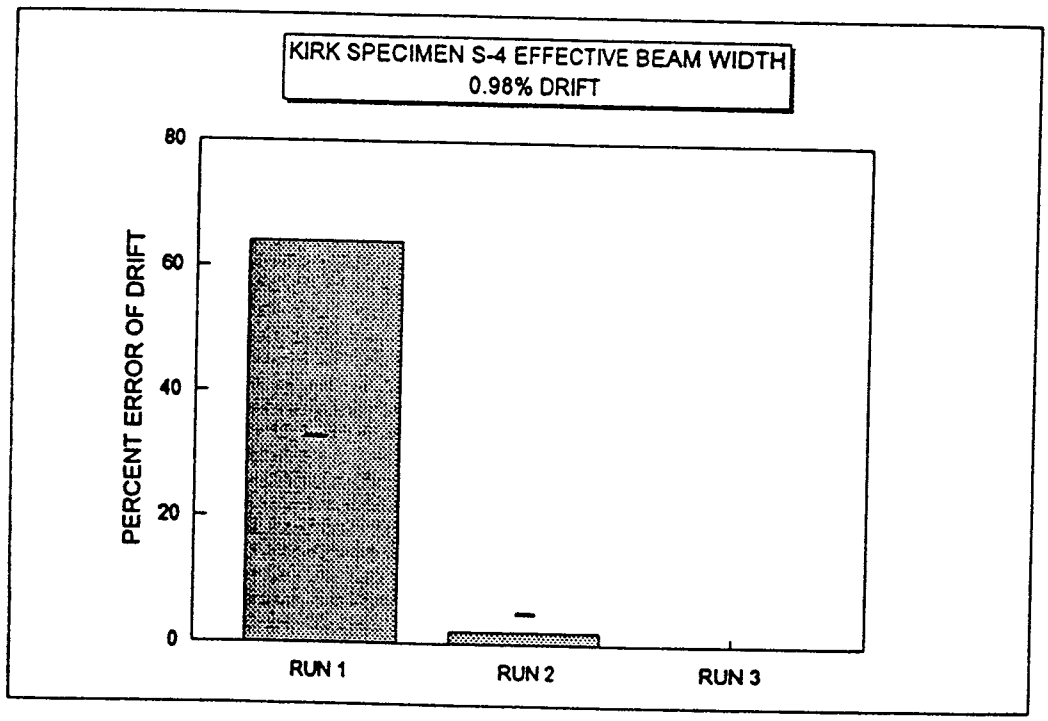

Figure 18 Total Average Percent Error Of Moments And Percent Error Of Drift Of Kirk Specimen S-4 At 0.98% Drift For Runs 1, 2 And 3

are consistent with the expected cracking behavior as discussed in the results for the effective beam width two-beam model.

Both specimens required an adjusted β value of 1.0 in the region of positive bending. However, specimen S-2 required an adjusted β value of 0.5 in the negative region of bending, while specimen S-4 required an adjusted β value of 0.33. This difference can be attributed to the lower lateral force applied to specimen S-2 in the experimental test.

Tables 16 and 22 list the analytical vs. experimental results at approximately 0.75% drift for specimens S-2 and S-4 respectively. At the 0.75% drift level, the adjusted β values of 0.75 in the region of positive bending and 0.3 in the region of negative bending are consistent with the expected cracking behavior as discussed in the results for the effective beam width two-beam model. The adjusted β values at the 0.75% drift level produced accurate drift results. However, the percent error of ETABS moment to ACTUAL moment increased slightly as compared to the results obtained from the equivalent frame model applied without cracking (Run 1).

Tables 18 and 24 list the analytical vs. experimental results at approximately 1.0% drift for specimens S-2 and S-4 respectively. At the 1.0% drift level, the adjusted β values of 0.65 in the region of positive bending and 0.3 in the region of negative bending are consistent with the expected cracking behavior as discussed in the results for the effective beam width two-beam model.

Overall, the equivalent frame two-beam model was able to accurately predict lateral drift. Although the correlation between analytical and experimental moments became

slightly worse at the 0.75% drift level, the model's combined prediction of moments and drift at all drift levels improved significantly as compared with Runs 1 and 2.

5.5 APPLICATION OF TWO-BEAM MODEL TO MOEHLE SPECIMEN

5.5.1 NORTH-SOUTH DIRECTION

As mentioned in section 4.5, only the effective beam width model was applied to the Moehle specimen. The application of the effective beam width two-beam model to the Moehle specimen in the North-South direction required splitting each span at the inflection point located 39.6 inches (1006 mm) from the centerline of the first column of each span in the direction of analysis. The effective beam width two-beam model in the North-South direction is shown in Figure 19.

An α of 0.4 was applied to the positive and negative regions of bending for all slab-beam elements connected to the columns along gridlines 2 and 3. However, a modification was made to the α values in the region of positive bending of end span 1-2 and in the region of negative bending of end span 3-4.

In Hwang's report (14), a summary of effective width factors obtained by Banchik using a finite element approach is presented. From Banchik's results, a lower effective width factor should be applied at the corner connections. In order to simplify the analytical two-beam model, a reduced α of 0.3 was applied to the region of positive bending in span 1-2 for all first exterior connections at the 0.5% drift level. An α of 0.2 was applied in the region of negative bending in span 3-4 for all exterior connections. At the 1.0% drift level, an α of 0.2 was applied to the region of positive bending in span 1-2 and in the region of negative bending in span 3-4.

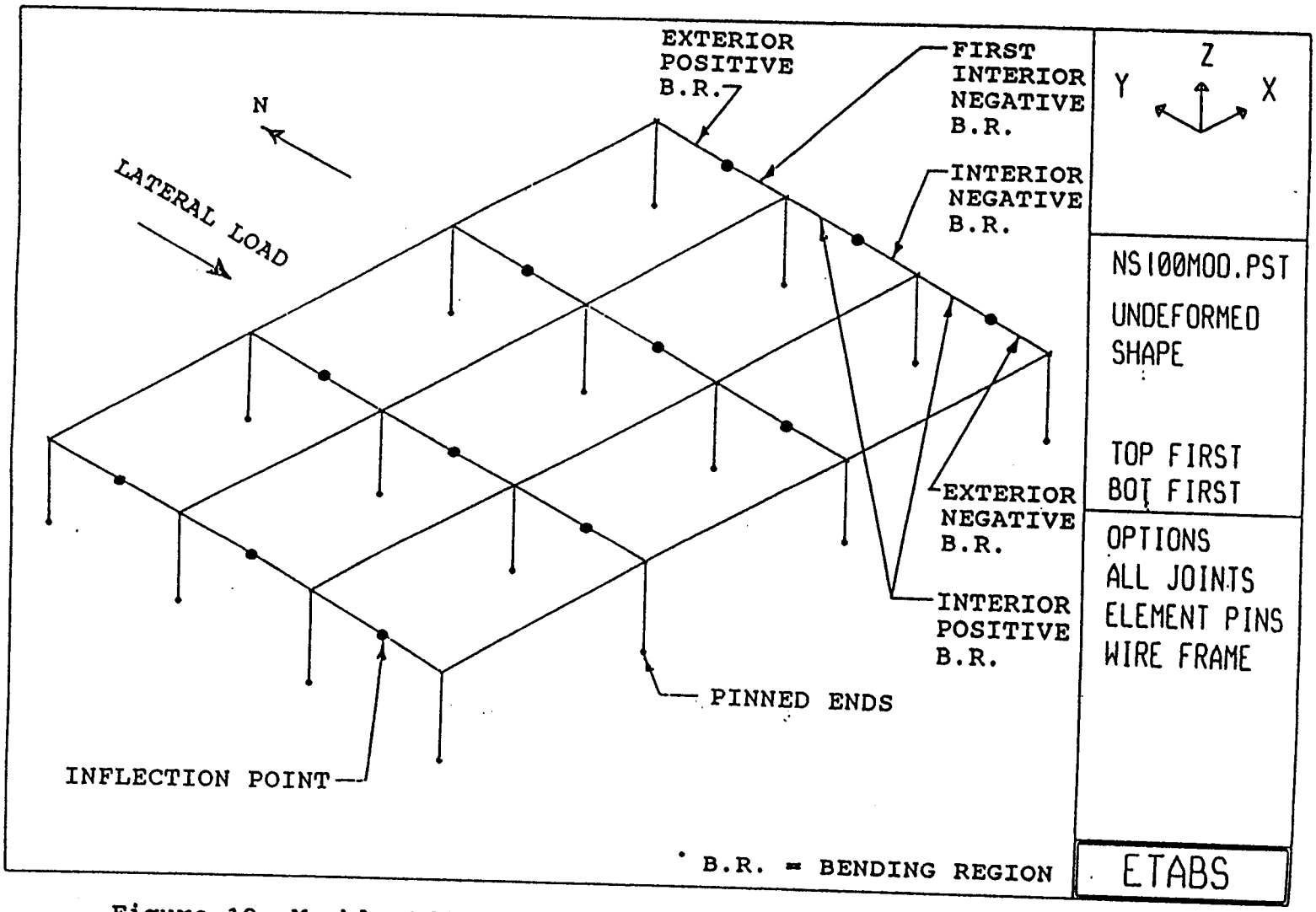

Figure 19 Moehle Effective Beam Width Two-Beam Model in the North-South Direction

The beta values were then adjusted by trial and error until the moments at the slab column connections and lateral drift matched the experimental values.

5.5.2 EAST-WEST DIRECTION

The application of the effective beam width two-beam model to the Moehle specimen in the East-West direction again required splitting each span at the inflection point located 70.2 inches (1783 mm) from the centerline of the first column of each span in the direction of analysis. The effective beam width two-beam model in the East-West direction is shown in Figure 20.

At the 0.5% drift level, an α of 0.4 was applied to the positive and negative regions of bending for all slab-beam elements connected to the columns along gridlines A, B, and C. However, an α of 0.5 was used in the region of positive bending in end span D-C. This increased α value was required due to the severe underestimation of stiffness in this region in Runs 1 and 2.

At the 1.0% drift level, an α of 0.4 was used throughout each span. The beta values were then adjusted by trial and error until the moments at the slab-column connections and lateral drift matched the experimental values.

5.6 OBSERVATIONS OF TWO-BEAM MODEL APPLIED TO MOEHLE SPECIMEN

5.6.1 PRESENTATION OF RESULTS

The results obtained from the analysis along with the experimental results are listed in tabular form as previously described in section 4.6.1. The heading on each table titled "Run 3" denotes the results of the two-beam model analysis.

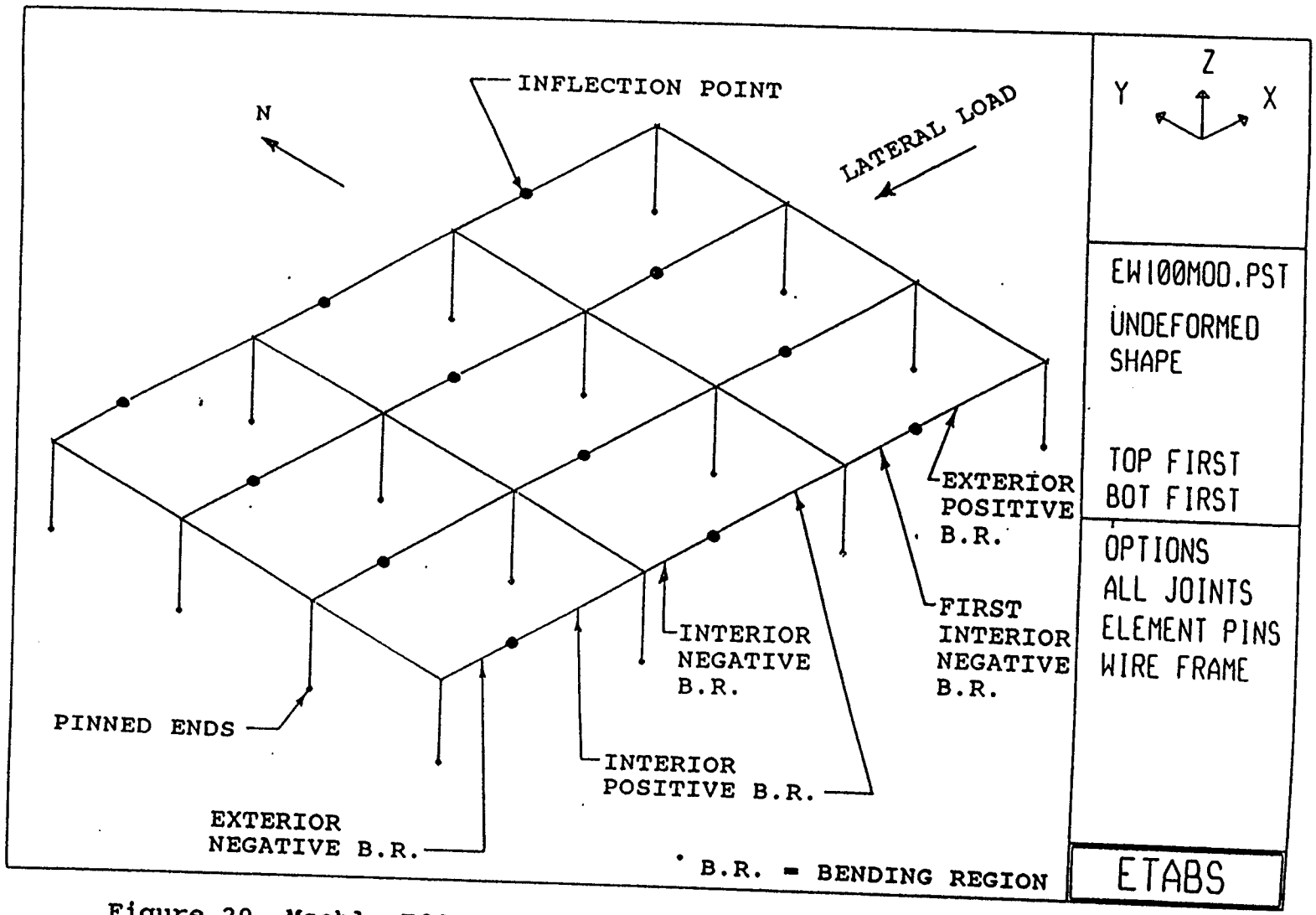

Figure 20 Moehle Effective Beam Width Two-Beam Model in the East-West Direction

However, the table listing the α and β values used in each span was modified. The first column lists the region of positive or negative bending in which the α and β values are being applied along the beam span. The second through fourth columns list the span in which the α and β factors are applied (see Figure 6), along with the α and β values used. Due to the symmetry of the specimen in the East-West direction, only the moments along gridlines 3 and 4 are reported.

5.6.2 EFFECTIVE BEAM WIDTH TWO-BEAM MODEL APPLIED IN NORTH-SOUTH DIRECTION AT 0.5% DRIFT

Table 27 lists the analytical vs. experimental results for the two-beam model analysis in the North-South direction at 0.5% drift.

At the 0.5% drift level, an adjusted β of 0.5 was used in all regions of positive bending. The reduced stiffness in the regions of positive bending can be attributed to the prior construction and lateral loading applied to the specimen. An adjusted β of 0.15 in the region of negative bending at the first interior connection is consistent with the expected cracking behavior under combined vertical and lateral loading. An adjusted β of 0.3 at the regions of negative bending in spans 2-3 and 3-4 is consistent with the expected deterioration in stiffness at these connections.

Lateral drift obtained with the two-beam model improved to within 8% of the experimental drift. Although the two-beam model's correlation between analytical and experimental moments became slightly worse as compared to Run 1, the model's combined prediction of moments and drift improved.

Figures 21 and 22 show the effective beam widths of the Moehle specimen at 0.5% drift for Runs 1 through 3 in the North-South direction. Figure 23 shows a graphical comparison of the TOTAL AVERAGE PERCENT ERROR OF MOMENTS and PERCENT ERROR OF DRIFT of the Moehle specimen at 0.5% drift for Runs 1 through 3 in the North-South direction.

5.6.3 EFFECTIVE BEAM WIDTH TWO-BEAM MODEL APPLIED IN NORTH-SOUTH DIRECTION AT 1.0% DRIFT

Table 30 lists the analytical vs. experimental results for the two-beam model analysis in the North-South direction at 1.0% drift.

At the 1.0% drift level, an adjusted β of 0.35 was used in all regions of positive bending. The reduced β value in the regions of positive bending is consistent with the increased cracking expected to occur at the 1.0% drift level. In the regions of negative bending, increased deterioration in stiffness is expected. The adjusted β values in the regions of negative bending represent this behavior. The adjusted β values in the regions of positive and negative bending were two-thirds of the values used in the 0.5% drift analysis.

Lateral drift obtained with the adjusted β values was accurate. Correlation between analytical and experimental moments improved significantly. Overall, the two-beam model in the North-South direction was successful in improving the combined correlation of analytical moments and drift with experimental results.

Figures 24 and 25 show the effective beam widths of the Moehle specimen at 1.0% drift for Runs 1 through 3 in the North-South direction. Figure 26 shows a graphical

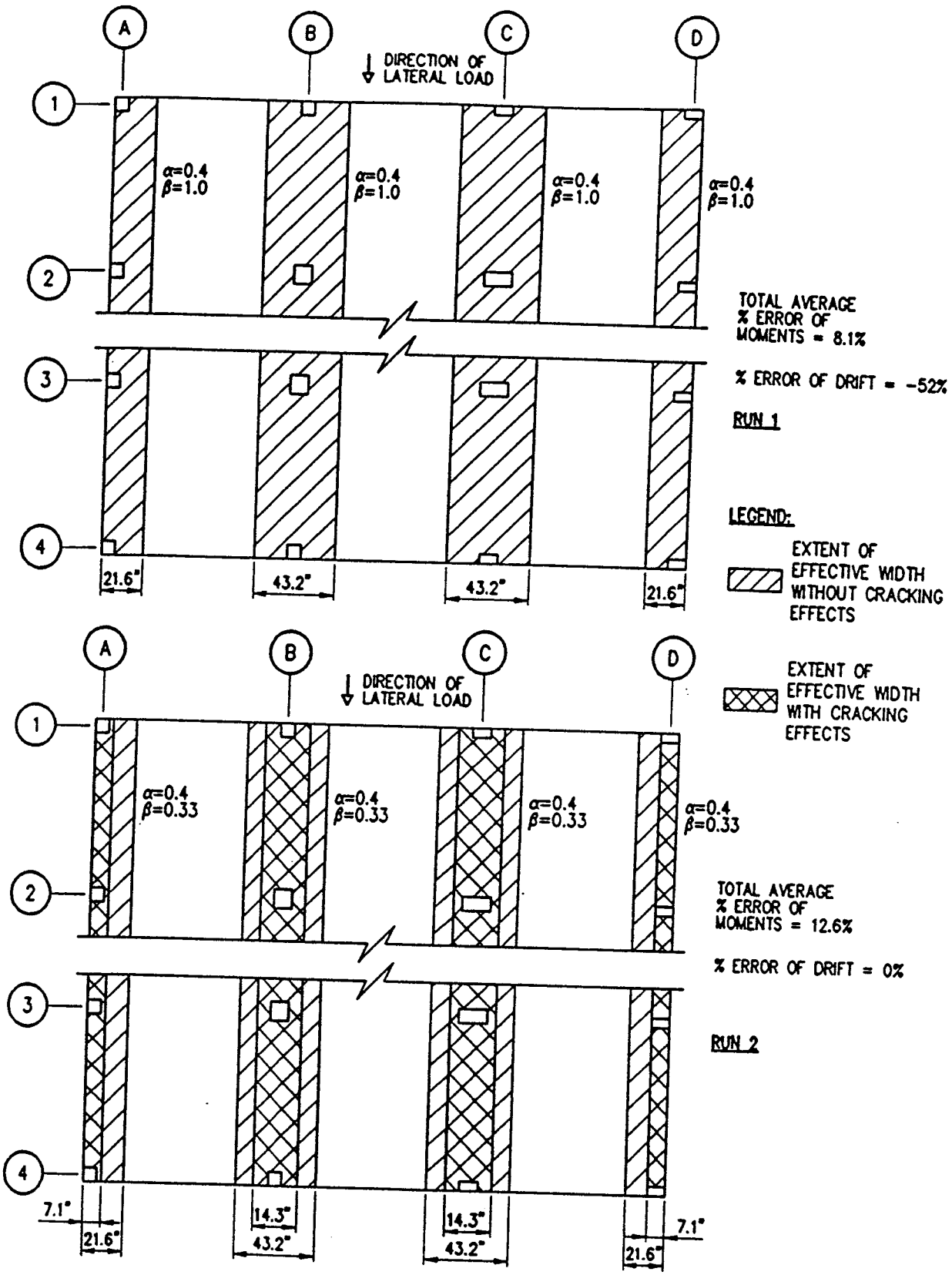

Figure 21 Effective Beam Widths Of Moehle Specimen North-South Direction At 0.5% Drift For Runs 1 and 2

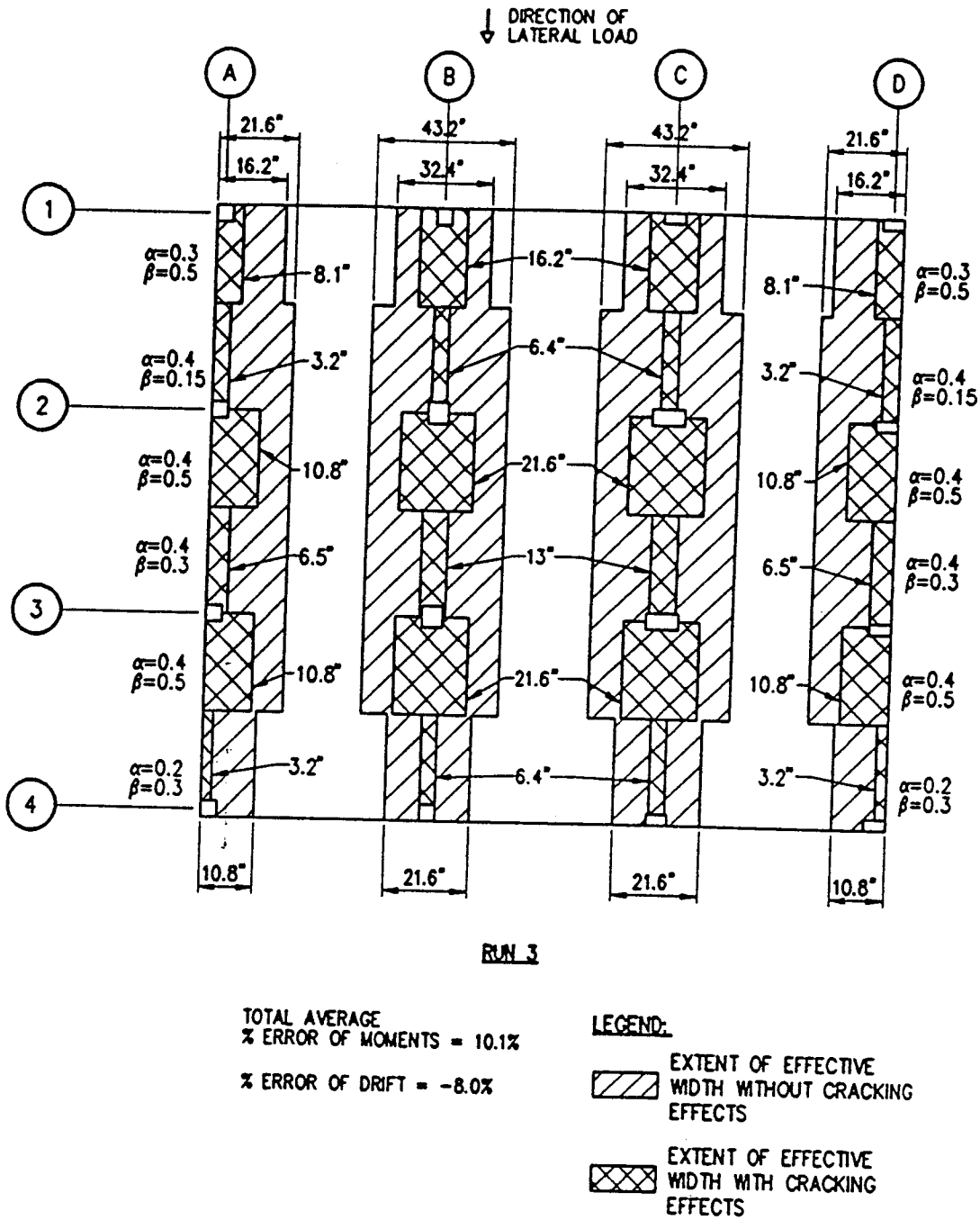

Figure 22 Effective Beam Widths Of Moehle Specimen North-South Direction At 0.5% Drift For Run 3

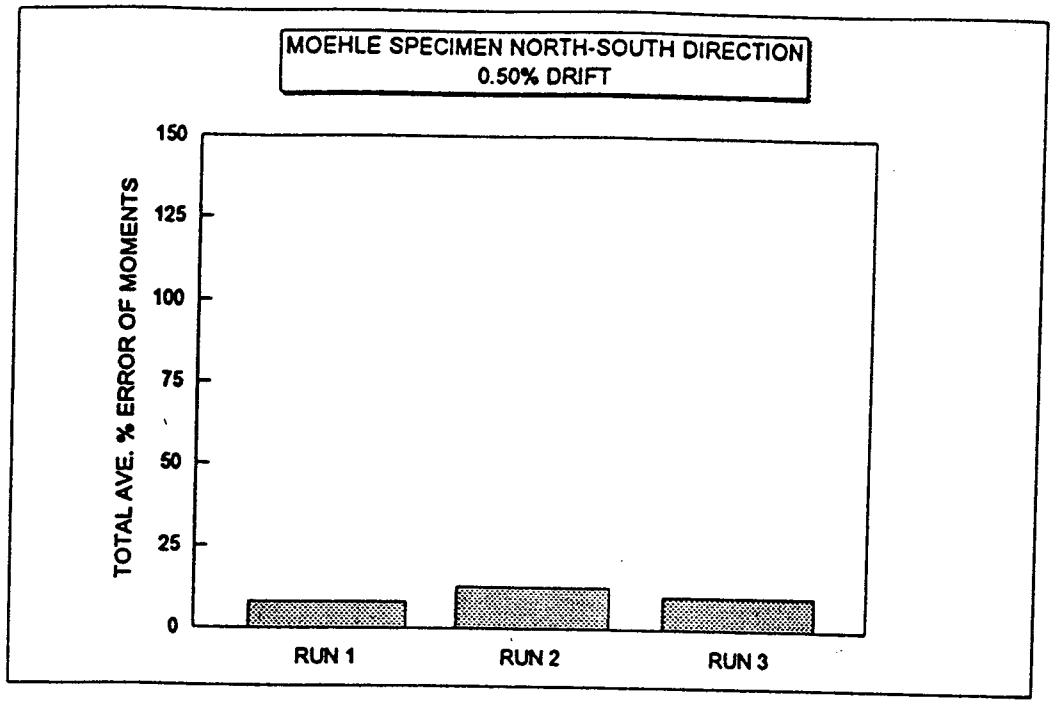

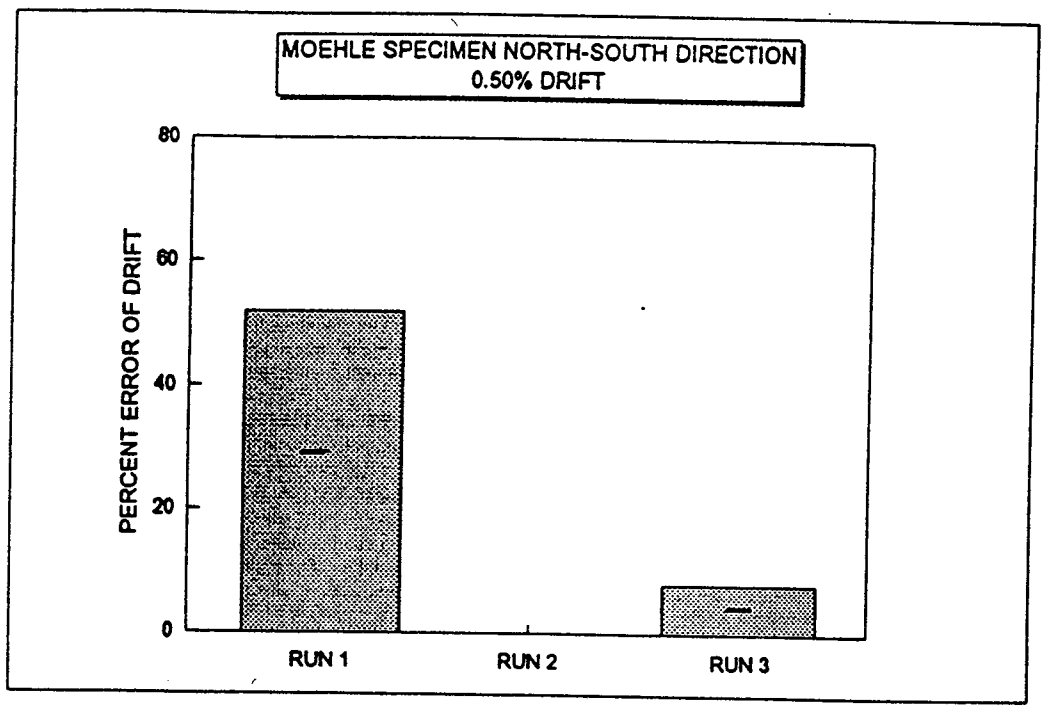

Figure 23 Total Average Percent Error Of Moments And Percent Error Of Drift Of Moehle Specimen North-South Direction At 0.5% Drift For Runs 1, 2 And 3

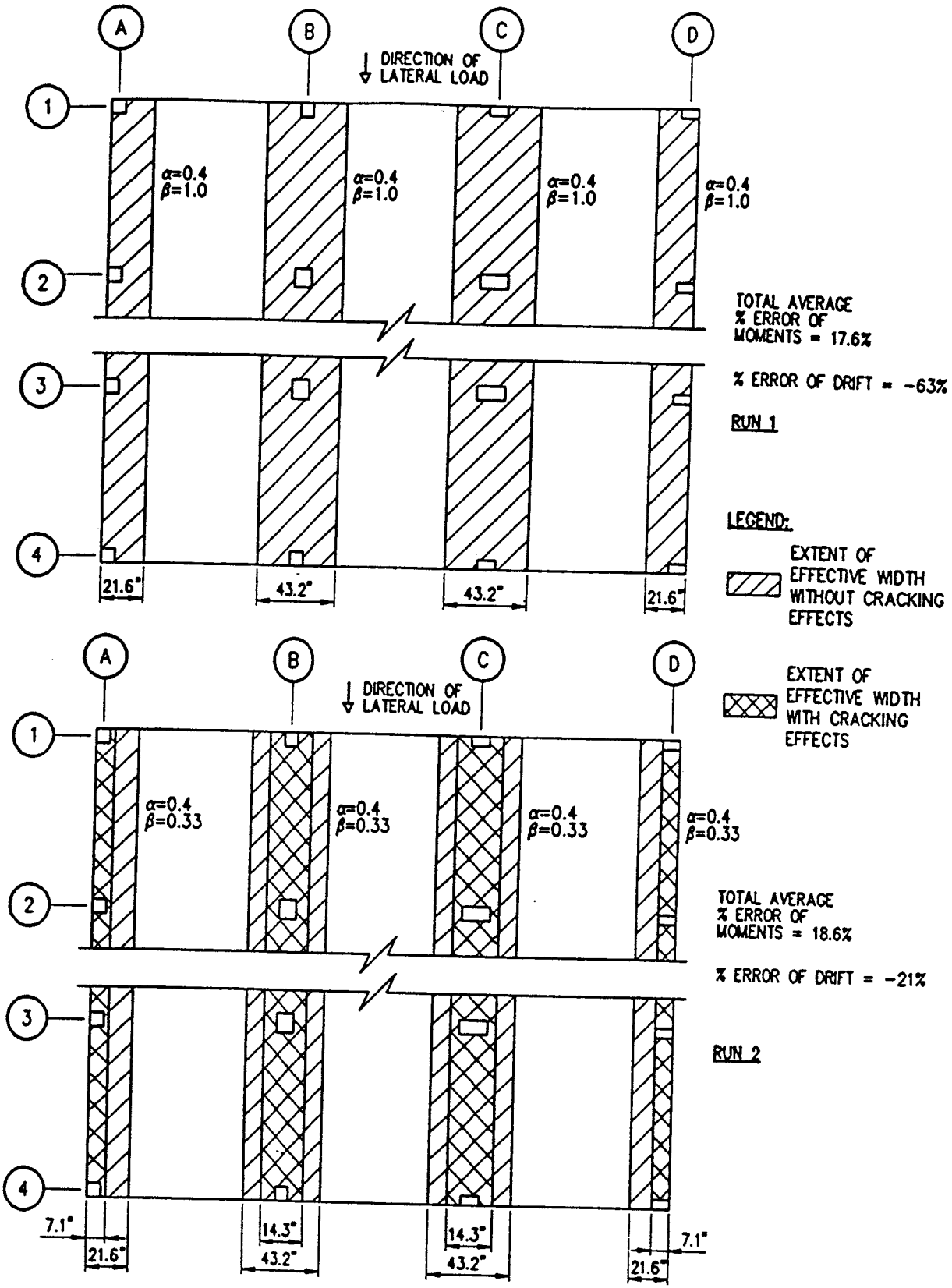

Figure 24 Effective Beam Widths Of Moehle Specimen North-South Direction At 1.0% Drift For Runs 1 and 2

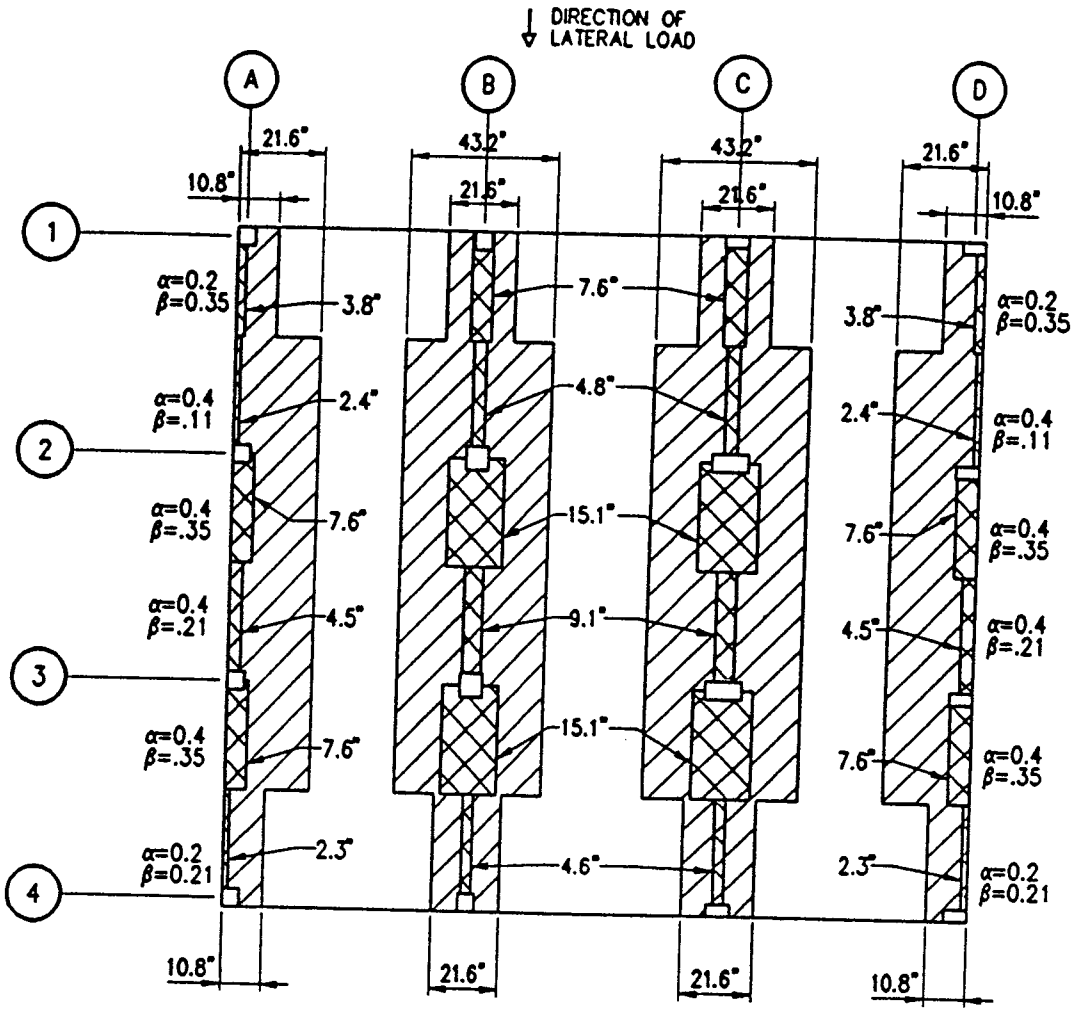

Figure 25 Effective Beam Widths Of Moehle Specimen North-South Direction At 1.0% Drift For Run 3

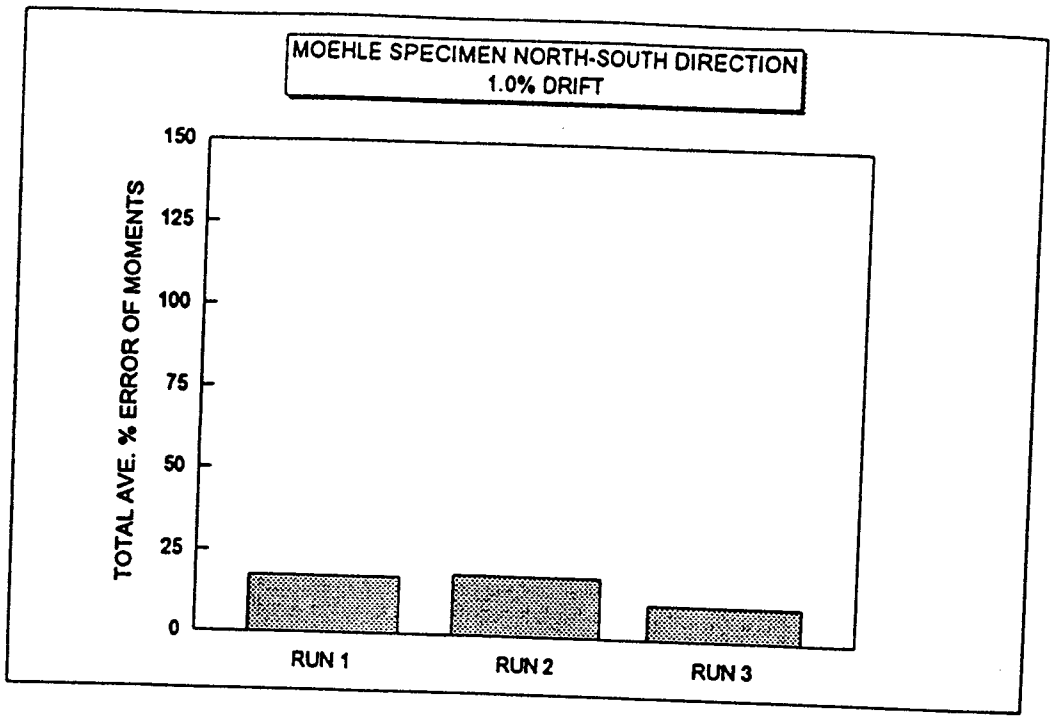

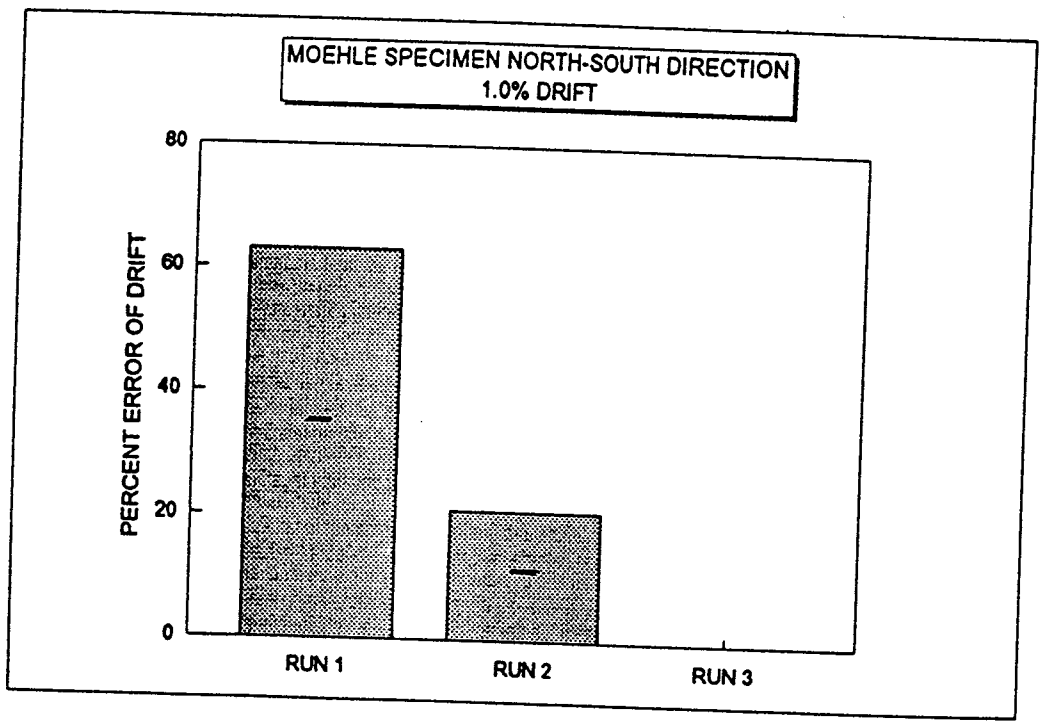

Figure 26 Total Average Percent Error of Moments And Percent Error Of Drift Of Moehle Specimen North-South Direction At 1.0% Drift For Runs 1, 2 And 3

comparison of the TOTAL AVERAGE PERCENT ERROR OF MOMENTS and PERCENT ERROR OF DRIFT of the Moehle specimen at 1.0% drift for Runs 1 through 3 in the North-South direction.

5.6.4 EFFECTIVE BEAM WIDTH TWO-BEAM MODEL APPLIED IN EAST-WEST DIRECTION AT 0.5% DRIFT

Table 33 lists the analytical vs. experimental results for the two-beam model analysis in the East-West direction at 0.5% drift.

Due to the flexibility of the specimen in the East-West direction, not much cracking is expected to occur at the 0.5% drift level. However, the region of negative bending in span B-A is expected to undergo cracking due to the increased negative moments in this region under combined vertical and lateral loading. The adjusted β of 0.3 in the negative region of span B-A is consistent with the expected cracking behavior. The β value at all other regions of positive and negative bending remained at 1.0.

Lateral drift obtained with the adjusted β values was accurate. Correlation between analytical and experimental moments at the exterior connections improved. However, the experimental moments were still slightly underestimated at the first exterior connections along gridline D.

Figures 27 and 28 show the effective beam widths of the Moehle specimen at 0.5% drift for Runs 1 through 3 in the East-West direction. Figure 29 shows a graphical comparison of the TOTAL AVERAGE PERCENT ERROR OF MOMENTS and PERCENT ERROR OF DRIFT of the Moehle specimen at 0.5% drift for Runs 1 through 3 in the East-West direction.

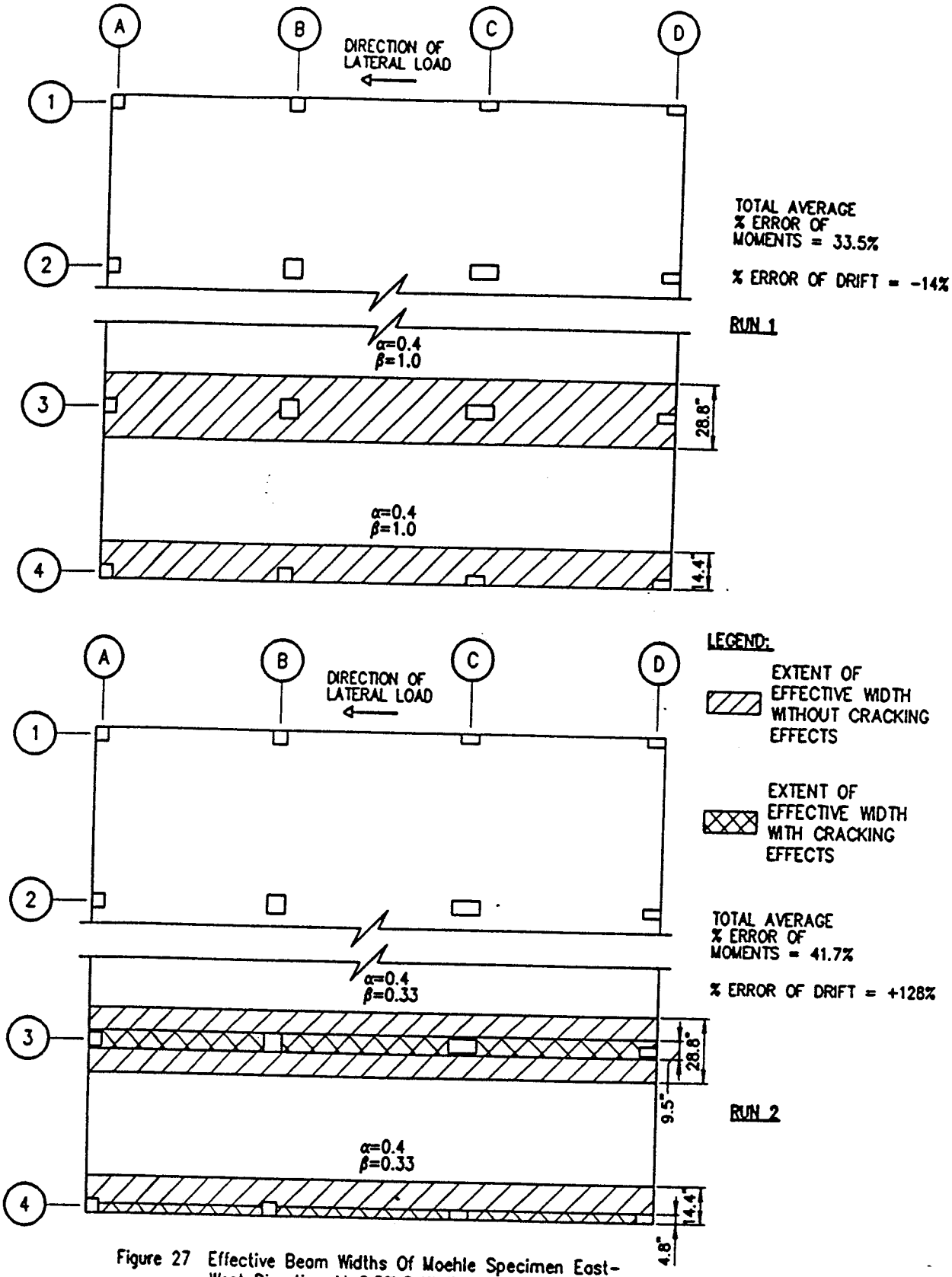

Figure 27 Effective Beam Widths Of Moehle Specimen East-West Direction At 0.5% Drift For Runs 1 And 2

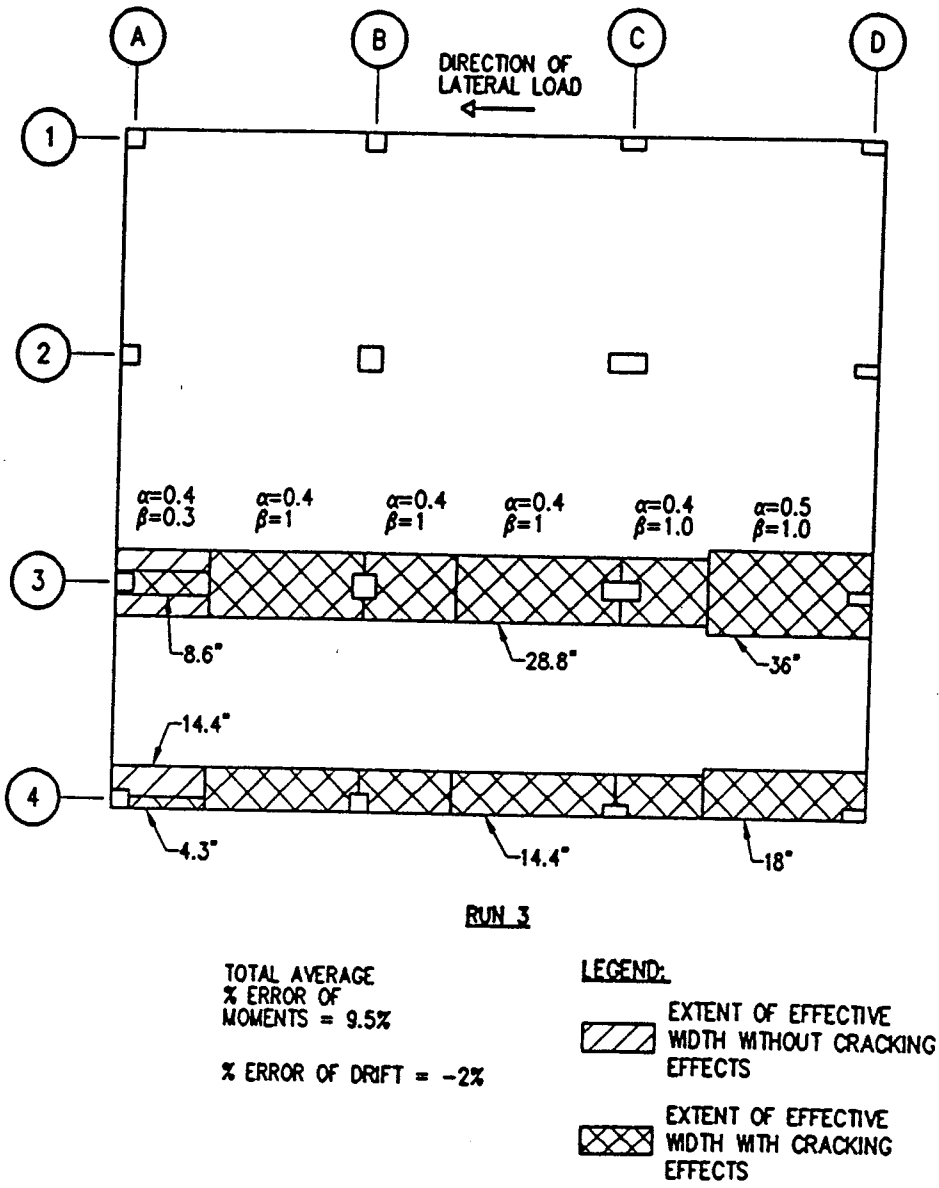

Figure 28 Effective Beam Widths Of Moehle Specimen East-West Direction At 0.5% Drift For Run 3

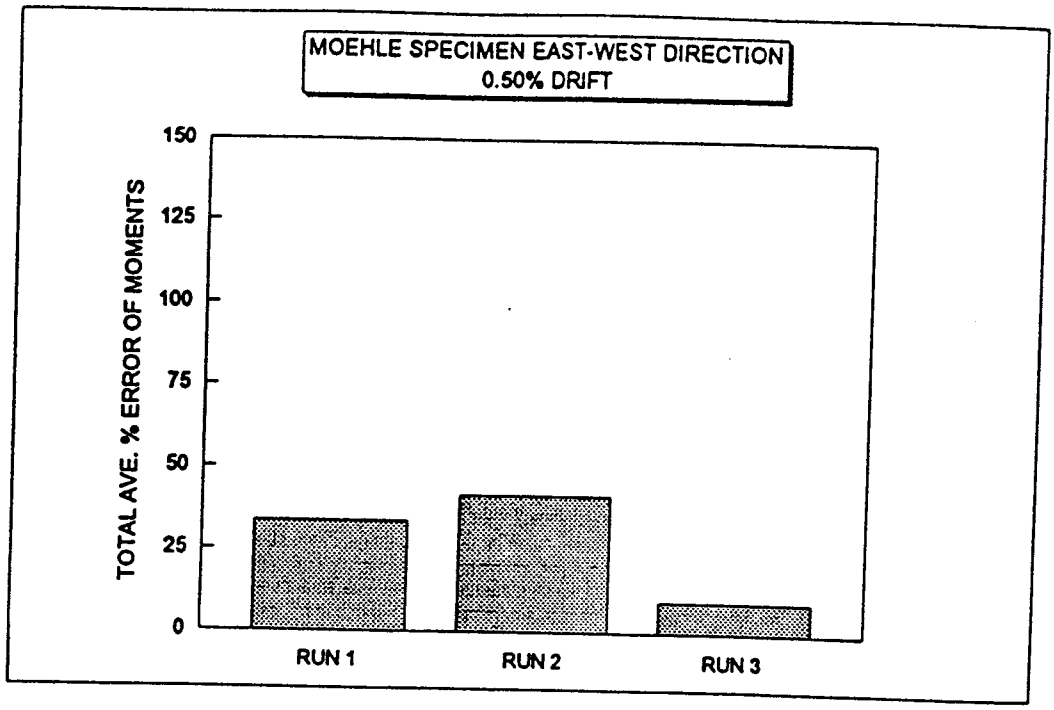

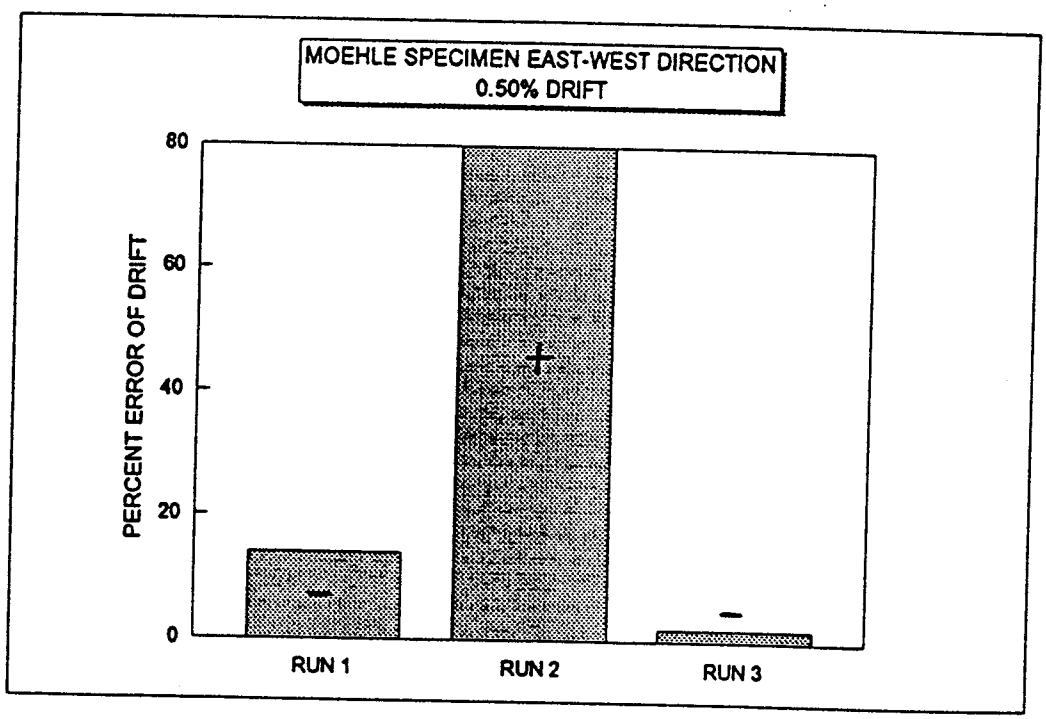

Figure 29 Total Average Percent Error Of Moments And Percent Error Of Drift Of Moehle Specimen East-West Direction At 0.5% Drift For Runs 1, 2 And 3

5.6.5 EFFECTIVE BEAM WIDTH TWO-BEAM MODEL APPLIED IN EAST-WEST DIRECTION AT 1.0% DRIFT

Table 36 lists the analytical vs. experimental results for the two-beam model analysis in the East-West direction at 1.0% drift.

At the 1.0% drift level, an increased reduction in stiffness in the regions of negative bending is expected. This reduction in stiffness leads to a redistribution of negative moments to the regions of positive bending. An adjusted β of 0.25 was applied in the region of negative bending in span B-A. An adjusted β of 0.7 was used throughout the remaining spans. These adjusted β values are consistent with the expected cracking behavior at the 1.0% drift level. Lateral drift obtained with the adjusted β values improved significantly, but remained 8% below the experimental drift. Correlation between analytical and experimental moments at the exterior connections improved significantly.

Figures 30 and 31 show the effective beam widths of the Moehle specimen at 1.0% drift for Runs 1 through 3 in the East-West direction. Figure 32 shows a graphical comparison of the TOTAL AVERAGE PERCENT ERROR OF MOMENTS and PERCENT ERROR OF DRIFT of the Moehle specimen at 1.0% drift for Runs 1 through 3 in the East-West direction.

Overall, the adjusted β values required in the East-West direction two-beam models were higher than those required in the North-South direction. This is due to the longer slab-beam lengths in the East-West direction, giving the specimen greater flexibility in this direction. The two-beam model was successful in improving the combined correlation of

analytical moments and drift with the experimental results, and reduced the total average percent error of analytical to experimental moments.

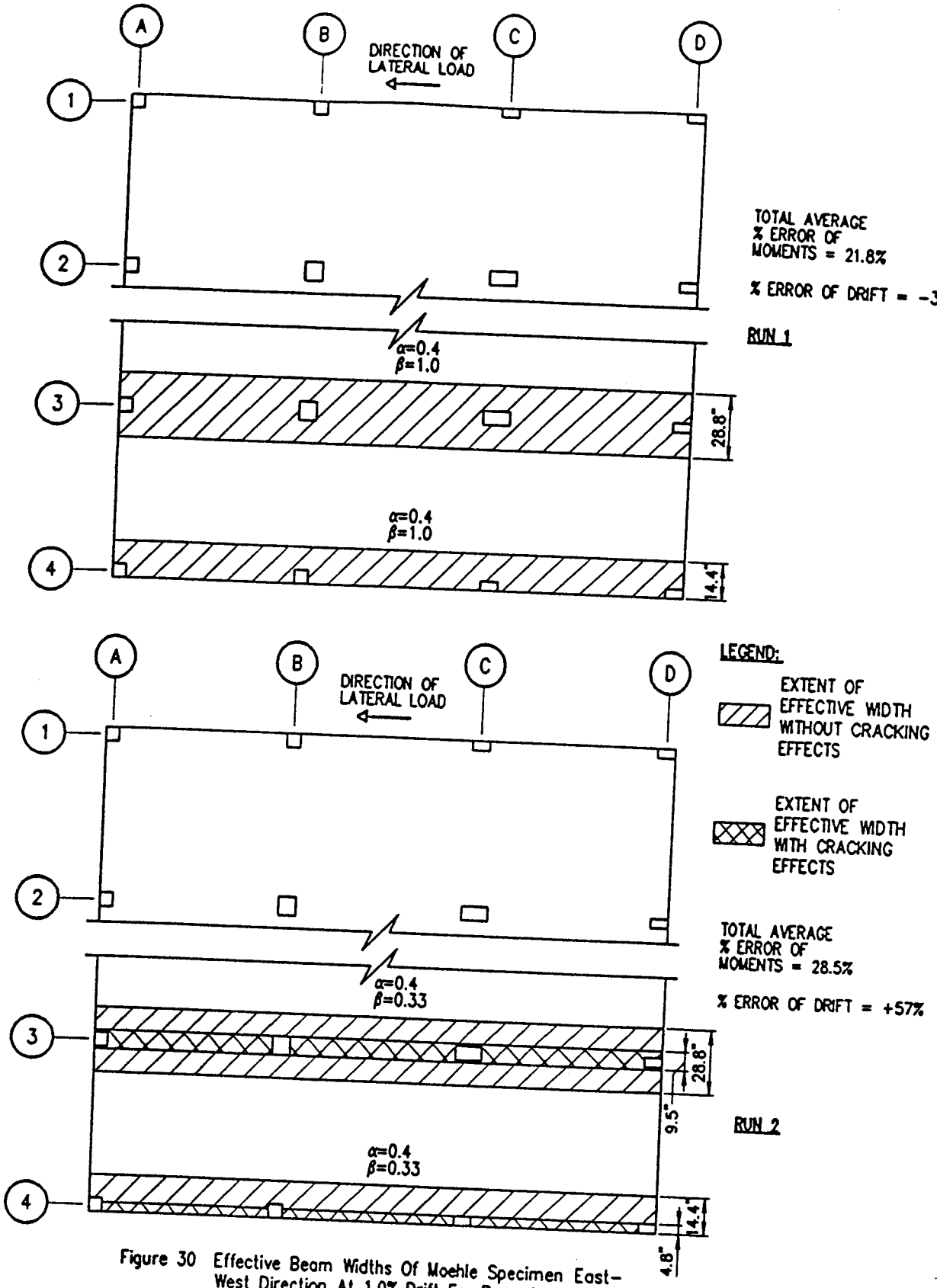

Figure 30 Effective Beam Widths Of Moehle Specimen East-West Direction At 1.0% Drift For Runs 1 And 2

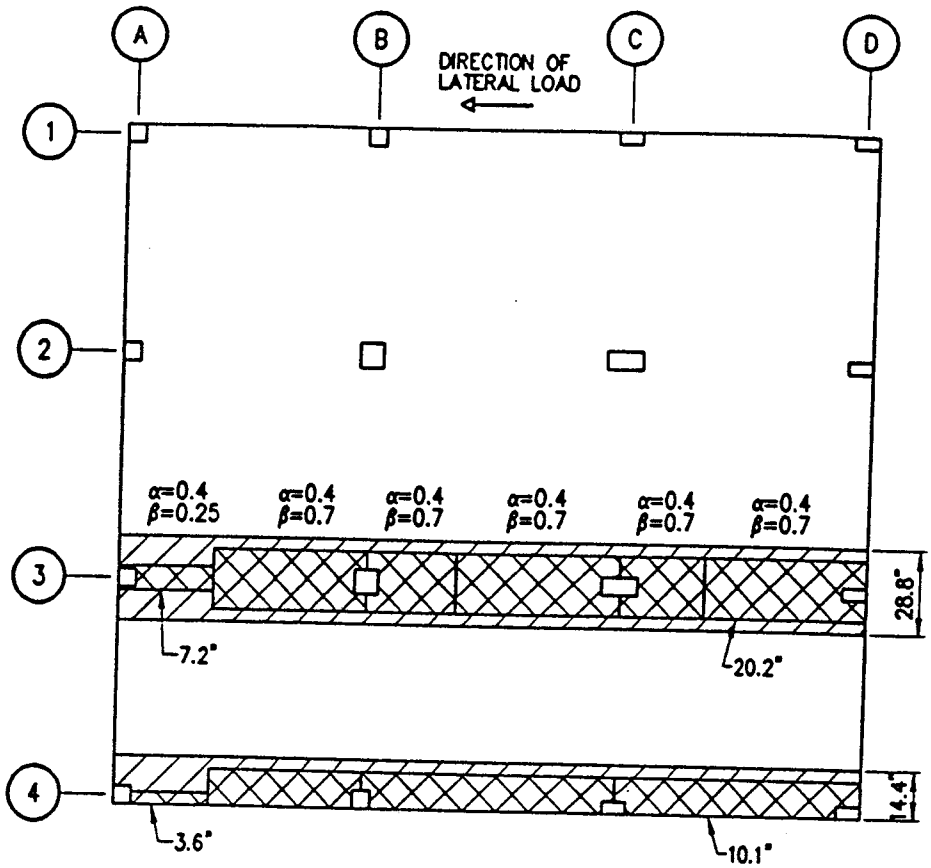

Figure 31 Effective Beam Widths Of Moehle Specimen East-West Direction At 1.0% Drift For Run 3

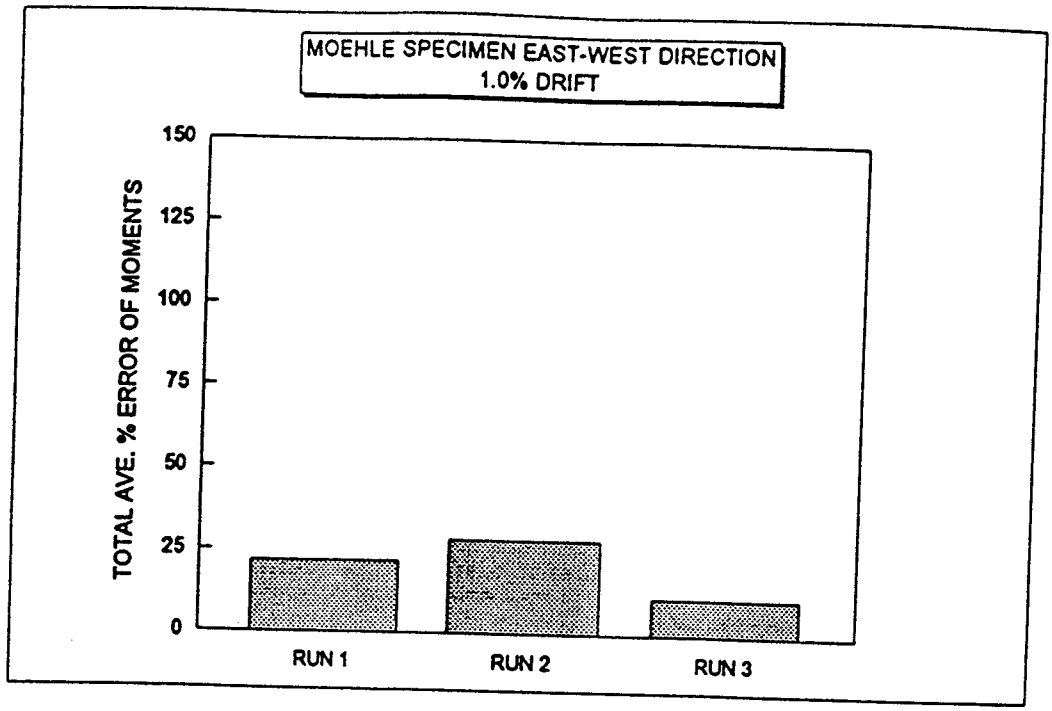

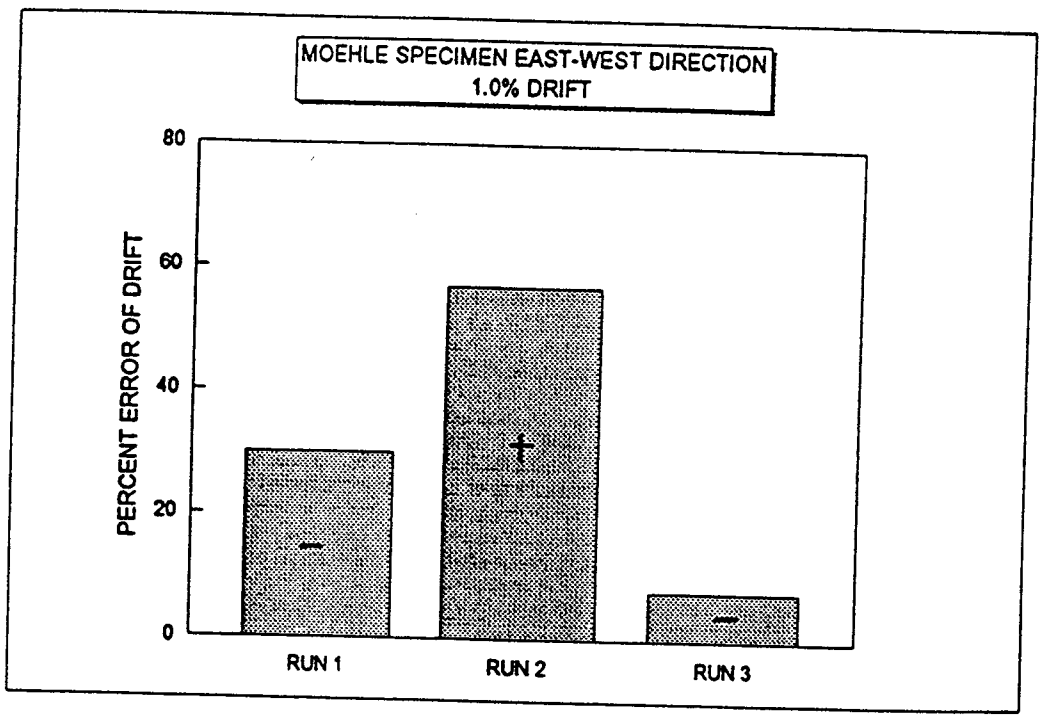

Figure 32 Total Average Percent Error Of Moments And Percent Error Of Drift Of Moehle Specimen East-West Direction At 1.0% Drift For Runs 1, 2 And 3

CHAPTER 6

SUMMARY RECOMMENDATIONS AND CONCLUSIONS

SUMMARY, RECOMMENDATIONS AND CONCLUSIONS

6.1 SUMMARY

An analytical study using the effective beam width and equivalent frame methods was performed on two flat plate specimens previously built and tested by Scavuzzo [27], and Hwang and Moehle [14].

The study was carried out to examine the ability of the analytical models to produce reasonable estimates of member actions and lateral drift under combined gravity and lateral loading.

The results of the study showed that the effective beam width method gave a poor prediction of bending moments and lateral drift. This was true when it was applied with, and without, cracking effects. The equivalent frame method, when applied without cracking effects, gave a good prediction of bending moments, but underestimated lateral drift. When applied with cracking effects, the equivalent frame method's prediction of bending moments worsened, while its prediction of lateral drift improved.

In order to improve prediction of moments and drift, and to better represent cracking behavior under combined vertical and lateral loading, a two-beam model is proposed. The two-beam model separates the slab-beam in each span into regions of positive and negative bending. The separation is made at the inflection point along each span. The proposed two-beam model can accommodate differences in the extent of cracking in positive and negative bending regions of the slab.

Alpha (α) values representing the effective slab width, and β values representing the extent of cracking, were applied to each slab-beam element of the Kirk and Moehle two-

beam models. These values were adjusted until reasonable correlation was obtained between experimental and analytical moment distribution and lateral drift.

Application of the proposed two-beam model to the Kirk specimens showed significant improvement in analytical estimation of moments and drift. However, due to the discontinuity of the Kirk specimen, it is less representative of a real structure than the Moehle specimen. The results of the Kirk study were therefore used only to confirm the recommendations drawn from the Moehle study. Notably, the modified beta values in the exterior positive region of bending compared well with the values obtained from the Moehle specimen.

Based on α and β values obtained from the two-beam model applied to the Moehle experimental specimen, the following recommendations are suggested for use in flat-plate analysis for combined vertical and lateral loads.

6.2 RECOMMENDATIONS

The recommended α and β values which follow are based upon the results of the Moehle specimen only. This specimen represents a realistic model of an actual flat-plate structure. The recommendations are based on the results of the two-beam model analysis applied to the Moehle specimen in the North-South and East-West directions. The various assumptions made in the analysis are listed in Chapters 4 and 5. The α and β values are related to the average clear span-to-depth ratio l_n/h of the Moehle specimen in the North-South and East-West directions.

It is recommended that for a clear span-to-depth ratio of $l_n/h = 20$, the inflection point be located at $0.55\ l_1$ measured from the first column in each span in the direction of

analysis. For $l_n/h = 30$, it is recommended that the inflection point be located at 0.65 l_l measured from the first column in each span in the direction of analysis. These values are based on the test specimens considered in this study. The actual point of contraflexure will vary depending on a number of factors, particularly the gravity load to lateral load ratio. Appropriate adjustments to these recommended locations can be made if desired, but slight changes in the point of contraflexure location are unlikely to have a substantial effect on the analysis results.

For a clear span-to-depth ratio $l_n/h = 20$ (short span in the Moehle specimen), the following recommendations are made at the 0.5% and 1.0% drift levels. (See Table 37 for a listing of the recommended α and β values.)

At the 0.5% drift level, corresponding to service loading, an α of 0.4 is recommended for all interior slab-beam elements of the two-beam model. Exterior connections are significantly less stiff than equivalent interior connections. Consequently, less of the slab is effective at these connections, and reduced α values are suggested. At the exterior connection subjected to negative slab bending, an α of 0.2 is recommended. At the exterior connection subjected to positive slab bending, an α of 0.3 was required to achieve good correlation between analytical and experimental results (Table 27). However, for consistency with the negative exterior connections, it is recommended that an α of 0.2 be applied.

For the low span-to-depth ratio of $l_n/h = 20$, significant slab cracking has occurred at the 0.5% drift level. To represent the extent of cracking, the following β values are recommended.

At the interior positive bending regions, a beta value of 0.5 is recommended. At the interior negative bending regions, a beta value of 0.3 is recommended. This lower beta value represents the increased cracking resulting from combined negative moments under vertical and lateral loads. Because of the weak exterior connections, larger bending moments are present at the first interior negative region. A beta value of 0.15 is recommended.

At the exterior positive region, a beta value of 0.5 is recommended. The gravity and lateral load moments counteract each other, resulting in the same cracking reduction as the interior positive connections. At the exterior negative region, as at interior negative regions, a beta value of 0.3 is recommended.

At the 1.0% drift level, which corresponds to ultimate load conditions, the recommended alpha values are the same as at the 0.5% drift level. The beta values at the 1.0% drift level are consistently 0.7 times the values at the 0.5% drift level.

For a span-to-depth ratio $l_n/h = 30$ (long span in the Moehle specimen), the following recommendations are made at the 0.5% and 1.0% drift levels. At 0.5% drift, an alpha value of 0.4 is recommended for both positive and negative bending regions of the two-beam model in all spans, except for the exterior negative bending region where an alpha value of 0.2 is suggested. Although an alpha value of 0.5 was initially used in the exterior positive region of bending (Table 33), the recommended alpha value of 0.4 in this region simplifies the modeling process without substantial change in the results.

At all regions of bending, except the exterior negative region, a beta value of 1.0 is recommended. This beta value reflects the observation that little or no cracking had

occurred at the 0.5% drift level when loading in the long span direction. The limited cracking is attributed to the flexibility of the long span slab-beam elements.

At the exterior negative bending region, a beta value of 0.6 is required at the 0.5% drift level. Due to the weakness of the exterior connection and the increased negative moment in this region, cracking occurs resulting in this reduced beta value.

At the 1.0% drift level, the recommended alpha values are the same as at the 0.5% drift level. The recommended beta values are again approximately 0.7 times the values at the 0.5% drift level.

The recommended alpha and beta values for $l_n/h = 20$ and $l_n/h = 30$ at the 0.5% and 1.0% drift levels are summarized in Table 37 and Figure 33. An example of the recommended alpha and beta values applied to a realistic flat-plate structure is provided in the appendix.

6.3 CONCLUSIONS

The following conclusions are made based on the findings of this study:

1) Under combined vertical and lateral loading, the effective beam width method gives a poor prediction of bending moments and lateral drift when applied with and without cracking effects.

2) Under combined vertical and lateral loading, the equivalent frame method gives a good prediction of bending moments but underestimates drift when applied without cracking effects ($\beta = 1.0$).

3) Under combined vertical and lateral loading, the equivalent frame method gives a poor prediction of bending moments and a better approximation of lateral drift when applied with cracking effects ($\beta = 0.33$).

4) A two-beam model is proposed which more accurately represents the cracking behavior of a flat-plate structure under combined vertical and lateral loading. The two-beam model separates each span of the original effective beam width and equivalent frame model into positive and negative bending regions. The separation is make at the inflection point in each span. Alpha (α) and beta (β) values can then be adjusted in each region of bending to more accurately model the slab stiffness and cracking behavior under combined vertical and lateral loading.

5) The inflection points should be located at 0.55 l_1 for a clear span-to-depth ratio $l_n/h = 20$, and 0.65 l_1 for a clear span-to-depth ratio $l_n/h = 30$. The location of the inflection points is measured from the first column in each span in the direction of lateral loading. Linear interpolation is recommended for clear span-to-depth ratios between 20 and 30.

6) By applying the two-beam model to the Kirk and Moehle specimens, alpha and beta values were obtained which produced improved correlation between experimental and analytical bending moments and lateral drift.

7) Based on the alpha and beta values obtained from the two-beam model analysis, a table of recommended alpha and beta values for flat-plate analysis using the effective beam width two-beam model was prepared. The

recommended alpha and beta values are listed for analysis at 0.5% drift (service load analysis) and 1.0% drift (ultimate load analysis). The recommended values are also listed for clear span-to-depth ratios of 20 and 30. Linear interpolation is recommended for clear span-to-depth ratios between 20 and 30.

Table 1 Kirk Specimen S-2 Effective Beam Width Runs 1 & 2
Lateral Load = 1.26 Kips

RUN 1	SPECIMEN S-2	EFF. BM. WIDTH	LATERAL LOAD = 1.26 KIPS	
CONNECTION	ACTUAL MOMENT KIP-IN	ETABS MOMENT KIP-IN	ETABS M/ACTUAL M	% ERROR
EXTERIOR	3.1	-7.1	-2.29	329.03
INTERIOR	47.3	58	1.23	22.62
TOTAL AVERAGE RATIO OF ETABS/ACTUAL MOMENT			1.76	
TOTAL AVERAGE PERCENT ERROR				175.83

ALPHA AND BETA VALUES USED FOR ANALYSIS		
	SPAN 1-2	SPAN 2-3
ALPHA	0.4	0.4
BETA	1	1

ACTUAL DRIFT (%)	0.39
ETABS DRIFT (%)	0.18

RUN 2	SPECIMEN S-2	EFF. BM. WIDTH	LATERAL LOAD = 1.26 KIPS	
CONNECTION	ACTUAL MOMENT KIP-IN	ETABS MOMENT KIP-IN	ETABS M/ACTUAL M	% ERROR
EXTERIOR	3.1	-9.6	-3.10	409.68
INTERIOR	47.3	60	1.27	26.85
TOTAL AVERAGE RATIO OF ETABS/ACTUAL MOMENT			2.18	
TOTAL AVERAGE PERCENT ERROR				218.26

ALPHA AND BETA VALUES USED FOR ANALYSIS		
	SPAN 1-2	SPAN 2-3
ALPHA	0.4	0.4
BETA	0.33	0.33

ACTUAL DRIFT (%)	0.39
ETABS DRIFT (%)	0.49

NOTE: COLUMN MOMENTS AT JOINT ARE POSITIVE CLOCKWISE!

Table 2 Kirk Specimen S-2 Effective Beam Width Run 3
Lateral Load = 1.26 Kips

RUN 3	SPECIMEN S-2	EFF. BM. WIDTH	LATERAL LOAD = 1.26 KIPS	
CONNECTION	ACTUAL MOMENT KIP-IN	ETABS MOMENT KIP-IN	ETABS M/ACTUAL M	% ERROR
EXTERIOR	3.1	4	1.29	29.03
INTERIOR	47.3	46.4	0.98	1.90
TOTAL AVERAGE RATIO OF ETABS/ACTUAL MOMENT			1.14	
TOTAL AVERAGE PERCENT ERROR				15.47

ALPHA AND BETA VALUES USED FOR ANALYSIS		
	SPAN 1-2	SPAN 2-3
ALPHA (POSITIVE)	0.4	0.4
ALPHA (NEGATIVE)	0.4	0.4
BETA (POSITIVE)	1	0.33
BETA (NEGATIVE)	0.33	0.33

ACTUAL DRIFT (%)	0.39
ETABS DRIFT (%)	0.38

NOTE: COLUMN MOMENTS AT JOINT ARE POSITIVE CLOCKWISE!

Table 3 Kirk Specimen S-2 Effective Beam Width Runs 1 & 2
Lateral Load = 2.205 Kips

RUN 1	SPECIMEN S-2	EFF. BM. WIDTH	LATERAL LOAD = 2.205 KIPS	
CONNECTION	ACTUAL MOMENT KIP-IN	ETABS MOMENT KIP-IN	ETABS M/ACTUAL M	% ERROR
EXTERIOR	16.6	4.8	0.29	71.08
INTERIOR	71.8	83.6	1.16	16.43
TOTAL AVERAGE RATIO OF ETABS/ACTUAL MOMENT			0.73	
TOTAL AVERAGE PERCENT ERROR				43.76

ALPHA AND BETA VALUES USED FOR ANALYSIS		
	SPAN 1-2	SPAN 2-3
ALPHA	0.4	0.4
BETA	1	1

ACTUAL DRIFT (%)	0.73
ETABS DRIFT (%)	0.29

RUN 2	SPECIMEN S-2	EFF. BM. WIDTH	LATERAL LOAD = 2.205 KIPS	
CONNECTION	ACTUAL MOMENT KIP-IN	ETABS MOMENT KIP-IN	ETABS M/ACTUAL M	% ERROR
EXTERIOR	16.6	3.2	0.19	80.72
INTERIOR	71.8	85.2	1.19	18.66
TOTAL AVERAGE RATIO OF ETABS/ACTUAL MOMENT			0.69	
TOTAL AVERAGE PERCENT ERROR				49.69

ALPHA AND BETA VALUES USED FOR ANALYSIS		
	SPAN 1-2	SPAN 2-3
ALPHA	0.4	0.4
BETA	0.33	0.33

ACTUAL DRIFT (%)	0.73
ETABS DRIFT (%)	0.81

NOTE: COLUMN MOMENTS AT JOINT ARE POSITIVE CLOCKWISE!

Table 4 Kirk Specimen S-2 Effective Beam Width Run 3
Lateral Load = 2.205 Kips

RUN 3	SPECIMEN S-2	EFF. BM. WIDTH	LATERAL LOAD = 2.205 KIPS	
CONNECTION	ACTUAL MOMENT KIP-IN	ETABS MOMENT KIP-IN	ETABS M/ACTUAL M	% ERROR
EXTERIOR	16.6	20.4	1.23	22.89
INTERIOR	71.8	68	0.95	5.29
TOTAL AVERAGE RATIO OF ETABS/ACTUAL MOMENT			1.09	
TOTAL AVERAGE PERCENT ERROR				14.09

ALPHA AND BETA VALUES USED FOR ANALYSIS		
	SPAN 1-2	SPAN 2-3
ALPHA (POSITIVE)	0.4	0.4
ALPHA (NEGATIVE)	0.4	0.4
BETA (POSITIVE)	0.75	0.25
BETA (NEGATIVE)	0.25	0.25

ACTUAL DRIFT (%)	0.73
ETABS DRIFT (%)	0.73

NOTE: COLUMN MOMENTS AT JOINT ARE POSITIVE CLOCKWISE!

Table 5 Kirk Specimen S-2 Effective Beam Width Runs 1 & 2
Lateral Load = 2.6 Kips

RUN 1	SPECIMEN S-2	EFF. BM. WIDTH	LATERAL LOAD = 2.6 KIPS	
CONNECTION	ACTUAL MOMENT KIP-IN	ETABS MOMENT KIP-IN	ETABS M/ACTUAL M	% ERROR
EXTERIOR	20.5	10	0.49	51.22
INTERIOR	83.5	94	1.13	12.57
TOTAL AVERAGE RATIO OF ETABS/ACTUAL MOMENT			0.81	
TOTAL AVERAGE PERCENT ERROR				31.90

ALPHA AND BETA VALUES USED FOR ANALYSIS		
	SPAN 1-2	SPAN 2-3
ALPHA	0.4	0.4
BETA	1	1

ACTUAL DRIFT (%)	0.84
ETABS DRIFT (%)	0.34

RUN 2	SPECIMEN S-2	EFF. BM. WIDTH	LATERAL LOAD = 2.6 KIPS	
CONNECTION	ACTUAL MOMENT KIP-IN	ETABS MOMENT KIP-IN	ETABS M/ACTUAL M	% ERROR
EXTERIOR	20.5	8.4	0.41	59.02
INTERIOR	83.5	95.6	1.14	14.49
TOTAL AVERAGE RATIO OF ETABS/ACTUAL MOMENT			0.78	
TOTAL AVERAGE PERCENT ERROR				36.76

ALPHA AND BETA VALUES USED FOR ANALYSIS		
	SPAN 1-2	SPAN 2-3
ALPHA	0.4	0.4
BETA	0.33	0.33

ACTUAL DRIFT (%)	0.84
ETABS DRIFT (%)	0.94

NOTE: COLUMN MOMENTS AT JOINT ARE POSITIVE CLOCKWISE!

Table 6 Kirk Specimen S-2 Effective Beam Width Run 3
Lateral Load = 2.6 Kips

RUN 3	SPECIMEN S-2	EFF. BM. WIDTH	LATERAL LOAD = 2.6 KIPS	
CONNECTION	ACTUAL MOMENT KIP-IN	ETABS MOMENT KIP-IN	ETABS M/ACTUAL M	% ERROR
EXTERIOR	20.5	24	1.17	17.07
INTERIOR	83.5	80	0.96	4.19
TOTAL AVERAGE RATIO OF ETABS/ACTUAL MOMENT			1.06	
TOTAL AVERAGE PERCENT ERROR				10.63

ALPHA AND BETA VALUES USED FOR ANALYSIS		
	SPAN 1-2	SPAN 2-3
ALPHA (POSITIVE)	0.4	0.4
ALPHA (NEGATIVE)	0.4	0.4
BETA (POSITIVE)	0.65	0.25
BETA (NEGATIVE)	0.25	0.25

ACTUAL DRIFT (%)	0.84
ETABS DRIFT (%)	0.84

NOTE: COLUMN MOMENTS AT JOINT ARE POSITIVE CLOCKWISE!

Table 7 Kirk Specimen S-4 Effective Beam Width Runs 1 & 2
Lateral Load = 1.313 Kips

RUN 1	SPECIMEN S-4	EFF. BM. WIDTH	LATERAL LOAD = 1.313 KIPS	
CONNECTION	ACTUAL MOMENT KIP-IN	ETABS MOMENT KIP-IN	ETABS M/ACTUAL M	% ERROR
EXTERIOR	7.3	-6	-0.82	182.19
INTERIOR	45.5	58.8	1.29	29.23
TOTAL AVERAGE RATIO OF ETABS/ACTUAL MOMENT			1.06	
TOTAL AVERAGE PERCENT ERROR				105.71

ALPHA AND BETA VALUES USED FOR ANALYSIS		
	SPAN 1-2	SPAN 2-3
ALPHA	0.4	0.4
BETA	1	1

ACTUAL DRIFT (%)	0.48
ETABS DRIFT (%)	0.2

RUN 2	SPECIMEN S-4	EFF. BM. WIDTH	LATERAL LOAD = 1.313 KIPS	
CONNECTION	ACTUAL MOMENT KIP-IN	ETABS MOMENT KIP-IN	ETABS M/ACTUAL M	% ERROR
EXTERIOR	7.3	-7.6	-1.04	204.11
INTERIOR	45.5	60	1.32	31.87
TOTAL AVERAGE RATIO OF ETABS/ACTUAL MOMENT			1.18	
TOTAL AVERAGE PERCENT ERROR				117.99

ALPHA AND BETA VALUES USED FOR ANALYSIS		
	SPAN 1-2	SPAN 2-3
ALPHA	0.4	0.4
BETA	0.33	0.33

ACTUAL DRIFT (%)	0.48
ETABS DRIFT (%)	0.54

NOTE: COLUMN MOMENTS AT JOINT ARE POSITIVE CLOCKWISE!

Table 8 Kirk Specimen S-4 Effective Beam Width Run 3
Lateral Load = 1.313 Kips

RUN 3	SPECIMEN S-4	EFF. BM. WIDTH	LATERAL LOAD = 1.313 KIPS	
CONNECTION	ACTUAL MOMENT KIP-IN	ETABS MOMENT KIP-IN	ETABS M/ACTUAL M	% ERROR
EXTERIOR	7.3	8	1.10	9.59
INTERIOR	45.5	44.4	0.98	2.42
TOTAL AVERAGE RATIO OF ETABS/ACTUAL MOMENT			1.04	
TOTAL AVERAGE PERCENT ERROR				6.00

ALPHA AND BETA VALUES USED FOR ANALYSIS		
	SPAN 1-2	SPAN 2-3
ALPHA (POSITIVE)	0.4	0.4
ALPHA (NEGATIVE)	0.4	0.4
BETA (POSITIVE)	1	0.3
BETA (NEGATIVE)	0.3	0.3

ACTUAL DRIFT (%)	0.48
ETABS DRIFT (%)	0.5

NOTE: COLUMN MOMENTS AT JOINT ARE POSITIVE CLOCKWISE!

Table 9 Kirk Specimen S-4 Effective Beam Width Runs 1 & 2
Lateral Load = 1.970 Kips

RUN 1	SPECIMEN S-4	EFF. BM. WIDTH	LATERAL LOAD = 1.970 KIPS	
CONNECTION	ACTUAL MOMENT KIP-IN	ETABS MOMENT KIP-IN	ETABS M/ACTUAL M	% ERROR
EXTERIOR	16.3	5.2	0.32	68.10
INTERIOR	62.5	73.6	1.18	17.76
TOTAL AVERAGE RATIO OF ETABS/ACTUAL MOMENT			0.75	
TOTAL AVERAGE PERCENT ERROR				42.93

ALPHA AND BETA VALUES USED FOR ANALYSIS		
	SPAN 1-2	SPAN 2-3
ALPHA	0.4	0.4
BETA	1	1

ACTUAL DRIFT (%)	0.7
ETABS DRIFT (%)	0.27

RUN 2	SPECIMEN S-4	EFF. BM. WIDTH	LATERAL LOAD = 1.970 KIPS	
CONNECTION	ACTUAL MOMENT KIP-IN	ETABS MOMENT KIP-IN	ETABS M/ACTUAL M	% ERROR
EXTERIOR	16.3	3.6	0.22	77.91
INTERIOR	62.5	75.2	1.20	20.32
TOTAL AVERAGE RATIO OF ETABS/ACTUAL MOMENT			0.71	
TOTAL AVERAGE PERCENT ERROR				49.12

ALPHA AND BETA VALUES USED FOR ANALYSIS		
	SPAN 1-2	SPAN 2-3
ALPHA	0.4	0.4
BETA	0.33	0.33

ACTUAL DRIFT (%)	0.7
ETABS DRIFT (%)	0.75

NOTE: COLUMN MOMENTS AT JOINT ARE POSITIVE CLOCKWISE!

Table 10 Kirk Specimen S-4 Effective Beam Width Run 3
Lateral Load = 1.970 Kips

RUN 3	SPECIMEN S-4	EFF. BM. WIDTH	LATERAL LOAD = 1.970 KIPS	
CONNECTION	ACTUAL MOMENT KIP-IN	ETABS MOMENT KIP-IN	ETABS M/ACTUAL M	% ERROR
EXTERIOR	16.3	20.4	1.25	25.15
INTERIOR	62.5	58.4	0.93	6.56
TOTAL AVERAGE RATIO OF ETABS/ACTUAL MOMENT			1.09	
TOTAL AVERAGE PERCENT ERROR				15.86

ALPHA AND BETA VALUES USED FOR ANALYSIS		
	SPAN 1-2	SPAN 2-3
ALPHA (POSITIVE)	0.4	0.4
ALPHA (NEGATIVE)	0.4	0.4
BETA (POSITIVE)	0.75	0.25
BETA (NEGATIVE)	0.25	0.25

ACTUAL DRIFT (%)	0.7
ETABS DRIFT (%)	0.71

NOTE: COLUMN MOMENTS AT JOINT ARE POSITIVE CLOCKWISE!

Table 11 Kirk Specimen S-4 Effective Beam Width Runs 1 & 2
Lateral Load = 2.6 Kips

RUN 1	SPECIMEN S-4	EFF. BM. WIDTH	LATERAL LOAD = 2.6 KIPS	
CONNECTION	ACTUAL MOMENT KIP-IN	ETABS MOMENT KIP-IN	ETABS M/ACTUAL M	% ERROR
EXTERIOR	23.9	14.8	0.62	38.08
INTERIOR	80.1	89.2	1.11	11.36
TOTAL AVERAGE RATIO OF ETABS/ACTUAL MOMENT			0.87	
TOTAL AVERAGE PERCENT ERROR				24.72

ALPHA AND BETA VALUES USED FOR ANALYSIS		
	SPAN 1-2	SPAN 2-3
ALPHA	0.4	0.4
BETA	1	1

ACTUAL DRIFT (%)	0.98
ETABS DRIFT (%)	0.35

RUN 2	SPECIMEN S-4	EFF. BM. WIDTH	LATERAL LOAD = 2.6 KIPS	
CONNECTION	ACTUAL MOMENT KIP-IN	ETABS MOMENT KIP-IN	ETABS M/ACTUAL M	% ERROR
EXTERIOR	23.9	13.2	0.55	44.77
INTERIOR	80.1	90.8	1.13	13.36
TOTAL AVERAGE RATIO OF ETABS/ACTUAL MOMENT			0.84	
TOTAL AVERAGE PERCENT ERROR				29.06

ALPHA AND BETA VALUES USED FOR ANALYSIS		
	SPAN 1-2	SPAN 2-3
ALPHA	0.4	0.4
BETA	0.33	0.33

ACTUAL DRIFT (%)	0.98
ETABS DRIFT (%)	0.96

NOTE: COLUMN MOMENTS AT JOINT ARE POSITIVE CLOCKWISE!

Table 12 Kirk Specimen S-4 Effective Beam Width Run 3
Lateral Load = 2.6 Kips

RUN 3	SPECIMEN S-4	EFF. BM. WIDTH	LATERAL LOAD = 2.6 KIPS	
CONNECTION	ACTUAL MOMENT KIP-IN	ETABS MOMENT KIP-IN	ETABS M/ACTUAL M	% ERROR
EXTERIOR	23.9	28.8	1.21	20.50
INTERIOR	80.1	75.2	0.94	6.12
TOTAL AVERAGE RATIO OF ETABS/ACTUAL MOMENT			1.07	
TOTAL AVERAGE PERCENT ERROR				13.31

ALPHA AND BETA VALUES USED FOR ANALYSIS		
	SPAN 1-2	SPAN 2-3
ALPHA (POSITIVE)	0.4	0.4
ALPHA (NEGATIVE)	0.4	0.4
BETA (POSITIVE)	0.6	0.25
BETA (NEGATIVE)	0.25	0.25

ACTUAL DRIFT (%)	0.98
ETABS DRIFT (%)	0.98

NOTE: COLUMN MOMENTS AT JOINT ARE POSITIVE CLOCKWISE!

Table 13 Kirk Specimen S-2 Equivalent Frame Runs 1 & 2
Lateral Load = 1.26 Kips

RUN 1	SPECIMEN S-2	EQUIVALENT FRAME LATERAL LOAD = 1.26 KIPS		
CONNECTION	ACTUAL MOMENT KIP-IN	ETABS MOMENT KIP-IN	ETABS M/ACTUAL M	% ERROR
EXTERIOR	3.1	4	1.29	29.03
INTERIOR	47.3	46.4	0.98	1.90
TOTAL AVERAGE RATIO OF ETABS/ACTUAL MOMENT			1.14	
TOTAL AVERAGE PERCENT ERROR				15.47

ALPHA AND BETA VALUES USED FOR ANALYSIS		
	SPAN 1-2	SPAN 2-3
ALPHA	1	1
BETA	1	1

ACTUAL DRIFT (%)	0.39
ETABS DRIFT (%)	0.17

RUN 2	SPECIMEN S-2	EQUIVALENT FRAME LATERAL LOAD = 1.26 KIPS		
CONNECTION	ACTUAL MOMENT KIP-IN	ETABS MOMENT KIP-IN	ETABS M/ACTUAL M	% ERROR
EXTERIOR	3.1	-3.2	-1.03	203.23
INTERIOR	47.3	53.6	1.13	13.32
TOTAL AVERAGE RATIO OF ETABS/ACTUAL MOMENT			1.08	
TOTAL AVERAGE PERCENT ERROR				108.27

ALPHA AND BETA VALUES USED FOR ANALYSIS		
	SPAN 1-2	SPAN 2-3
ALPHA	1	1
BETA	0.33	0.33

ACTUAL DRIFT (%)	0.39
ETABS DRIFT (%)	0.3

NOTE: COLUMN MOMENTS AT JOINT ARE POSITIVE CLOCKWISE!

Table 14 Kirk Specimen S-2 Equivalent Frame Run 3
Lateral Load = 1.26 Kips

RUN 3	SPECIMEN S-2	EQUIVALENT FRAME LATERAL LOAD = 1.26 KIPS		
CONNECTION	ACTUAL MOMENT KIP-IN	ETABS MOMENT KIP-IN	ETABS M/ACTUAL M	% ERROR
EXTERIOR	3.1	2.8	0.90	9.68
INTERIOR	47.3	47.6	1.01	0.63
TOTAL AVERAGE RATIO OF ETABS/ACTUAL MOMENT			0.95	
TOTAL AVERAGE PERCENT ERROR				5.16

ALPHA AND BETA VALUES USED FOR ANALYSIS		
	SPAN 1-2	SPAN 2-3
ALPHA (POSITIVE)	0.4	0.4
ALPHA (NEGATIVE)	0.4	0.4
BETA (POSITIVE)	1	0.5
BETA (NEGATIVE)	0.5	0.5

ACTUAL DRIFT (%)	0.39
ETABS DRIFT (%)	0.37

NOTE: COLUMN MOMENTS AT JOINT ARE POSITIVE CLOCKWISE!

Table 15 Kirk Specimen S-2 Equivalent Frame Runs 1 & 2
Lateral Load = 2.205 Kips

RUN 1	SPECIMEN S-2	EQUIVALENT FRAME	LATERAL LOAD = 2.205 KIPS	
CONNECTION	ACTUAL MOMENT KIP-IN	ETABS MOMENT KIP-IN	ETABS M/ACTUAL M	% ERROR
EXTERIOR	16.5	18	1.09	9.09
INTERIOR	71.5	70	0.98	2.10
TOTAL AVERAGE RATIO OF ETABS/ACTUAL MOMENT			1.03	
TOTAL AVERAGE PERCENT ERROR				5.59

ALPHA AND BETA VALUES USED FOR ANALYSIS		
	SPAN 1-2	SPAN 2-3
ALPHA	1	1
BETA	1	1

ACTUAL DRIFT (%)	0.73
ETABS DRIFT (%)	0.27

RUN 2	SPECIMEN S-2	EQUIVALENT FRAME	LATERAL LOAD = 2.205 KIPS	
CONNECTION	ACTUAL MOMENT KIP-IN	ETABS MOMENT KIP-IN	ETABS M/ACTUAL M	% ERROR
EXTERIOR	16.5	9.6	0.58	41.82
INTERIOR	71.5	78.8	1.10	10.21
TOTAL AVERAGE RATIO OF ETABS/ACTUAL MOMENT			0.84	
TOTAL AVERAGE PERCENT ERROR				26.01

ALPHA AND BETA VALUES USED FOR ANALYSIS		
	SPAN 1-2	SPAN 2-3
ALPHA	1	1
BETA	0.33	0.33

ACTUAL DRIFT (%)	0.73
ETABS DRIFT (%)	0.48

NOTE: COLUMN MOMENTS AT JOINT ARE POSITIVE CLOCKWISE!

Table 16 Kirk Specimen S-2 Equivalent Frame Run 3
Lateral Load = 2.205 Kips

RUN 3	SPECIMEN S-2	EQUIVALENT FRAME	LATERAL LOAD = 2.205 KIPS	
CONNECTION	ACTUAL MOMENT KIP-IN	ETABS MOMENT KIP-IN	ETABS M/ACTUAL M	% ERROR
EXTERIOR	16.5	19.2	1.16	16.36
INTERIOR	71.5	69.2	0.97	3.22
TOTAL AVERAGE RATIO OF ETABS/ACTUAL MOMENT			1.07	
TOTAL AVERAGE PERCENT ERROR				9.79

ALPHA AND BETA VALUES USED FOR ANALYSIS		
	SPAN 1-2	SPAN 2-3
ALPHA (POSITIVE)	0.4	0.4
ALPHA (NEGATIVE)	0.4	0.4
BETA (POSITIVE)	0.75	0.33
BETA (NEGATIVE)	0.33	0.33

ACTUAL DRIFT (%)	0.73
ETABS DRIFT (%)	0.76

NOTE: COLUMN MOMENTS AT JOINT ARE POSITIVE CLOCKWISE!

Table 17 Kirk Specimen S-2 Equivalent Frame Runs 1 & 2
Lateral Load = 2.6 Kips

RUN 1	SPECIMEN S-2	EQUIVALENT FRAME	LATERAL LOAD = 2.6 KIPS	
CONNECTION	ACTUAL MOMENT KIP-IN	ETABS MOMENT KIP-IN	ETABS M/ACTUAL M	% ERROR
EXTERIOR	20.5	24.4	1.19	19.02
INTERIOR	83.5	79.6	0.95	4.67
TOTAL AVERAGE RATIO OF ETABS/ACTUAL MOMENT			1.07	
TOTAL AVERAGE PERCENT ERROR				11.85

ALPHA AND BETA VALUES USED FOR ANALYSIS		
	SPAN 1-2	SPAN 2-3
ALPHA	1	1
BETA	1	1

ACTUAL DRIFT (%)	0.84
ETABS DRIFT (%)	0.32

RUN 2	SPECIMEN S-2	EQUIVALENT FRAME	LATERAL LOAD = 2.6 KIPS	
CONNECTION	ACTUAL MOMENT KIP-IN	ETABS MOMENT KIP-IN	ETABS M/ACTUAL M	% ERROR
EXTERIOR	20.5	15.2	0.74	25.85
INTERIOR	83.5	88.8	1.06	6.35
TOTAL AVERAGE RATIO OF ETABS/ACTUAL MOMENT			0.90	
TOTAL AVERAGE PERCENT ERROR				16.10

ALPHA AND BETA VALUES USED FOR ANALYSIS		
	SPAN 1-2	SPAN 2-3
ALPHA	1	1
BETA	0.33	0.33

ACTUAL DRIFT (%)	0.84
ETABS DRIFT (%)	0.56

NOTE: COLUMN MOMENTS AT JOINT ARE POSITIVE CLOCKWISE!

Table 18 Kirk Specimen S-2 Equivalent Frame Run 3
Lateral Load = 2.6 Kips

RUN 3	SPECIMEN S-2	EQUIVALENT FRAME LATERAL LOAD = 2.6 KIPS		
CONNECTION	ACTUAL MOMENT KIP-IN	ETABS MOMENT KIP-IN	ETABS M/ACTUAL M	% ERROR
EXTERIOR	20.5	24	1.17	17.07
INTERIOR	83.5	80	0.96	4.19
TOTAL AVERAGE RATIO OF ETABS/ACTUAL MOMENT			1.06	
TOTAL AVERAGE PERCENT ERROR				10.63

ALPHA AND BETA VALUES USED FOR ANALYSIS		
	SPAN 1-2	SPAN 2-3
ALPHA (POSITIVE)	0.4	0.4
ALPHA (NEGATIVE)	0.4	0.4
BETA (POSITIVE)	0.65	0.33
BETA (NEGATIVE)	0.33	0.33

ACTUAL DRIFT (%)	0.84
ETABS DRIFT (%)	0.92

NOTE: COLUMN MOMENTS AT JOINT ARE POSITIVE CLOCKWISE!

Table 19 Kirk Specimen S-4 Equivalent Frame Runs 1 & 2
Lateral Load = 1.313 Kips

RUN 1	SPECIMEN S-4	EQUIVALENT FRAME LATERAL LOAD = 1.313 KIPS		
CONNECTION	ACTUAL MOMENT KIP-IN	ETABS MOMENT KIP-IN	ETABS M/ACTUAL M	% ERROR
EXTERIOR	7.2	5.2	0.72	27.78
INTERIOR	45.2	47.2	1.04	4.42
TOTAL AVERAGE RATIO OF ETABS/ACTUAL MOMENT			0.88	
TOTAL AVERAGE PERCENT ERROR				16.10

ALPHA AND BETA VALUES USED FOR ANALYSIS		
	SPAN 1-2	SPAN 2-3
ALPHA	1	1
BETA	1	1

ACTUAL DRIFT (%)	0.48
ETABS DRIFT (%)	0.18

RUN 2	SPECIMEN S-4	EQUIVALENT FRAME LATERAL LOAD = 1.313 KIPS		
CONNECTION	ACTUAL MOMENT KIP-IN	ETABS MOMENT KIP-IN	ETABS M/ACTUAL M	% ERROR
EXTERIOR	7.2	-2	-0.28	127.78
INTERIOR	45.2	54.4	1.20	20.35
TOTAL AVERAGE RATIO OF ETABS/ACTUAL MOMENT			0.74	
TOTAL AVERAGE PERCENT ERROR				74.07

ALPHA AND BETA VALUES USED FOR ANALYSIS		
	SPAN 1-2	SPAN 2-3
ALPHA	1	1
BETA	0.33	0.33

ACTUAL DRIFT (%)	0.48
ETABS DRIFT (%)	0.32

NOTE: COLUMN MOMENTS AT JOINT ARE POSITIVE CLOCKWISE!

Table 20 Kirk Specimen S-4 Equivalent Frame Run 3
Lateral Load = 1.313 Kips

RUN 3	SPECIMEN S-4	EQUIVALENT FRAME	LATERAL LOAD = 1.313 KIPS	
CONNECTION	ACTUAL MOMENT KIP-IN	ETABS MOMENT KIP-IN	ETABS M/ACTUAL M	% ERROR
EXTERIOR	7.2	6.4	0.89	11.11
INTERIOR	45.2	46	1.02	1.77
TOTAL AVERAGE RATIO OF ETABS/ACTUAL MOMENT			0.95	
TOTAL AVERAGE PERCENT ERROR				6.44

ALPHA AND BETA VALUES USED FOR ANALYSIS		
	SPAN 1-2	SPAN 2-3
ALPHA (POSITIVE)	0.4	0.4
ALPHA (NEGATIVE)	0.4	0.4
BETA (POSITIVE)	1	0.33
BETA (NEGATIVE)	0.33	0.33

ACTUAL DRIFT (%)	0.48
ETABS DRIFT (%)	0.49

NOTE: COLUMN MOMENTS AT JOINT ARE POSITIVE CLOCKWISE!

Table 21 Kirk Specimen S-4 Equivalent Frame Runs 1 & 2
Lateral Load = 1.970 Kips

RUN 1	SPECIMEN S-4	EQUIVALENT FRAME	LATERAL LOAD = 1.970 KIPS	
CONNECTION	ACTUAL MOMENT KIP-IN	ETABS MOMENT KIP-IN	ETABS M/ACTUAL M	% ERROR
EXTERIOR	16.3	16.8	1.03	3.07
INTERIOR	62.5	62	0.99	0.80
TOTAL AVERAGE RATIO OF ETABS/ACTUAL MOMENT			1.01	
TOTAL AVERAGE PERCENT ERROR				1.93

ALPHA AND BETA VALUES USED FOR ANALYSIS		
	SPAN 1-2	SPAN 2-3
ALPHA	1	1
BETA	1	1

ACTUAL DRIFT (%)	0.7
ETABS DRIFT (%)	0.25

RUN 2	SPECIMEN S-4	EQUIVALENT FRAME	LATERAL LOAD = 1.970 KIPS	
CONNECTION	ACTUAL MOMENT KIP-IN	ETABS MOMENT KIP-IN	ETABS M/ACTUAL M	% ERROR
EXTERIOR	16.3	9.2	0.56	43.56
INTERIOR	62.5	69.6	1.11	11.36
TOTAL AVERAGE RATIO OF ETABS/ACTUAL MOMENT			0.84	
TOTAL AVERAGE PERCENT ERROR				27.46

ALPHA AND BETA VALUES USED FOR ANALYSIS		
	SPAN 1-2	SPAN 2-3
ALPHA	1	1
BETA	0.33	0.33

ACTUAL DRIFT (%)	0.7
ETABS DRIFT (%)	0.44

NOTE: COLUMN MOMENTS AT JOINT ARE POSITIVE CLOCKWISE!

Table 22 Kirk Specimen S-4 Equivalent Frame Run 3
Lateral Load = 1.970 Kips

RUN 3	SPECIMEN S-4	EQUIVALENT FRAME	LATERAL LOAD = 1.970 KIPS	
CONNECTION	ACTUAL MOMENT KIP-IN	ETABS MOMENT KIP-IN	ETABS M/ACTUAL M	% ERROR
EXTERIOR	16.3	19.6	1.20	20.25
INTERIOR	62.5	59.2	0.95	5.28
TOTAL AVERAGE RATIO OF ETABS/ACTUAL MOMENT			1.07	
TOTAL AVERAGE PERCENT ERROR				12.76

ALPHA AND BETA VALUES USED FOR ANALYSIS		
	SPAN 1-2	SPAN 2-3
ALPHA (POSITIVE)	0.4	0.4
ALPHA (NEGATIVE)	0.4	0.4
BETA (POSITIVE)	0.75	0.3
BETA (NEGATIVE)	0.3	0.3

ACTUAL DRIFT (%)	0.7
ETABS DRIFT (%)	0.74

NOTE: COLUMN MOMENTS AT JOINT ARE POSITIVE CLOCKWISE!

Table 23 Kirk Specimen S-4 Equivalent Frame Runs 1 & 2
Lateral Load = 2.6 Kips

RUN 1	SPECIMEN S-4	EQUIVALENT FRAME LATERAL LOAD = 2.6 KIPS		
CONNECTION	ACTUAL MOMENT KIP-IN	ETABS MOMENT KIP-IN	ETABS M/ACTUAL M	% ERROR
EXTERIOR	23.9	27.2	1.14	13.81
INTERIOR	80.1	76.8	0.96	4.12
TOTAL AVERAGE RATIO OF ETABS/ACTUAL MOMENT			1.05	
TOTAL AVERAGE PERCENT ERROR				8.96

ALPHA AND BETA VALUES USED FOR ANALYSIS		
	SPAN 1-2	SPAN 2-3
ALPHA	1	1
BETA	1	1

ACTUAL DRIFT (%)	0.98
ETABS DRIFT (%)	0.32

RUN 2	SPECIMEN S-4	EQUIVALENT FRAME LATERAL LOAD = 2.6 KIPS		
CONNECTION	ACTUAL MOMENT KIP-IN	ETABS MOMENT KIP-IN	ETABS M/ACTUAL M	% ERROR
EXTERIOR	23.9	19.6	0.82	17.99
INTERIOR	80.1	84.4	1.05	5.37
TOTAL AVERAGE RATIO OF ETABS/ACTUAL MOMENT			0.94	
TOTAL AVERAGE PERCENT ERROR				11.68

ALPHA AND BETA VALUES USED FOR ANALYSIS		
	SPAN 1-2	SPAN 2-3
ALPHA	1	1
BETA	0.33	0.33

ACTUAL DRIFT (%)	0.98
ETABS DRIFT (%)	0.57

NOTE: COLUMN MOMENTS AT JOINT ARE POSITIVE CLOCKWISE!

Table 24 Kirk Specimen S-4 Equivalent Frame Run 3
Lateral Load = 2.6 Kips

RUN 3	SPECIMEN S-4	EQUIVALENT FRAME LATERAL LOAD = 2.6 KIPS		
CONNECTION	ACTUAL MOMENT KIP-IN	ETABS MOMENT KIP-IN	ETABS M/ACTUAL M	% ERROR
EXTERIOR	23.9	28.4	1.19	18.83
INTERIOR	80.1	75.6	0.94	5.62
TOTAL AVERAGE RATIO OF ETABS/ACTUAL MOMENT			1.07	
TOTAL AVERAGE PERCENT ERROR				12.22

ALPHA AND BETA VALUES USED FOR ANALYSIS		
	SPAN 1-2	SPAN 2-3
ALPHA (POSITIVE)	0.4	0.4
ALPHA (NEGATIVE)	0.4	0.4
BETA (POSITIVE)	0.65	0.3
BETA (NEGATIVE)	0.3	0.3

ACTUAL DRIFT (%)	0.98
ETABS DRIFT (%)	0.98

NOTE: COLUMN MOMENTS AT JOINT ARE POSITIVE CLOCKWISE!

Table 25 Moehle Specimen Run 1 North-South Direction 0.5% Drift
Lateral Load = 15.15 Kips

RUN 1	MOEHLE SPECIMEN	N-S 0.5% DRIFT	LATERAL LOAD = 15.15 KIPS	
CONNECTION	ACTUAL MOMENT KIP-IN	ETABS MOMENT KIP-IN	ETABS M/ ACTUAL M	% ERROR OF COLUMN GROUP
A1	18.4	17.9	0.97	
B1	28.9	31.3	1.08	
C1	20.7	22.8	1.10	
D1	13.6	14.4	1.06	
AVERAGE RATIO OF ETABS/ACTUAL MOMENT (A1-D1)			1.05	6.76
A2	47.2	40.2	0.85	
B2	128.1	112.1	0.88	
C2	85.2	79.4	0.93	
D2	31.8	32.2	1.01	
AVERAGE RATIO OF ETABS/ACTUAL MOMENT (A2-D2)			0.92	8.85
A3	42	38.7	0.92	
B3	118.2	105.2	0.89	
C3	84.1	73.4	0.87	
D3	31.2	30.8	0.99	
AVERAGE RATIO OF ETABS/ACTUAL MOMENT (A3-D3)			0.92	8.22
A4	28.6	32.2	1.13	
B4	50.2	53.1	1.06	
C4	41.2	40.7	0.99	
D4	23.9	27.3	1.14	
AVERAGE RATIO OF ETABS/ACTUAL MOMENT (A4-D4)			1.08	8.45
TOTAL AVERAGE RATIO OF ETABS/ACTUAL MOMENT			0.99	
TOTAL AVERAGE PERCENT ERROR				8.07

ALPHA AND BETA VALUES USED FOR ANALYSIS			
	SPAN 1-2	SPAN 2-3	SPAN 3-4
ALPHA	0.4	0.4	0.4
BETA	1	1	1

ACTUAL DRIFT (%)	0.5
ETABS DRIFT (%)	0.24

Table 26 Moehle Specimen Run 2 North-South Direction 0.5% Drift
Lateral Load = 15.15 Kips

RUN 2	MOEHLE SPECIMEN	N-S 0.5% DRIFT	LATERAL LOAD = 15.15 KIPS	
CONNECTION	ACTUAL MOMENT KIP-IN	ETABS MOMENT KIP-IN	ETABS M/ ACTUAL M	% ERROR OF COLUMN GROUP
A1	18.4	14.9	0.81	
B1	28.9	27.8	0.96	
C1	20.7	22.8	1.10	
D1	13.6	13.4	0.99	
AVERAGE RATIO OF ETABS/ACTUAL MOMENT (A1-D1)			0.96	8.61
A2	47.2	40.2	0.85	
B2	128.1	99.2	0.77	
C2	85.2	82.3	0.97	
D2	31.8	36.2	1.14	
AVERAGE RATIO OF ETABS/ACTUAL MOMENT (A2-D2)			0.93	13.66
A3	42	39.7	0.95	
B3	118.2	94.7	0.80	
C3	84.1	77.9	0.93	
D3	31.2	35.2	1.13	
AVERAGE RATIO OF ETABS/ACTUAL MOMENT (A3-D3)			0.95	11.39
A4	28.6	31.7	1.11	
B4	50.2	57	1.14	
C4	41.2	48.6	1.18	
D4	23.9	29.8	1.25	
AVERAGE RATIO OF ETABS/ACTUAL MOMENT (A4-D4)			1.17	16.76
TOTAL AVERAGE RATIO OF ETABS/ACTUAL MOMENT			1.00	
TOTAL AVERAGE PERCENT ERROR				12.60

ALPHA AND BETA VALUES USED FOR ANALYSIS			
	SPAN 1-2	SPAN 2-3	SPAN 3-4
ALPHA	0.4	0.4	0.4
BETA	0.33	0.33	0.33

ACTUAL DRIFT (%)	0.5
ETABS DRIFT (%)	0.5

Table 27 Moehle Specimen Run 3 North-South Direction 0.5% Drift
Lateral Load = 15.15 Kips

RUN 3	MOEHLE SPECIMEN	N-S 0.5% DRIFT	LATERAL LOAD = 15.15 KIPS	
CONNECTION	ACTUAL MOMENT KIP-IN	ETABS MOMENT KIP-IN	ETABS M/ ACTUAL M	% ERROR OF COLUMN GROUP
A1	18.4	14.9	0.81	
B1	26.9	27.3	0.94	
C1	20.7	21.8	1.05	
D1	13.6	13.4	0.99	
AVERAGE RATIO OF ETABS/ACTUAL MOMENT (A1-D1)			0.95	7.84
A2	47.2	40.2	0.85	
B2	126.1	103.2	0.81	
C2	85.2	82.8	0.97	
D2	31.8	35.7	1.12	
AVERAGE RATIO OF ETABS/ACTUAL MOMENT (A2-D2)			0.94	12.34
A3	42	44.1	1.05	
B3	118.2	112.6	0.95	
C3	84.1	88.8	1.06	
D3	31.2	38.2	1.22	
AVERAGE RATIO OF ETABS/ACTUAL MOMENT (A3-D3)			1.07	9.44
A4	28.6	23.8	0.83	
B4	50.2	44.6	0.89	
C4	41.2	37.7	0.92	
D4	23.9	22.3	0.93	
AVERAGE RATIO OF ETABS/ACTUAL MOMENT (A4-D4)			0.89	10.78
TOTAL AVERAGE RATIO OF ETABS/ACTUAL MOMENT			0.96	
TOTAL AVERAGE PERCENT ERROR				10.10

ALPHA AND BETA VALUES USED FOR ANALYSIS			
	SPAN 1-2	SPAN 2-3	SPAN 3-4
ALPHA (POSITIVE)	0.3	0.4	0.4
ALPHA (NEGATIVE)	0.4	0.4	0.2
BETA (POSITIVE)	0.5	0.5	0.5
BETA (NEGATIVE)	0.15	0.3	0.3

ACTUAL DRIFT (%)	0.5
ETABS DRIFT (%)	0.46

Table 28 Moehle Specimen Run 1 North-South Direction 1% Drift
Lateral Load = 23.74 Kips

RUN 1	MOEHLE SPECIMEN	N-S 1.0% DRIFT	LATERAL LOAD = 23.74 KIPS	
CONNECTION	ACTUAL MOMENT KIP-IN	ETABS MOMENT KIP-IN	ETABS M/ ACTUAL M	% ERROR OF COLUMN GROUP
A1	25.2	31.7	1.26	
B1	43	55.6	1.29	
C1	28.3	40.7	1.44	
D1	19.8	26.9	1.36	
AVERAGE RATIO OF ETABS/ACTUAL MOMENT (A1-D1)			1.34	33.69
A2	74.1	62.5	0.84	
B2	206.9	173.6	0.84	
C2	142.5	123	0.86	
D2	53	50.1	0.95	
AVERAGE RATIO OF ETABS/ACTUAL MOMENT (A2-D2)			0.87	12.73
A3	66.3	61	0.92	
B3	187.1	166.6	0.89	
C3	139.3	116.6	0.84	
D3	52.5	48.1	0.92	
AVERAGE RATIO OF ETABS/ACTUAL MOMENT (A3-D3)			0.89	10.91
A4	38.2	46.1	1.21	
B4	66.5	77.4	1.16	
C4	56.9	58.5	1.03	
D4	34.8	39.2	1.13	
AVERAGE RATIO OF ETABS/ACTUAL MOMENT (A4-D4)			1.13	13.13
TOTAL AVERAGE RATIO OF ETABS/ACTUAL MOMENT			1.06	
TOTAL AVERAGE PERCENT ERROR				17.61

ALPHA AND BETA VALUES USED FOR ANALYSIS			
	SPAN 1-2	SPAN 2-3	SPAN 3-4
ALPHA	0.4	0.4	0.4
BETA	1	1	1

ACTUAL DRIFT (%)	1
ETABS DRIFT (%)	0.37

Table 29 Moehle Specimen Run 2 North-South Direction 1% Drift
Lateral Load = 23.74 Kips

RUN 2	MOEHLE SPECIMEN	N-S 1.0% DRIFT	LATERAL LOAD = 23.74 KIPS	
CONNECTION	ACTUAL MOMENT KIP-IN	ETABS MOMENT KIP-IN	ETABS M/ ACTUAL M	% ERROR OF COLUMN GROUP
A1	25.2	27.8	1.10	
B1	43	52.1	1.21	
C1	28.3	43.7	1.54	
D1	19.8	25.8	1.30	
AVERAGE RATIO OF ETABS/ACTUAL MOMENT (A1-D1)			1.29	29.05
A2	74.1	63	0.85	
B2	206.9	154.3	0.75	
C2	142.5	127.5	0.89	
D2	53	56.5	1.07	
AVERAGE RATIO OF ETABS/ACTUAL MOMENT (A2-D2)			0.89	14.38
A3	66.3	62	0.94	
B3	187.1	149.8	0.80	
C3	139.3	123.5	0.89	
D3	52.5	55.6	1.06	
AVERAGE RATIO OF ETABS/ACTUAL MOMENT (A3-D3)			0.92	10.92
A4	38.2	45.1	1.18	
B4	66.5	80.9	1.22	
C4	56.9	68.9	1.21	
D4	34.8	41.7	1.20	
AVERAGE RATIO OF ETABS/ACTUAL MOMENT (A4-D4)			1.20	20.16
TOTAL AVERAGE RATIO OF ETABS/ACTUAL MOMENT			1.08	
TOTAL AVERAGE PERCENT ERROR				18.63

ALPHA AND BETA VALUES USED FOR ANALYSIS			
	SPAN 1-2	SPAN 2-3	SPAN 3-4
ALPHA	0.4	0.4	0.4
BETA	0.33	0.33	0.33

ACTUAL DRIFT (%)	1
ETABS DRIFT (%)	0.79

Table 30 Moehle Specimen Run 3 North-South Direction 1% Drift
Lateral Load = 23.74 Kips

RUN 3	MOEHLE SPECIMEN	N-S 1.0% DRIFT	LATERAL LOAD = 23.74 KIPS	
CONNECTION	ACTUAL MOMENT KIP-IN	ETABS MOMENT KIP-IN	ETABS M/ ACTUAL M	% ERROR OF COLUMN GROUP
A1	25.2	19.8	0.79	
B1	43	35.7	0.83	
C1	28.3	30.3	1.07	
D1	19.8	18.8	0.95	
AVERAGE RATIO OF ETABS/ACTUAL MOMENT (A1-D1)			0.91	12.63
A2	74.1	65	0.88	
B2	206.9	158.2	0.76	
C2	142.5	131.9	0.93	
D2	53	59	1.11	
AVERAGE RATIO OF ETABS/ACTUAL MOMENT (A2-D2)			0.92	13.64
A3	66.3	73.4	1.11	
B3	187.1	183	0.98	
C3	139.3	150.3	1.08	
D3	52.5	66	1.26	
AVERAGE RATIO OF ETABS/ACTUAL MOMENT (A3-D3)			1.11	11.63
A4	38.2	34.2	0.90	
B4	66.5	64	0.96	
C4	56.9	55.6	0.98	
D4	34.8	32.7	0.94	
AVERAGE RATIO OF ETABS/ACTUAL MOMENT (A4-D4)			0.94	5.64
TOTAL AVERAGE RATIO OF ETABS/ACTUAL MOMENT			0.97	
TOTAL AVERAGE PERCENT ERROR				10.89

ALPHA AND BETA VALUES USED FOR ANALYSIS			
	SPAN1-2	SPAN 2-3	SPAN 3-4
ALPHA (POSITIVE)	0.2	0.4	0.4
ALPHA (NEGATIVE)	0.4	0.4	0.2
BETA (POSITIVE)	0.35	0.35	0.35
BETA (NEGATIVE)	0.11	0.21	0.21

ACTUAL DRIFT (%)	1
ETABS DRIFT (%)	0.99

Table 31 Moehle Specimen Run 1 East-West Direction 0.5% Drift
Lateral Load = 17.93 Kips

RUN 1	MOEHLE SPECIMEN	E-W 0.5% DRIFT	LATERAL LOAD = 17.93 KIPS	
CONNECTION	ACTUAL MOMENT KIP-IN	ETABS MOMENT KIP-IN	ETABS M/ ACTUAL M	% ERROR OF COLUMN GROUP
D3	28.5	6.9	0.24	
D4	14.4	3	0.21	
AVERAGE RATIO OF ETABS/ACTUAL MOMENT (D3-D4)			0.23	77.48
C3	133.4	112.6	0.84	
C4	48.8	50.6	1.04	
AVERAGE RATIO OF ETABS/ACTUAL MOMENT (C3-C4)			0.94	9.64
B3	107.4	99.7	0.93	
B4	36.8	39.7	1.08	
AVERAGE RATIO OF ETABS/ACTUAL MOMENT (B3-B4)			1.00	7.52
A3	58.6	81.8	1.40	
A4	36	50.1	1.39	
AVERAGE RATIO OF ETABS/ACTUAL MOMENT (A3-A4)			1.39	39.38
TOTAL AVERAGE RATIO OF ETABS/ACTUAL MOMENT			0.89	
TOTAL AVERAGE PERCENT ERROR				33.51

ALPHA AND BETA VALUES USED FOR ANALYSIS			
	SPAN D-C	SPAN C-B	SPAN B-A
ALPHA	0.4	0.4	0.4
BETA	1	1	1

ACTUAL DRIFT (%)	0.5
ETABS DRIFT (%)	0.43

Table 32 Moehle Specimen Run 2 East-West Direction 0.5% Drift
Lateral Load = 17.93 Kips

RUN 2	MOEHLE SPECIMEN	E-W 0.5% DRIFT	LATERAL LOAD = 17.93 KIPS	
CONNECTION	ACTUAL MOMENT KIP-IN	ETABS MOMENT KIP-IN	ETABS M/ ACTUAL M	% ERROR OF COLUMN GROUP
D3	28.5	2	0.07	
D4	14.4	0.5	0.03	
AVERAGE RATIO OF ETABS/ACTUAL MOMENT (D3-D4)			0.05	94.76
C3	133.4	105.7	0.79	
C4	48.8	49.1	1.01	
AVERAGE RATIO OF ETABS/ACTUAL MOMENT (C3-C4)			0.90	10.69
B3	107.4	101.7	0.95	
B4	36.8	42.2	1.15	
AVERAGE RATIO OF ETABS/ACTUAL MOMENT (B3-B4)			1.05	9.99
A3	58.6	90.3	1.54	
A4	36	53.6	1.49	
AVERAGE RATIO OF ETABS/ACTUAL MOMENT (A3-A4)			1.51	51.49
TOTAL AVERAGE RATIO OF ETABS/ACTUAL MOMENT			0.88	
TOTAL AVERAGE PERCENT ERROR				41.73

ALPHA AND BETA VALUES USED FOR ANALYSIS			
	SPAN D-C	SPAN C-B	SPAN B-A
ALPHA	0.4	0.4	0.4
BETA	0.33	0.33	0.33

ACTUAL DRIFT (%)	0.5
ETABS DRIFT (%)	1.14

Table 33 Moehle Specimen Run 3 East-West Direction 0.5% Drift
Lateral Load = 17.93 Kips

RUN 3	MOEHLE SPECIMEN	E-W 0.5% DRIFT	LATERAL LOAD = 17.93 KIPS	
CONNECTION	ACTUAL MOMENT KIP-IN	ETABS MOMENT KIP-IN	ETABS M/ ACTUAL M	% ERROR OF COLUMN GROUP
D3	28.5	23.8	0.84	
D4	14.4	12.9	0.90	
AVERAGE RATIO OF ETABS/ACTUAL MOMENT (D3-D4)			0.87	13.45
C3	133.4	125	0.94	
C4	48.8	57.5	1.18	
AVERAGE RATIO OF ETABS/ACTUAL MOMENT (C3-C4)			1.06	12.06
B3	107.4	98.2	0.91	
B4	36.8	38.2	1.04	
AVERAGE RATIO OF ETABS/ACTUAL MOMENT (B3-B4)			0.98	6.19
A3	58.6	56.5	0.96	
A4	36	32.7	0.91	
AVERAGE RATIO OF ETABS/ACTUAL MOMENT (A3-A4)			0.94	6.38
TOTAL AVERAGE RATIO OF ETABS/ACTUAL MOMENT			0.96	
TOTAL AVERAGE PERCENT ERROR				9.52

ALPHA AND BETA VALUES USED FOR ANALYSIS			
	SPAN D-C	SPAN C-B	SPAN B-A
ALPHA (POSITIVE)	0.5	0.4	0.4
ALPHA (NEGATIVE)	0.4	0.4	0.4
BETA (POSITIVE)	1	1	1
BETA (NEGATIVE)	1	1	0.3

ACTUAL DRIFT (%)	0.5
ETABS DRIFT (%)	0.49

Table 34 Moehle Specimen Run 1 East-West Direction 1% Drift
Lateral Load = 24.93 Kips

RUN 1	MOEHLE SPECIMEN	E-W 1.0% DRIFT	LATERAL LOAD = 24.93 KIPS	
CONNECTION	ACTUAL MOMENT KIP-IN	ETABS MOMENT KIP-IN	ETABS M/ ACTUAL M	% ERROR OF COLUMN GROUP
D3	44	26.8	0.61	
D4	22.1	13.9	0.63	
AVERAGE RATIO OF ETABS/ACTUAL MOMENT (D3-D4)			0.62	38.10
C3	185	153.8	0.83	
C4	66.6	69.4	1.04	
AVERAGE RATIO OF ETABS/ACTUAL MOMENT (C3-C4)			0.94	10.53
B3	154.2	140.4	0.91	
B4	52.8	55.6	1.05	
AVERAGE RATIO OF ETABS/ACTUAL MOMENT (B3-B4)			0.98	7.13
A3	71.5	98.2	1.37	
A4	47.8	60	1.26	
AVERAGE RATIO OF ETABS/ACTUAL MOMENT (A3-A4)			1.31	31.43
TOTAL AVERAGE RATIO OF ETABS/ACTUAL MOMENT			0.96	
TOTAL AVERAGE PERCENT ERROR				21.80

ALPHA AND BETA VALUES USED FOR ANALYSIS			
	SPAN D-C	SPAN C-B	SPAN B-A
ALPHA	0.4	0.4	0.4
BETA	1	1	1

ACTUAL DRIFT (%)	1
ETABS DRIFT (%)	0.7

Table 35 Moehle Specimen Run 2 East-West Direction 1% Drift
Lateral Load = 24.93 Kips

RUN 2	MOEHLE SPECIMEN	E-W 1.0% DRIFT	LATERAL LOAD = 24.93 KIPS	
CONNECTION	ACTUAL MOMENT KIP-IN	ETABS MOMENT KIP-IN	ETABS M/ ACTUAL M	% ERROR OF COLUMN GROUP
D3	44	21.3	0.48	
D4	22.1	10.9	0.49	
AVERAGE RATIO OF ETABS/ACTUAL MOMENT (D3-D4)			0.49	51.13
C3	185	145.8	0.79	
C4	66.6	67.5	1.01	
AVERAGE RATIO OF ETABS/ACTUAL MOMENT (C3-C4)			0.90	11.27
B3	154.2	142.4	0.92	
B4	52.8	58.5	1.11	
AVERAGE RATIO OF ETABS/ACTUAL MOMENT (B3-B4)			1.02	9.22
A3	71.5	108.1	1.51	
A4	47.8	64	1.34	
AVERAGE RATIO OF ETABS/ACTUAL MOMENT (A3-A4)			1.43	42.54
TOTAL AVERAGE RATIO OF ETABS/ACTUAL MOMENT			0.96	
TOTAL AVERAGE PERCENT ERROR				28.54

ALPHA AND BETA VALUES USED FOR ANALYSIS			
	SPAN D-C	SPAN C-B	SPAN B-A
ALPHA	0.4	0.4	0.4
BETA	0.33	0.33	0.33

ACTUAL DRIFT (%)	1
ETABS DRIFT (%)	1.57

Table 36 Moehle Specimen Run 3 East-West Direction 1% Drift
Lateral Load = 24.93 Kips

RUN 3	MOEHLE SPECIMEN	E-W 1.0% DRIFT	LATERAL LOAD = 24.93 KIPS	
CONNECTION	ACTUAL MOMENT KIP-IN	ETABS MOMENT KIP-IN	ETABS M/ ACTUAL M	% ERROR OF COLUMN GROUP
D3	44	35.7	0.81	
D4	22.1	18.8	0.85	
AVERAGE RATIO OF ETABS/ACTUAL MOMENT (D3-D4)			0.83	16.90
C3	185	170.1	0.92	
C4	66.6	78.9	1.18	
AVERAGE RATIO OF ETABS/ACTUAL MOMENT (C3-C4)			1.05	13.26
B3	154.2	144.8	0.94	
B4	52.8	57.5	1.09	
AVERAGE RATIO OF ETABS/ACTUAL MOMENT (B3-B4)			1.01	7.50
A3	71.5	70.9	0.99	
A4	47.8	41.2	0.86	
AVERAGE RATIO OF ETABS/ACTUAL MOMENT (A3-A4)			0.93	7.32
TOTAL AVERAGE RATIO OF ETABS/ACTUAL MOMENT			0.96	
TOTAL AVERAGE PERCENT ERROR				11.25

ALPHA AND BETA VALUES USED FOR ANALYSIS			
	SPAN D-C	SPAN C-B	SPAN B-A
ALPHA (POSITIVE)	0.4	0.4	0.4
ALPHA (NEGATIVE)	0.4	0.4	0.4
BETA (POSITIVE)	0.7	0.7	0.7
BETA (NEGATIVE)	0.7	0.7	0.25

ACTUAL DRIFT (%)	1
ETABS DRIFT (%)	0.92

Table 37. Recommended Alpha and Beta Values for the Effective Beam Width Two-Beam Model

Clear Span/Depth Ratio = 20	0.5% DRIFT		1.0% DRIFT	
LOCATION	ALPHA	BETA	ALPHA	BETA
Exterior Negative	0.2	0.3	0.2	0.21
Exterior Positive	0.2	0.5	0.2	0.35
Ist Interior Negative	0.4	0.15	0.4	0.11
Interior Positive	0.4	0.5	0.4	0.35
Interior Negative	0.4	0.3	0.4	0.21

Clear Span/Depth Ratio = 30	0.5% DRIFT		1.0% DRIFT	
LOCATION	ALPHA	BETA	ALPHA	BETA
Exterior Negative	0.2	0.6	0.2	0.46
Exterior Positive	0.4	1	0.4	0.7
Ist Interior Negative	0.4	1	0.4	0.7
Interior Positive	0.4	1	0.4	0.7
Interior Negative	0.4	1	0.4	0.7

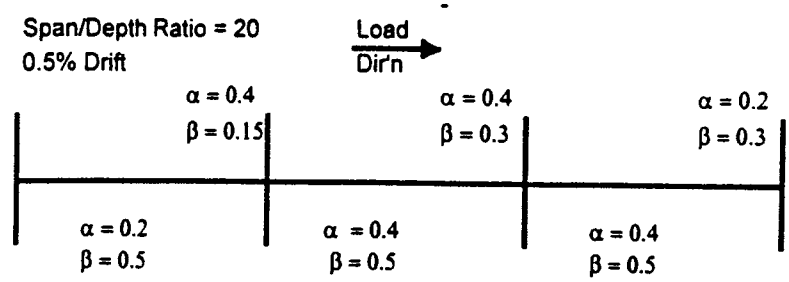

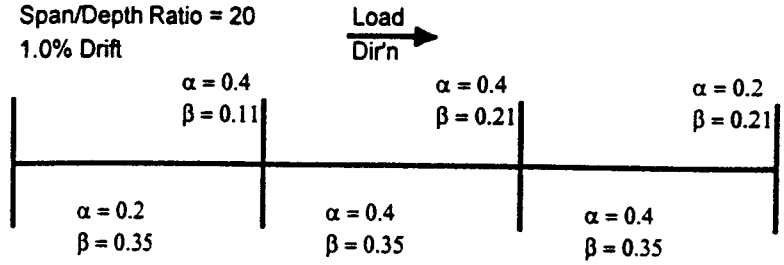

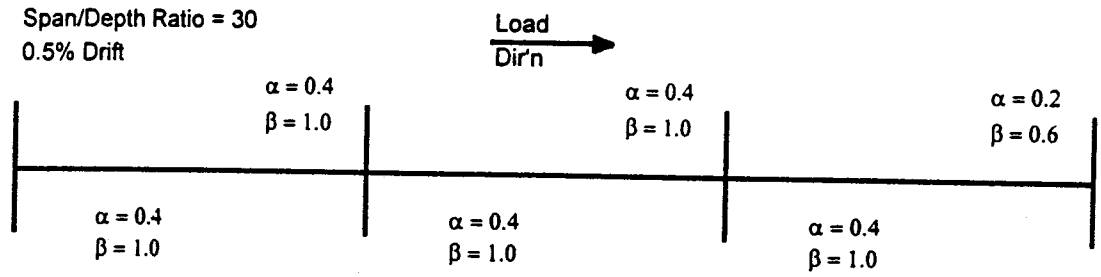

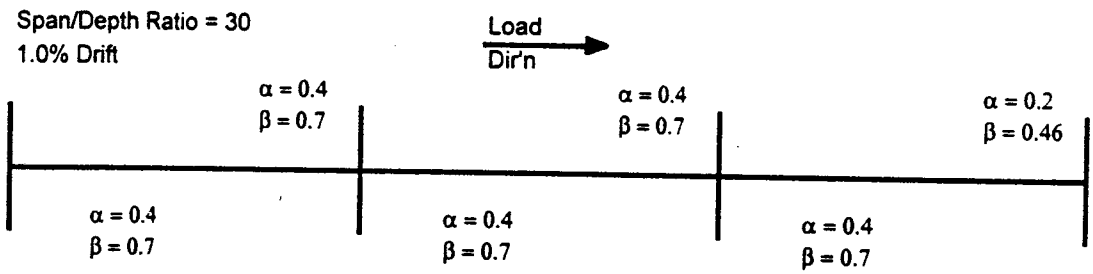

Figure 33 Recommended Alpha and Beta Values for the Effective Beam Width Two-Beam Model.

APPENDIX

APPENDIX

In order to demonstrate the application of the recommended alpha and beta values for flat-plate analysis using the two-beam model, a realistic example of a flat-plate structure was developed (Figures 34 and 35). The structure is 5 bays by 5 bays, with two I-shaped shear walls running vertically through the center of the building. The span lengths vary in dimension, allowing for different l_n/h ratios. All columns are 24" x 24" (610 x 610 mm) square, while the shearwalls are 12" (305 mm) thick throughout. The slab is 9" (229 mm) thick.

Figure 34 shows the recommended effective beam widths for the two-beam model analysis in the North direction. The effective beam widths along gridlines 1 through 3 represent service load analysis (0.5% drift). The effective beam widths along gridlines 4 through 6 represent ultimate load analysis (1.0% drift).

Figure 35 shows the recommended effective beam widths for the two-beam model analysis in the East direction. The effective beam widths along gridlines A through C represent service load analysis (0.5% drift). The effective beam widths along gridlines D through F represent ultimate load analysis (1.0% drift).

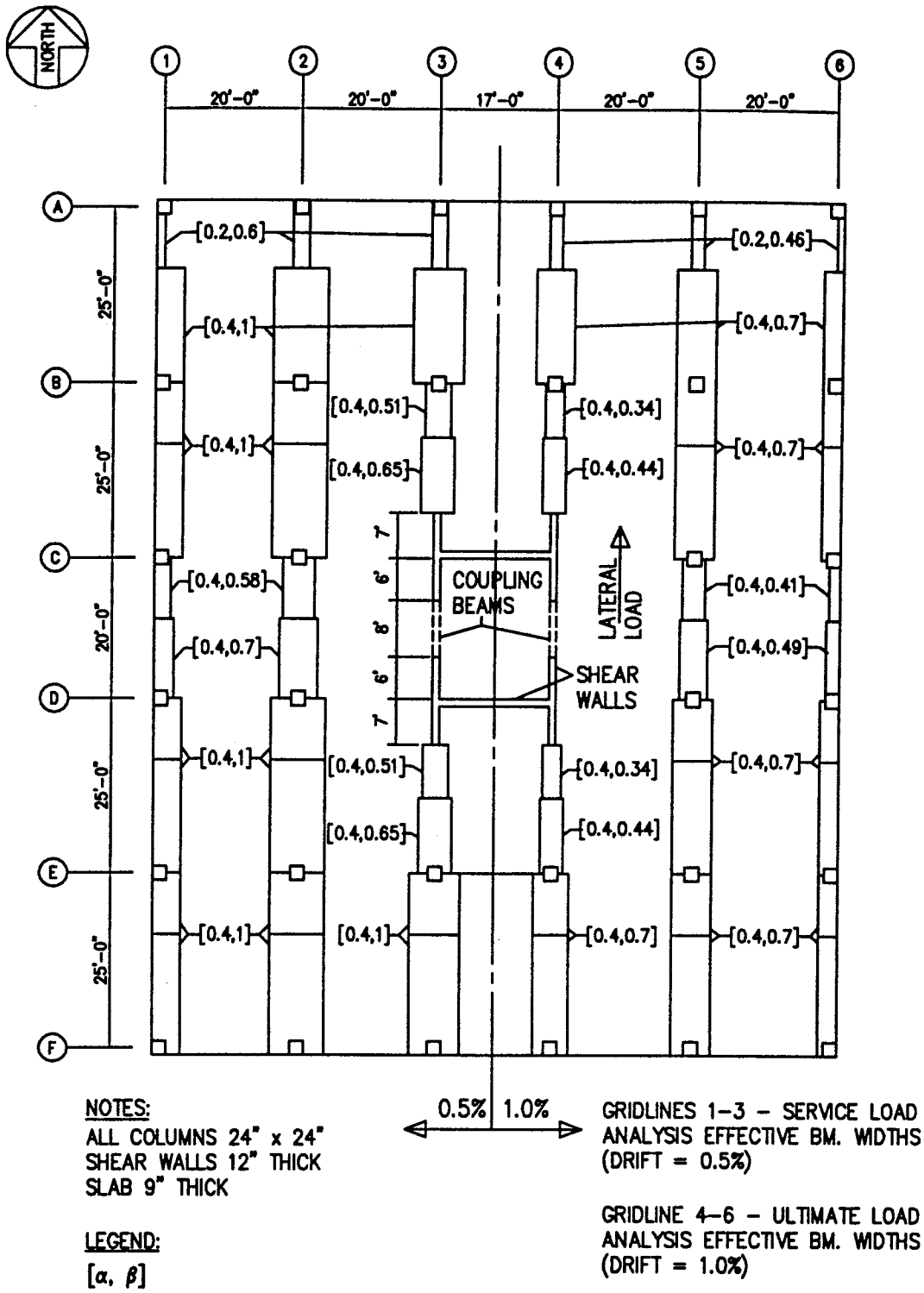

NOTES:
ALL COLUMNS 24" x 24"
SHEAR WALLS 12" THICK
SLAB 9" THICK

LEGEND:
$[\alpha, \beta]$

GRIDLINES 1–3 – SERVICE LOAD ANALYSIS EFFECTIVE BM. WIDTHS (DRIFT = 0.5%)

GRIDLINE 4–6 – ULTIMATE LOAD ANALYSIS EFFECTIVE BM. WIDTHS (DRIFT = 1.0%)

Figure 34 Application of Recommended Alpha and Beta Values for Two–Beam Model Analysis in the North Direction.

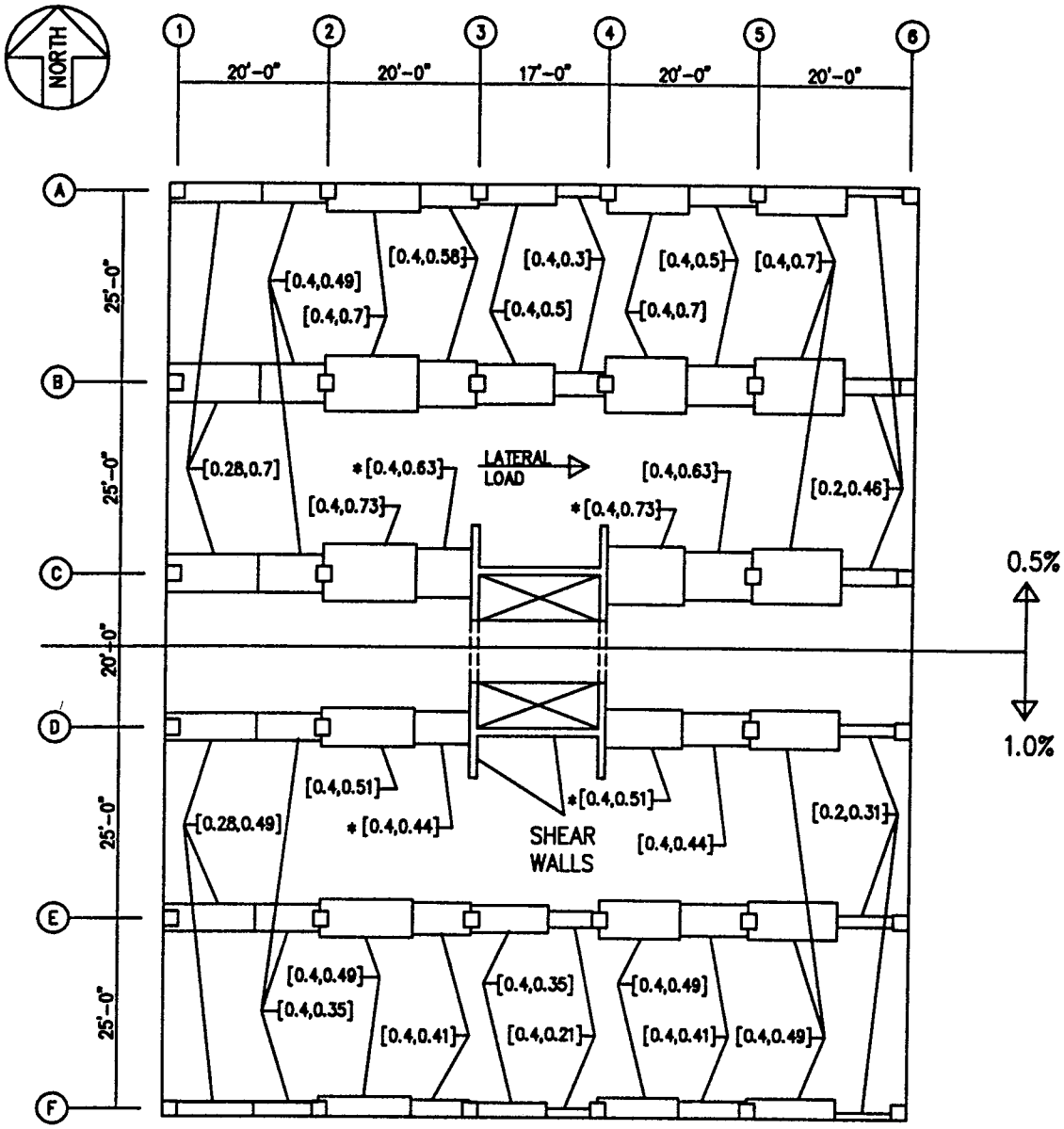

NOTES:

ALL COLUMNS 24" x 24"
SHEAR WALLS 12" THICK
SLAB 9" THICK
* CONNECTION TO SHEAR WALL WOULD SUGGEST LARGER ALPHA VALUE FOR SLAB.

GRIDLINES A–C – SERVICE LOAD ANALYSIS EFFECTIVE BM. WIDTHS (DRIFT = 0.5%)

GRIDLINE D–F – ULTIMATE LOAD ANALYSIS EFFECTIVE BM. WIDTHS (DRIFT = 1.0%)

LEGEND:

$[\alpha, \beta]$

Figure 35 Application of Recommended Alpha and Beta Values for Two–Beam Model Analysis in the East Direction.

REFERENCES

REFERENCE

(1) Aalami, B., "Moment-Rotation Relation Between Column and Slab," ACI Journal, Proceedings, Vol. 69, No. 5, May 1972, pp. 263-269. Also, Discussion by James Carpenter, Vol. 69, No. 11, November 1972, pp. 706-707.

(2) ADOSS, Analysis and Design of Slab Systems, Portland Cement Association, 1991.

(3) Allen, F. H., and Darvall, P., "Lateral Load Equivalent Frame," ACI Journal, Proceedings, Vol. 74, No. 7, July 1977, pp. 294-299.

(4) "Building Code Requirements for Reinforced Concrete (ACI 318-89) and Commentary - ACI 318R-89," American Concrete Institute, Detroit, 1989, 353 pp.

(5) Cano, M. T., and Klingner, R. E., "Comparison of Analysis Procedures for Two-Way Slabs," ACI Journal, Vol.85, No. 6, Nov.-Dec. 1988, pp. 597-608.

(6) Corley, G. W., and Jirsa, J. O., "Equivalent Frame Analysis For Slab Design," ACI Journal, Vol. 67, No. 11, Nov. 1970, pp. 875-884.

(7) Darvall, P., and Allen, F., "Lateral Load Effective Width of Flat Plates with Drop Panels," ACI Journal, Vol. 81, No. 6, Nov.-Dec. 1984, pp. 613-617.

(8) Domel, A., and Ghosh, S. K., "Economical Floor Systems for Multi-story Residential Buildings," Concrete International, Vol. 12, No. 9, Sept. 1990, pp. 37-40.

(9) Elias, Z. M., "Lateral Stiffness of Flat Plate Structures," ACI Journal, Vol. 80, No. 1, Jan.-Feb. 1983, pp. 50-54.

(10) Fraser, D. J., "Simplified Frame Analysis for Flat Plate Construction," Concrete International, Vol. 6, No. 9, Sept. 1984, pp. 32-41.

(11) Habibullah, Ashraf, "ETABS," Three Dimensional Analysis of Building Systems, Computers and Structures, Inc., 1983-1991.

(12) Hawkins, N. M. and Mitchell, D., "Progressive collapse of Flat-Plate Structures," ACI Journal, Vol. 76, No. 7, July 1979, pp. 775-808.

(13) Hawkins, N. M., "Seismic Response of Reinforced Concrete Flat Plate Structures," Proceedings of the Seventh World Conference on Earthquake Engineering, Istanbul, Turkey, Sept. 8-13, 1980, pp.33-40.

(14) Hwang, S., and Moehle, J. P., "An Experimental Study of Flat-Plate Structures Under Vertical and Lateral Loads," Structural engineering, Mechanics and Materials, Report No. UCB/SEMM-90/11, July 1990, University of California at Berkeley, 271 pp.

(15) Long, A. E., and Kirk, D. W., "Lateral Load Stiffness of Slab-Column Structures," Reinforced Concrete Structures Subjected To Wind And Earthquake Forces, SP-63, American Concrete Institute, Detroit, 1980, pp. 197-220.

(16) McCormac, J. C., "Design of Reinforced Concrete," Second Edition, Harper & Row, New York, 1986, 628 pp.

(17) Mehrain, M., and Aalami, B., "Rotational Stiffness of Concrete Slabs," ACI Journal, Proceedings, Vol. 71, No. 9, September 1974, pp. 429-435.

(18) Moehle, J. P., and Diebold, J. W., "Experimental Study of the Seismic Response of a Two-Story Flat-Plate Structure," Earthquake Engineering Research Center, Report No. UCB/EERC-84/08, August 1984, University of California at Berkeley, 238 pp.

(19) Morrison, D. G., Hirasawa, I., and Sozen, M. A., "Lateral Load Tests of R/C Slab Column Connection," Journal of Structural Engineering, ASCE, Vol. 109, No. 11, November 1983, pp. 2698-2714.

(20) Mulcahy, J. F., and Rotter, J. M., "Moment Rotation Characteristics of Flat Plate and Column Systems," ACI Journal, Vol. 80, No.2, March-April 1983, pp. 85-92.

(21) Pan, A., and Moehle, J. P., "Lateral Displacement Ductility of Reinforced Concrete Flat Plates," ACI Journal, Vol. 86, No. 3, May-June 1989, pp. 250-258.

(22) PCACOL, Strength Design of Reinforced Concrete Column Sections, Portland Cement Association, 1992.

(23) Pecknold, D. A., "Slab Effective Width for Equivalent Frame Analysis," ACI Journal, Vol. 72, No. 4, April 1975, pp. 135-137. Also discussion by F. H. Allen and P. Darvall, Robert Glover, and Author, ACI Proceedings, Vol. 72, No. 10, October 1975, pp.583-586.

(24) Pillai, S. U., Kirk, W., and Scavuzzo, L., "Shear Reinforcement at Slab-Column Connections in a Reinforced Concrete Flat Plate Structure," ACI Journal, Vol. 79, No. 1, Jan.-Feb. 1982, pp. 36-42.

(25) Rangan, B. V., and Hall, A. S., "Moment Redistribution in Flat Plate Floors," ACI Journal, Vol. 81, No. 6, Nov.-Dec. 1984, pp. 601-608.

(26) Robertson, I. N., and Durrani, A. J., "Seismic Response of connections in Indeterminate Flat-Slab Subassemblies," Structural Research at Rice, Report No. 41, July 1990, Rice University, 266 pp.

(27) Scavuzzo, L., "Shear Reinforcement of Slab-Column Connections in a Reinforced Concrete Structure," ME Thesis, Royal Military College of Canada, Kingston, 1978.

(28) Vanderbilt, D. M., and Corley, G. W., "Frame Analysis of Concrete Buildings," Concrete International, Vol. 5, No. 12, December 1983, pp. 33-43.

NOTATION

NOTATION

c_1	=	dimension of rectangular column parallel to direction of loading
c_2	=	dimension of rectangular column transverse to direction of loading
h	=	slab thickness
K_c	=	actual column stiffness
K_{ec}	=	equivalent column stiffness
l_1	=	length of span parallel to direction of loading
l_2	=	length of span transverse to direction of loading
l_n/h	=	clear span-to-depth ratio
α	=	effective beam width factor, alpha
β	=	stiffness reduction factor for cracking, beta